Theses and Dissertations   1. Thesis and Dissertation Collection, all items

1966

An analysis of the effect of initial web tilt upon the stresses induced in a stiffened plate panel subjected to uniform lateral load

Johnston, Donald Hendrie.; Rosenqvist, Harald S.

Massachusetts Institute of Technology

http://hdl.handle.net/10945/9432

AN ANALYSIS OF THE EFFECT OF INITIAL WEB TILT UPON

THE STRESSES INDUCED IN A STIFFENED PLATE PANEL SUBJECTED

TO UNIFORM LATERAL LOAD

by

DONALD HENDRIE JOHNSTON JR.

LIEUTENANT COMMANDER, UNITED STATES NAVY

B.S., U.S. Naval Academy

(1956)

and

HARALD S. ROSENQVIST

LIEUTENANT, CHILEAN NAVY

B.S.M.E., Naval Engineering School

Valparaiso, Chile

(1961)

June, 1966

AN ANALYSIS OF THE EFFECT OF INITIAL WEB TILT UPON
THE STRESSES INDUCED IN A STIFFENED PLATE PANEL SUBJECTED
TO UNIFORM LATERAL LOAD

by

DONALD HENDRIE JOHNSTON JR.
LIEUTENANT COMMANDER, UNITED STATES NAVY
B.S., U.S. Naval Academy
(1956)

and

HARALD S. ROSENQVIST
LIEUTENANT, CHILEAN NAVY
B.S.M.E., Naval Engineering School
Valparaiso, Chile
(1961)

Submitted in Partial Fulfillment of the
Requirements for the Degree of
Naval Engineer and the Degree of
Master of Science in Naval Architecture
and Marine Engineering
at the
MASSACHUSETTS INSTITUTE OF TECHNOLOGY
May, 1966

AN ANALYSIS OF THE EFFECT OF INITIAL WEB TILT UPON

THE STRESSES INDUCED IN A STIFFENED PLATE PANEL SUBJECTED

TO UNIFORM LATERAL LOAD

by

LIEUTENANT COMMANDER DONALD HENDRIE JOHNSTON, JR.
UNITED STATED NAVY

and

LIEUTENANT HARALD S. ROSENQVIST
CHILEAN NAVY

ABSTRACT

The object of this theoretical study is to determine
the overall magnitude of the effect of an initial stiffener
web tilt upon the bending stresses induced in a flat plate
panel subjected to a uniform lateral load.

A simplified plate geometry was set up, and analyzed
by use of the theory of small deflections. The theoretical
solution was programmed for the IBM 7094 computer. Input
data was selected to represent ship bottom plating, and
ranged from an aspect ratio (a/b) of 2.0 to 4.0.

The study revealed that the effect of such an initial
tilt is significant, and further that the magnitude of the
effect is essentially independent of the support conditions
assumed for the plate panel. In addition, a useful design
parameter, the depth ratio of the stiffener to plating
thickness (c/t), was disclosed, and the variation of the
web tilt effect with this parameter shown.

Thesis Supervisor: J. Harvey Evans
Title: Professor of Naval Architecture

TABLE OF CONTENTS

LIST OF TABLES AND FIGURES

Tables

Figures

I. INTRODUCTION

Background

"Web Tilt," as used in this thesis, is defined by
NAVSHIPS 250-637-3 [1] as "the deviation of the web of a
stiffening member from a reference plane normal to the base
line." In recent years, with the increasing importance of
submarine pressure hull design, the problem of determining
the magnitude of the effect of web tilt upon a stiffened,
circular cylinder has come into direct focus. Wenk and
Kennard [2] and Kennard [3], at the David Taylor Model Basin,
have studied the effect of such a tilt upon the twisting of
the stiffening member itself, with the attendant weakening
of the overall structure.

This approach to the problem implies that the twisting
of the stiffening members observed in cases of general in-
stability failure might have been at least a partial cause
of the failure rather than simply a resultant deformation.
Despite these theories, there remains an absence of any good,
experimentally verified theory covering the effect of such
a tilt upon the stresses obtained in the shell plating it-
self. In other words, if web tilt did in fact contribute
to failure, by just how much and in just what way? As a
result of this lack of theoretical or experimental informa-
tion, severe building specifications have been adopted to
limit the amount of web tilt acceptable in submarine con-
struction.

While the possible existence of a stress magnification which does not lend itself to analysis is of obvious concern to the submarine designer, whose structural design is a critical art, the possibility that some degree of stress magnification exists in shell plating due to web tilt is in no way limited to the cylindrical geometry. Virtually all ship hulls are made up of stiffened plate panels, both flat and curved, and a brief examination of representative plans indicates that the orientation of hull stiffeners with respect to the hull plating is by no means constant in any one ship. If the definition of web tilt given before were re-worded such that the angle of tilt was described by the angle between the web of the stiffening member and the line of action of the normal, or hydrostatic, loading on the plate, then the significance of the above statement becomes clearer. On some ships very large angles of tilt are formed intentionally by using one of the stiffening members near the turn of the bilge as a support for some internal part of the ship, such as a reduction gear.

In short, the presence of stiffened plate panels possessed of some degree of web tilt can be assumed on nearly every ship. Only the seriousness of this situation, that is, the value of any resulting stress magnification, remains a question. It is to this question that this thesis is directed.

Statement of the Problem

Reduced to its simplest form, the "tilt" problem arises from the fact that the line of action of the reaction force imparted to the stiffening member from the plate under conditions of lateral load does not pass directly through the flexural center of the stiffener. As discussed by Roark [4], this force (P) can be resolved into an equal and parallel force (P') passing through the flexural center (Q) of the beam, and a couple (T) equal to the moment of P and Q. As a result of this, an equal and opposite couple (T') will act on the plate from the stiffener, causing additional stresses and altering the effect of the hydrostatic load acting alone. (Figure (I))
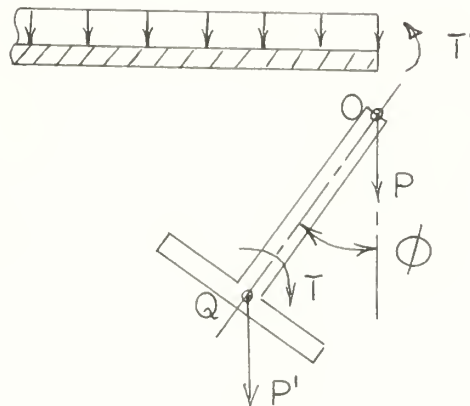
Fig. I Schematic of a tilted stiffener

Brief consideration of this problem as applied to a ship hull reveals that the actual performance of a tilted stiffening member under load is a complicated function of

many variables. Considering the major variables in turn, they are

1. Accurate description of the boundary conditions at each edge of any plate panel.

Traditionally, ship plate problems have been treated as either fully clamped at the edges or else simply supported. In an investigation of this sort, however, where the action of the stiffening member along one or more of the edges must be considered in detail, these approximations appear too general. If, as a first approximation of the problem, analysis in this thesis is limited to the case of a longitudinally framed ship, and the web tilt is considered to be applied along one of the longitudinal stiffeners, and, in addition, if attention is directed chiefly to the effect at or near the center of the plate panel, then the support conditions along the transverse edges of the plate panels might be reasonably assumed to approximate those of simple support. Use of this approximation represents a worst case of stress at the mid-panel section.

Along the longitudinal edges, it can be argued that the simple beam deflection of the stiffening member must at all times equal the deflection of the plate to which it is attached, and also, the rotation of the beam and the plate edge must be equal at the point of attachment. These conditions describe the conditions of elastic support described

by Timoshenko [5] and others, and seems most appropriate for
this case. The selected boundary conditions will be dis-
cussed in more detail in the following pages.

2. Accurate determination of the magnitude of the
force transmitted from the plate to the stiffener under
lateral load.

An exact analysis of this force can only be done for
a few individual cases, as it depends upon the panel dimen-
sions, the lateral load, the support conditions, and, in
some manner, upon the number of adjacent panels between theo-
retically rigid supports. This last statement can be visu-
alized if one makes an analogy to a simple beam continuous
over several supports and subjected to lateral load. Tabu-
lated solutions for this simple case [6] show that the value
of the reaction force at a central support will vary by a
factor of two or more as the number of spans increases from
one to four.

3. Exact behavior of the tilted stiffener under load.

Consideration of Figure II will indicate that a
stiffener with an initial angle of tilt will act in such a
way as to change the angle when deformed. The amount of
this change would be different for different points along
the length of the stiffener. This deformation arises from
the stress differentials set up in the flange of the member
as the beam is displaced from its initial position. If the

initial angle of tilt were not a constant along the length
of the stiffener, but changed from a positive to negative
value, as might occur in the case of an initial tilt caused
by variation in welding heat along the length, then it could
even be argued that the change could cause the final tilt
angle to decrease.
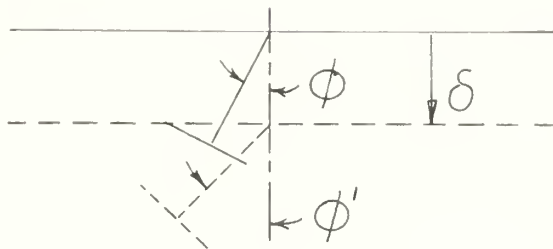
Fig. II   Schematic of stiffener action under load

4.   The effect of loading in the plane of the plate.

Clearly, as the stiffener is deflected from its
initial position by the action of the lateral load, the ef-
fect of any in-plane load becomes pronounced. In considera-
tion of ship hulls, such loads are always present, and, as
in the case above, could act to change the initial angle of
tilt in any manner, depending upon the sign of the load.

With all of these considerations in mind, a general
solution to the web tilt problem is clearly impossible. In
order to make a first approximation of the magnitude of tilt-
induced stresses, a simplified model of the situation must
be defined.

To this end, this thesis will analyze a single plate panel by use of the theory of small deflections. This approximation has been discussed by Bleich [9] and others, who state that the deflection of ship hull plating usually does not exceed one-half of the plating thickness, and concludes that linearized theory may be applied.

As stated before, two edges of the plate panel will be assumed to be simply supported, representing the transverse bulkhead connections. The other two plate edges, representing the longitudinal stiffening members, will be assumed to be elastically supported by the stiffening members, one of which will be subjected to various angles of initial tilt. Since a review of the literature revealed no treatment of the actual behavior of a skew stiffener under the action of a lateral load, the approximation will be made that the stiffener deflection will be small enough that the tilt angle might be considered a constant under the action of the lateral load, i.e., $\emptyset = \emptyset'$ in Fig. II.

The angle of initial tilt will be assumed to be a constant along the edge of the plate. With this assumption, the change brought about by the superposition of an in-plane load would be negligible, and will be neglected in this paper. Thus the investigation will be limited to the effect of the tilt on the plate bending stresses alone.

With this simplified approach, some idea of the
order of magnitude of the tilt-induced stresses as related
to those arising from the normal pressure alone will be ob-
tained. This will not represent a completely general solu-
tion to the problem in any case, in that no "design equation"
will be provided. Rather, this approach will represent a
first, crude look into the problem and, if indeed any prob-
lem is shown to exist, will point the way to the best
avenues for further research on the subject.

II.   THEORY
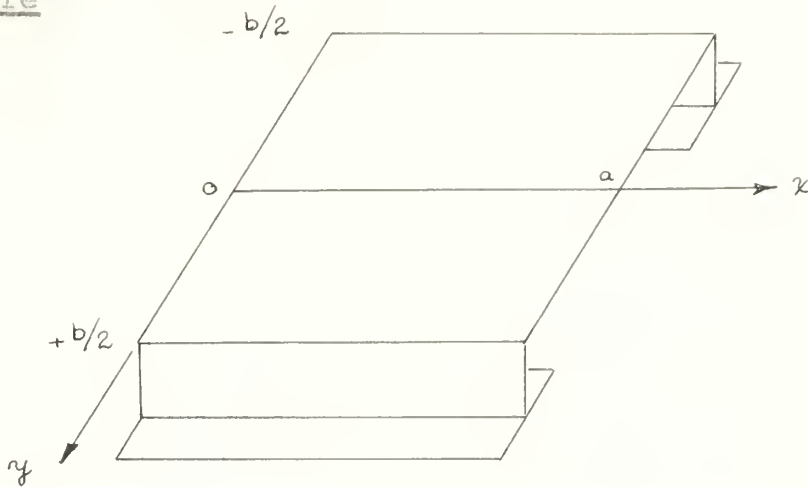
Fig. III   Schematic diagram of simplified plate panel

a   plate length in the x-direction (inches)

b   plate length in the y-direction (inches)

x,y   coordinate directions

h, t   plate thickness (inches)

w   plate deflection (inches)

E   Young's modulus of elasticity (psi)

           (note: a value of 30,000,000 psi is assumed in this

           work)

ν Poisson's ratio

           (note: a value of 0.3 is assumed in this work)

q   uniform lateral load on plate (psi)

e   distance from toe of frame web to the flexural center

           of the stiffener (OQ in Fig. I)

-9-

$\emptyset$ angle of tilt of the frame web

I   moment of inertia of the stiffener about the neutral axis of bending (inches^4)

D   flexural rigidity of plate ($Eh^3/12(1-\nu^2)$)

G   modulus of rigidity of the stiffener

K   a factor analogous to the polar moment of inertia of the stiffener section, but dependent on the form and dimensions of the cross section

Solution Technique

The problem of evaluating the tilt induced stresses will be undertaken in two separate phases. First, a solution will be obtained for the deflection equation of a flat plate panel subjected only to a lateral load. From the deflection equation, stresses in the plate can be computed. In addition, the force which the plate exerts on the edge stiffeners can also be computed. This force, according to the theory of small deflections, is the sum of the shear force at the plate edge and the rate of change of the twisting moment along the plate edge, viz.,

$$V_y = \left[Q_y - \frac{\partial\ Mxy}{\partial x} \right] \tag{1}$$

This force will be referred to as the "shear pressure" in this thesis.

In the second phase of the solution, a similarly supported flat plate will be loaded solely by a moment along its longitudinal edge. This moment will be equal to the product of the shear pressure arising from the lateral load and the moment arm arising from the web tilt (ϵ SIN $\emptyset$). A solution for the plate deflection equation under this loading will be obtained.

If, for purposes of this analysis, the system is assumed to remain elastic under action of the loads, the principle of superposition may be applied and the separate deflection equations added directly. From this combined case, the total stress in the plate panel with a tilted stiffener may be obtained, as well as factors relating to the percentage of stress magnification at any point in the plate panel.

Fundamental Equations

The basic equation governing the small deflections of laterally loaded plates has been given by Timoshenko [5] and others, and is,

$$\nabla^4 \omega = q/D \tag{2a}$$

or,

$$\frac{\partial^4 \omega}{\partial x^4} + 2 \frac{\partial^4 \omega}{\partial x^2 \partial y^2} + \frac{\partial^4 \omega}{\partial y^4} = \frac{q}{D} \tag{2b}$$

In the discussion of bending of rectangular plates which have two sides simply supported, a solution of the following form has been proposed by Nádai [7] and Lévy [8].

$$\omega = \sum_{m=1}^{\infty} Y_m \, SIN \, \frac{m\pi x}{a} \tag{3}$$

where,

$$Y_m = \frac{qa^4}{D} \left[A_m COSH \, \frac{m\pi y}{a} + B_m \, \frac{m\pi y}{a} \, SINH \, \frac{m\pi y}{a} + C_m \, SINH \, \frac{m\pi y}{a} + \right.$$
$$\left. + D_m \, \frac{m\pi y}{a} \, COSH \, \frac{m\pi y}{a} \right] \tag{4}$$

The series constants in the above equation remain to be determined by the particular boundary conditions of the case in question, and by the equation of the deflection surface (2b).

Since the simplified model selected for examination in this thesis has been assumed to be simply supported along its transverse edges (x = 0, a), this form of solution is considered appropriate for use.

Boundary Conditions

As stated before, the solution to the problem is to be divided into two parts, each of which having its own particular boundary conditions. Certain conditions, however, will remain constant throughout the problem, these are

a) The deflection and moment of the plate edge at a simply supported edge must always be zero, viz.,

$$\omega = 0, \quad \frac{\partial^2 \omega}{\partial x^2} = 0 \qquad \text{at } x = 0, a \qquad (5)$$

b) The condition of elastic support requires that the load on the stiffening member at the plate edge be equal to the force transmitted from the plate to the stiffener, i.e., the shear pressure, viz.,

$$EI \frac{\partial^4 \omega}{\partial x^4} = - V_y \qquad \text{at } y = \pm b/2 \qquad (6a)$$

or,

$$EI \frac{\partial^4 \omega}{\partial x^4} = D \left[\frac{\partial^3 \omega}{\partial y^3} + (2-\nu) \frac{\partial^3 \omega}{\partial x^2 \partial y} \right] \text{ at } y = \pm b/2 \qquad (6b)$$

Considering other conditions which must exist along the plate edges, it can easily be seen that the rotation of the stiffener at its point of attachment to the plate must equal the rotation of the plate at the same point. Stated in mathematical terms, this would be

$$-GK \frac{\partial^3 \omega}{\partial x^2 \partial y} = D \left[\frac{\partial^2 \omega}{\partial y^2} + \nu \frac{\partial^2 \omega}{\partial x^2} \right] \quad \text{at } y = \pm b/2 \qquad (7)$$

In most actual cases, however, plating stiffeners are T-sections, and it can be shown that the value of the torsional stiffness constant (K) is only a fraction of the value of the polar moment of inertia (J) of these sections [4]. Hence, the resistance of such a structural element to a rotation about its point of attachment is quite small. This is obviously not a good approximation at or near the ends of the stiffener, where some form of connection is made to a transverse member, but near the center of the panel, where the bending stresses resulting from boundary condition (5) would be the greatest, the assumption seems reasonable.

Considering this, one further assumption which might be made concerning the longitudinal plate edge would be that the stiffener, near the center of its span, offers no resistance to rotation about its point of attachment, or,

$$D \left[\frac{\partial^2 \omega}{\partial y^2} + \nu \frac{\partial^2 \omega}{\partial x^2} \right] = 0 \qquad \text{at } y = \pm \, b/2 \qquad (8)$$

It is just this assumption which has been made by Timoshenko [5] in his treatment of a somewhat similar case. There, the value of the stiffness constant (K) was equal to the polar moment (J), a fact which serves to affirm the assumption made in (8).

Another approach to the condition existing along the ± b/2 edges may be defined if one considers an ideal plate deflection pattern as shown in Fig. IV.
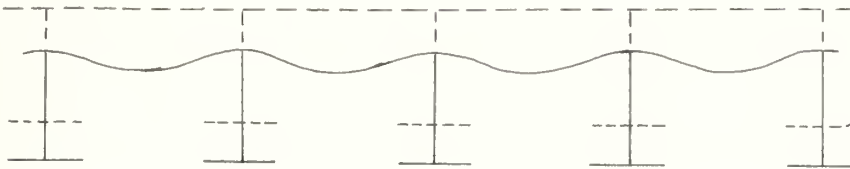
Fig. IV. Ideal deflection pattern of an infinite series of similar plate panels under lateral load

While this deflection pattern is obviously an ideal situation in which each plate panel affects its neighbor in such a way that all rotation of the plate panel at the stiffener is removed, viz.,

$$\frac{\partial w}{\partial y} = 0 \qquad \text{at } y = \pm \, b/2 \qquad (9)$$

it would appear reasonable to assume that this situation is no more ideal than that which assumes no residual bending moment at the stiffeners (8). Actually, it seems most likely that the actual situation lies somewhere between the two extremes. Accordingly, both of these approximations will be made in the solution of the plate under lateral load alone.

For purposes of identification, the solution using boundary condition (8) will be referred to as the "simple support" approximation to the lateral load case, and that using boundary condition (9) as the "clamped" approximation to the lateral load case. This terminology will be retained throughout.

The second phase of the solution, that dealing with the plate panel loaded only by a moment applied along a longitudinal edge, has been discussed by Timoshenko [5] for somewhat different boundary conditions. A completely general edge moment loading may be described by the following two conditions:

$$- D \left[\frac{\partial^2 \omega}{\partial y^2} + \nu \frac{\partial^2 \omega}{\partial x^2} \right] = f_1(x) \quad \text{at } y = + b/2 \qquad (10)$$

$$- D \left[\frac{\partial^2 \omega}{\partial y^2} + \nu \frac{\partial^2 \omega}{\partial x^2} \right] = f_2(x) \quad \text{at } y = - b/2 \qquad (11)$$

Using these conditions, together with (5) and (6), the complete solution for the plate deflection equation under moment load alone may be obtained in general form. Specialization of this solution, by setting the moment at one of the longitudinal edges equal to zero and the other equal to that transmitted from the tilted stiffener, will lead to the solution sought in this phase. This method of specialization is further described in appendix B.

Lateral Load Case

1. Simple support approximation

The boundary conditions appropriate to this case are

$$\omega = 0, \quad \frac{\partial^2 \omega}{\partial x^2} = 0 \qquad \text{at } x = 0, a \qquad (5)$$

$$EI \frac{\partial^4 \omega}{\partial x^4} = D \left[\frac{\partial^3 \omega}{\partial y^3} + (2-\nu) \frac{\partial^3 \omega}{\partial x^2 \partial y} \right] \qquad \text{at } y = \pm b/2 \qquad (6)$$

$$D \left[\frac{\partial^2 \omega}{\partial y^2} + \nu \frac{\partial^2 \omega}{\partial x^2} \right] = 0 \qquad \text{at } y = \pm b/2 \qquad (7)$$

The solution of equation (2a) for these conditions has been carried out by Timoshenko [5] and, with a slight change in notation, is reproduced below.

$$\omega = \frac{4qa^4}{\pi^5 D} \sum_{m=1,3,\ldots}^{\infty} \frac{1}{m^5} \left[1 + A_m \text{ COSH } \frac{m\pi y}{a} \right.$$

$$\left. + B_m \frac{m\pi y}{a} \text{ SINH } \frac{m\pi y}{a} \right] \text{ SIN } \frac{m\pi x}{a} \qquad (12)$$

in which,

$$A_m = \frac{\nu(1+\nu)\text{SINH } \lambda_m - \nu(1-\nu)\lambda_m \text{COSH } \lambda_m - \alpha_m (2\text{COSH } \lambda_m + \lambda_m \text{SINH } \lambda_m)}{(3+\nu)(1-\nu)\text{SINH } \lambda_m \text{COSH } \lambda_m - (1-\nu^2)\lambda_m + 2\alpha_m \text{COSH}^2 \lambda_m}$$

$$(13)$$

$$B_m = \frac{\nu(1-\nu)\text{SINH } \lambda_m + \alpha_m \text{COSH } \lambda_m}{(3+\nu)(1-\nu)\text{SINH } \lambda_m \text{COSH } \lambda_m - (1-\nu^2)\lambda_m + 2\alpha_m \text{COSH}^2 \lambda_m}$$

$$(14)$$

$$\lambda_m = \frac{m\pi b}{2a} \tag{15}$$

$$\alpha_m = \frac{EI}{D} \cdot \frac{m\pi}{a} \tag{16}$$

With this solution for the plate deflection surface, surface stresses in the plate may be found from the following relationships:

$$\sigma_x = \frac{6M_x}{h^2} = -\frac{6D}{h^2}\left[\frac{\partial^2 w}{\partial x^2} + \nu \frac{\partial^2 w}{\partial y^2}\right] \tag{17}$$

$$\sigma_y = \frac{6M_y}{h^2} = -\frac{6D}{h^2}\left[\frac{\partial^2 w}{\partial y^2} + \nu \frac{\partial^2 w}{\partial x^2}\right] \tag{18}$$

Upon differentiation of (12), and substitution, the equations for the stresses due to lateral load under the simple support approximation are

$$\sigma_{x_1} = \frac{24qa^2}{h^2\pi^3}\sum_{m=1,3,\ldots}^{\infty}\frac{1}{m^3}\Big[1+A_m(1-\nu)\cosh\frac{m\pi y}{a}$$

$$- 2\nu\,B_m\cosh\frac{m\pi y}{a} + B_m(1-\nu)\frac{m\pi y}{a}\sinh\frac{m\pi y}{a}\Big]\sin\frac{m\pi x}{a} \tag{19}$$

$$\sigma_{y_1} = \frac{24qa^2}{h^2\pi^3}\sum_{m=1,3,\ldots}^{\infty}\frac{1}{m^3}\Big[\nu+(\nu-1)A_m\cosh\frac{m\pi y}{a}$$

$$-2B_m\cosh\frac{m\pi y}{a} +(\nu-1)B_m\frac{m\pi y}{a}\sinh\frac{m\pi y}{a}\Big]\sin\frac{m\pi x}{a} \tag{20}$$

2. Clamped approximation

The boundary conditions appropriate to this case are

$$\omega = 0, \quad \frac{\partial^2 \omega}{\partial x^2} = 0 \qquad \text{at } x = 0, a \qquad (5)$$

$$EI \frac{\partial^4 \omega}{\partial x^4} = D \left[\frac{\partial^3 \omega}{\partial y^3} + (2-\nu) \frac{\partial^3 \omega}{\partial x^2 \partial y} \right] \quad \text{at } y = \pm b/2 \qquad (6)$$

$$\frac{\partial \omega}{\partial y} = 0 \qquad \text{at } y = \pm b/2 \qquad (9)$$

A detailed solution for this case is presented in Appendix A.

The solution for the deflection surface of the plate subject to the approximation that there is no rotation of the plate panel at the stiffeners under purely lateral load is

$$\omega = \frac{4qa^4}{\pi^5 D} \sum_{m=1,3,\ldots}^{\infty} \frac{1}{m^5} \left[1+A_m \text{COSH} \frac{m\pi y}{a} + B_m \frac{m\pi y}{a} \text{SINH} \frac{m\pi y}{a} \right] \text{SIN} \frac{m\pi y}{a}$$

$$(12)$$

where

$$A_m = \frac{-\alpha_m (\text{SINH } \lambda_m + \lambda_m \text{ COSH } \lambda_m)}{\alpha_m \lambda_m + \alpha_m \text{SINH } \lambda_m \text{COSH } \lambda_m + 2\text{SINH}^2 \lambda_m} \qquad (21)$$

$$B_m = \frac{\alpha_m \text{SINH } \lambda_m}{\alpha_m \lambda_m + \alpha_m \text{SINH } \lambda_m \text{COSH } \lambda_m + 2\text{SINH}^2 \lambda_m} \qquad (22)$$

with the terms λ_m and α_m as defined above by (15) and (16).

The solution is thus of the same form for both approximations. Only the series constants, A_m and B_m, change with different boundary conditions. With these same modifications then, the equations derived for the flat plate stresses are identical for both support approximations.

Tilt Load Case

Boundary conditions for this case are

$$\omega = 0, \quad \frac{\partial^2 \omega}{\partial x^2} = 0 \qquad \text{at } x = 0, a \qquad (5)$$

$$EI \frac{\partial^4 \omega}{\partial x^4} = D\left[\frac{\partial^3 \omega}{\partial y^3} + (2-\nu) \frac{\partial^3 \omega}{\partial x^2 \partial y} \right] \qquad \text{at } y = \pm b/2 \qquad (6)$$

$$-D\left[\frac{\partial^2 \omega}{\partial y^2} + \nu \frac{\partial^2 \omega}{\partial x^2} \right] = f_1(x) \qquad \text{at } y = + b/2 \qquad (10)$$

$$-D\left[\frac{\partial^2 \omega}{\partial y^2} + \nu \frac{\partial^2 \omega}{\partial x^2} \right] = f_2(x) \qquad \text{at } y = - b/2 \qquad (11)$$

A detailed solution for this case is presented in Appendix B.

If the arbitrary moments applied to the plate edge are assumed to be of the general form

$$f(x) = \sum_{m=1}^{\infty} E_m \, \text{SIN} \, \frac{m \pi x}{a} \qquad (23)$$

then the solution to this case can be given as follows

$$\omega = - \frac{a^2}{\pi^2 D} \sum_{m=1}^{\infty} \frac{E_m}{m^2} \left[\frac{\rho}{R_1} \cosh \frac{m\pi y}{a} + \frac{m\pi y}{aR_1} \sinh \frac{m\pi y}{a} \right.$$

$$\left. + \frac{\gamma}{R_2} \sinh \frac{m\pi y}{a} + \frac{m\pi y}{aR_2} \cosh \frac{m\pi y}{a} \right] \sin \frac{m\pi x}{a} \tag{24}$$

where the constants of the series terms are given by

$$\rho = \frac{(1+\nu-\alpha_m \lambda_m) \sinh \lambda_m - (1-\nu) \lambda_m \cosh \lambda_m}{(1-\nu) \sinh \lambda_m + \alpha_m \cosh \lambda_m} \tag{25}$$

$$\gamma = \frac{(1+\nu-\alpha_m \lambda_m) \cosh \lambda_m - (1-\nu) \lambda_m \sinh \lambda_m}{(1-\nu) \cosh \lambda_m + \alpha_m \sinh \lambda_m} \tag{26}$$

$$R_1 = \left[\rho(1-\nu)+2 \right] \cosh \lambda_m + \lambda_m (1-\nu) \sinh \lambda_m \tag{27}$$

$$R_2 = \left[\gamma(1-\nu)+2 \right] \sinh \lambda_m + \lambda_m (1-\nu) \cosh \lambda_m \tag{28}$$

with the terms λ_m and α_m as defined before, (15), (16).

In order to determine the value of the series constant E_m in (24), the nature of the loading moment must be considered. As stated earlier, the moment applied to the plate from the stiffener will be the product of the shear pressure at the edge of the plate times the moment arm arising from the angle of tilt, ($\epsilon \sin \emptyset$).

The shear pressure at the plate edge, by the theory of small deflections, is

$$V_y = Q_y - \frac{\partial Mxy}{\partial x} \tag{29}$$

or

$$V_y = -D \left[\frac{\partial^3 w}{\partial y^3} + (2-\nu) \frac{\partial^3 w}{\partial x^2 \partial y} \right] \tag{30}$$

The reaction force applied to the plate is then

$$-V_y \bigg|_{y=b/2} = D \left[\frac{\partial^3 w}{\partial y^3} + (2-\nu) \frac{\partial^3 w}{\partial x^2 \partial y} \right]_{y=b/2} \tag{31}$$

Differentiating the solution to the lateral load case (12) and substituting that value into (31) gives

$$-V_{(b/2)} = \frac{4qa}{\pi^2} \sum_{m=1,3,\ldots}^{\infty} \frac{1}{m^2} \left[(\nu-1)A_m \text{ SINH } \lambda_m + (\nu+1)B_m \text{SINH } \lambda_m \right.$$

$$\left. + (\nu-1)B_m \lambda_m \text{COSH } \lambda_m \right] \text{ SIN } \frac{m\pi x}{a} \tag{32}$$

This solution has the same form for both lateral load stress approximations, only the values of A_m and B_m change, as has been shown.

Since the moment applied to the plate is of the form

$$f(x) = -V_{(b/2)} \cdot \text{ SIN } \phi \tag{33}$$

and has been assumed to be

$$f(x) = \sum_{m=1}^{\infty} E_m \ SIN \ \frac{m\pi x}{a} \tag{23}$$

the final form of the solution for the series constant E_m is

$$E_m = \frac{4qa}{\pi^2 m^2} \left[(\nu-1)A_m \ SINH \ \lambda_m + (\nu+1)B_m \ SINH \ \lambda_m \right.$$

$$\left. + (\nu-1)B_m \lambda_m COSH \ \lambda_m \right] \varepsilon \ SIN \ \varnothing \tag{34}$$

With this, the solution for the deflection surface
of the plate panel subjected to both lateral and tilt loadings
separately is complete.

It should be noted at this point that when the two
deflections are combined by the principle of superposition,
a different form of the equation for the shear pressure at
the plate edge would arise. This is to say that the loading
by the tilt moment would give rise to its own shear pressure
and a separate moment load on the plate. This increment in
the shear pressure has been analyzed and shown to be second
order. The analysis is shown in detail in Appendix C. For
the purpose of this investigation, the second order terms
are disregarded.

The stresses induced in the plate subjected to web
tilt loading may be evaluated in the same manner as before,
by use of equations (17) and (18).

Differentiating (24), and substituting into (17) and (18) gives

$$\sigma_{x_2} = \frac{3}{h^2} \sum_{m=1,3,\ldots}^{\infty} E_m \left[\frac{(\rho(\nu-1)+2\nu)}{R_1} \text{COSH} \frac{m\pi y}{a} + \frac{m\pi y(\nu-1)}{aR_1} \text{SINH} \frac{m\pi y}{a} \right.$$

$$+ \frac{(\gamma(\nu-1)+2\nu)}{R_2} \text{SINH} \frac{m\pi y}{a} + \frac{m\pi y(\nu-1)}{aR_2} \text{COSH} \frac{m\pi y}{a} \left. \right] \text{SIN} \frac{m\pi x}{a}$$

(35)

$$\sigma_{y_2} = \frac{3}{h^2} \sum_{m=1,3,\ldots}^{\infty} E_m \left[\frac{(\rho(1-\nu)+2)}{R_1} \text{COSH} \frac{m\pi y}{a} + \frac{m\pi y(1-\nu)}{aR_1} \text{SINH} \frac{m\pi y}{a} \right.$$

$$+ \frac{(\gamma(1-\nu)+2)}{R_2} \text{SINH} \frac{m\pi y}{a} + \frac{m\pi y(1-\nu)}{aR_2} \text{COSH} \frac{m\pi y}{a} \left. \right] \text{SIN} \frac{m\pi x}{a}$$

(36)

According the the principle of superposition, the stresses obtained for the two separate cases may be added directly to give the total stress in the plate panel subjected to both the lateral load and the tilt load arising from a single tilted frame.

The total plate stresses are

$$\sigma_x = \sigma_{x_1} + \sigma_{x_2} \tag{37}$$

$$\sigma_y = \sigma_{y_1} + \sigma_{y_2} \tag{38}$$

and the stress magnification factor arising from the tilted
frame may be readily obtained as well.

$$F_x = \sigma_x / \sigma_{x_1} \qquad (39)$$

$$F_Y = \sigma_y / \sigma_{Y_1} \qquad (40)$$

The procedure shown thus far will determine the
magnitude of the effect of web tilt for each of the two ap-
proximations of plate restraint which have been proposed.
A computer program has been devised which will allow the
infinite series terms involved in the solution to be evalu-
ated out to vanishingly small terms. This program is pre-
sented in Appendix D.

Selection of Input Data

Having obtained an analytical solution for the effect
of web tilt loading on plate bending stresses, some numeri-
cal examples must be obtained for examination.

In order to obtain a set of representative input
data, the design path described by St. Denis [10] was fol-
lowed through a single cycle. Three values of ship length,
transverse frame spacing, and longitudinal frame spacing
were selected as typical values, and a design made for each
of the twenty-seven possible combinations. The assumed

initial values are shown in Table I.

Length	Transverse Spacing	Longitudinal Spacing
300	72	24
500	84	30
700	96	36

Table I. Initial Input Data

The value of the primary hull girder stress was assumed to be given by the relationship

$$\sigma_1 = 2240^3/L \tag{41}$$

then, following the procedure outlined in [10], stress schedules were set up for each case to give allowable values of the plate bending stress (σ_3). With this, the plate thickness required was obtained by using the maximum value given by the equations shown below.

1. plates in pure bending

$$t = \frac{b}{12}\sqrt{\frac{0.685\rho_o H}{2\ \sigma_3}} \tag{42}$$

2. stability of plates in compression

$$t = \frac{b}{\pi} \sqrt{\frac{12(1-\nu^2)\sigma_1}{4E}} \qquad (43)$$

The plate thus selected in each case was then checked to insure that a factor of safety of 1.25 was provided on the ultimate strength after buckling.

With the plating thus selected, the scantlings of the longitudinal stiffeners were selected by setting a limiting value of the slenderness ratio (L/k) for each span, viz.,

$$(L/k) \leq 30 \qquad (44)$$

The bending moment in each stiffener was approximated by means of the relationship

$$M = \frac{WL}{12} = \frac{\rho_o HbL^2}{12} \qquad (45)$$

where, in all cases in this thesis, the draft of the ship was held constant at thirty feet.

The required section modulus of the combined beam and plate was obtained by the relationship

$$\frac{I}{C} \text{ (required)} = \frac{M}{\sigma_2} \qquad (46)$$

where

$$\sigma_2 = (\sigma_{Y_s} / 1.25) - \sigma_1 \qquad (47)$$

Actual selection of the stiffener sections was ac-
complished by the use of references [6] and [11]. Medium
steel construction was assumed throughout.

A complete tabulation of the results of this first
design spiral is given in Table II. While it is acknowledged
that these scantlings are not likely to be appropriate for
specific ships of the assumed initial dimensions due to con-
siderations of overall section modulus, it is felt that the
values obtained in this limited analysis represent a minimum
design condition, and are thus appropriate for use in the
analysis for the effect of web tilt.

In order to provide a more orderly form for data pre-
sentation, the input data shown in Table II have been pre-
sented in non-dimensional form in Table III.

Since the most critical factor affecting the magni-
tude of the tilt moment can easily be seen to be the distance
from the toe to the flexural center (c), the input data,
(a/b) ratios, are shown plotted against the ratio (c/t) in
Figure V.

L	a	b	h	I_b	I_o	ϵ	Item	Case
300	72	24	0.375	78.0	11.4	5.78	6x6.5x13.5 T	1
300	72	30	0.5	117.7	15.3	5.85	6x6.5x18 T	2
300	72	36	0.5625	151.7	21.1	6.72	7x6.75x17 T	3
300	84	24	0.375	107.6	19.0	6.74	7x6.75x15 T	4
300	84	30	0.5	187.6	30.7	7.72	8x7x18 T	5
300	84	36	0.5625	198.7	30.7	7.72	8x7x18 T	6
300	96	24	0.375	158.1	30.7	7.72	8x7x18 T	7
300	96	30	0.5	228.6	37.8	7.78	8x7x22.5 T	8
300	96	36	0.5625	324.8	42.2	8.72	9x7.5x25 T	9
500	72	24	0.4375	96.1	13.0	5.82	6x6.5x15.5 T	10
500	72	30	0.5625	102.9	21.1	6.77	7x6.75x17 T	11
500	72	36	0.6875	216.2	30.7	7.72	8x7x18 T	12
500	84	24	0.4375	133.3	21.1	6.77	7x6.75x17 T	13
500	84	30	0.5625	198.7	30.7	7.72	8x7x18 T	14
500	84	36	0.6875	296.4	42.2	7.78	8x7x25 T	15
500	96	24	0.4375	174.4	30.7	7.72	8x7x18 T	16
500	96	30	0.5625	268.2	42.2	7.78	8x7x25 T	17
500	96	36	0.6975	391.1	59.6	8.75	9x7.5x27.5 T	18
700	72	24	0.5	125.8	19.0	6.74	7x6.75x15 T	19
700	72	30	0.625	176.3	23.5	6.8	7x6.75x19 T	20
700	72	36	0.75	249.9	33.2	7.75	8x7x20 T	21
700	84	24	0.5	187.6	30.7	7.72	8x7x18 T	22
700	84	30	0.625	256.3	37.8	7.78	8x7x22.5 T	23
700	84	36	0.75	342.0	43.6	7.61	8x8.5x29 T	24
700	96	24	0.5	228.6	37.8	7.78	8x7x22.5 T	25
700	96	30	0.625	342.5	42.2	8.72	9x7.5x25 T	26
700	96	36	0.75	441.6	64.8	8.78	9x7.5x30 T	27

Table II. Table of Panel Scantlings

INPUT DATA

NOMENCLATURE:

A: long side dimension.

B: short side dimension.

t: thickness of the plate

Io: moment of inertia of the stiffeners.

ϵ: distance from the flexural center of the stiffener to the plate edge.

L: length of the ship.

L: 300'

A/B	A/ϵ	ϵ/t	Io/Bϵ^3	A/t	Io/tϵ^3	A
2.0	10.65	12.0	$1.90*10^{-3}$	128	$12.1*10^{-2}$	72"
2.33	12.40	13.7	1.86	149	11.8	84
2.4	12.40	11.7	2.55	144	15.3	72
2.66	11.00	15.5	1.80	170	11.3	96
2.8	10.90	15.4	2.24	168	13.4	84
3.0	12.45	15.4	2.46	193	15.8	72
3.2	12.35	15.6	2.67	192	16.0	96
3.5	12.45	18.0	2.59	224	16.5	84
4.0	12.45	20.6	2.79	256	17.8	96

Table III. Non-dimensional Input Data

INPUT DATA

L: 500'

A/B	A/ε	ε/t	$Io/B\epsilon^3$	A/t	$Io/t\epsilon^3$	A
2.0	9.40	11.2	$1.86*10^{-3}$	105	$9.8*10^{-2}$	72"
2.33	10.80	11.3	2.48	122	13.0	84
2.4	10.65	12.0	2.28	128	12.1	72
2.66	10.95	12.7	2.46	139	12.8	96
2.8	10.90	13.7	2.23	149	12.0	84
3.0	12.40	13.3	2.75	164	15.1	72
3.2	12.35	13.8	2.96	171	15.7	96
3.5	12.40	15.5	2.83	192	15.5	84
4.0	12.45	17.6	2.80	220	15.3	96

L: 700'

A/B	A/ε	ε/t	$Io/B\epsilon^3$	A/t	$Io/t\epsilon^3$	A
2.0	9.3	10.3	$1.97*10^{-3}$	96	$9.6*10^{-2}$	72"
2.33	11.0	10.2	2.70	112	13.2	84
2.4	10.6	10.9	2.48	115	11.0	72
2.66	10.9	11.7	2.66	128	12.7	96
2.8	10.8	12.4	2.68	134	12.8	84
3.0	10.7	13.5	2.60	144	12.4	72
3.2	11.0	14.0	2.12	153	10.3	96
3.5	10.9	15.4	2.80	168	13.4	84
4.0	12.3	15.6	3.34	192	16.0	96
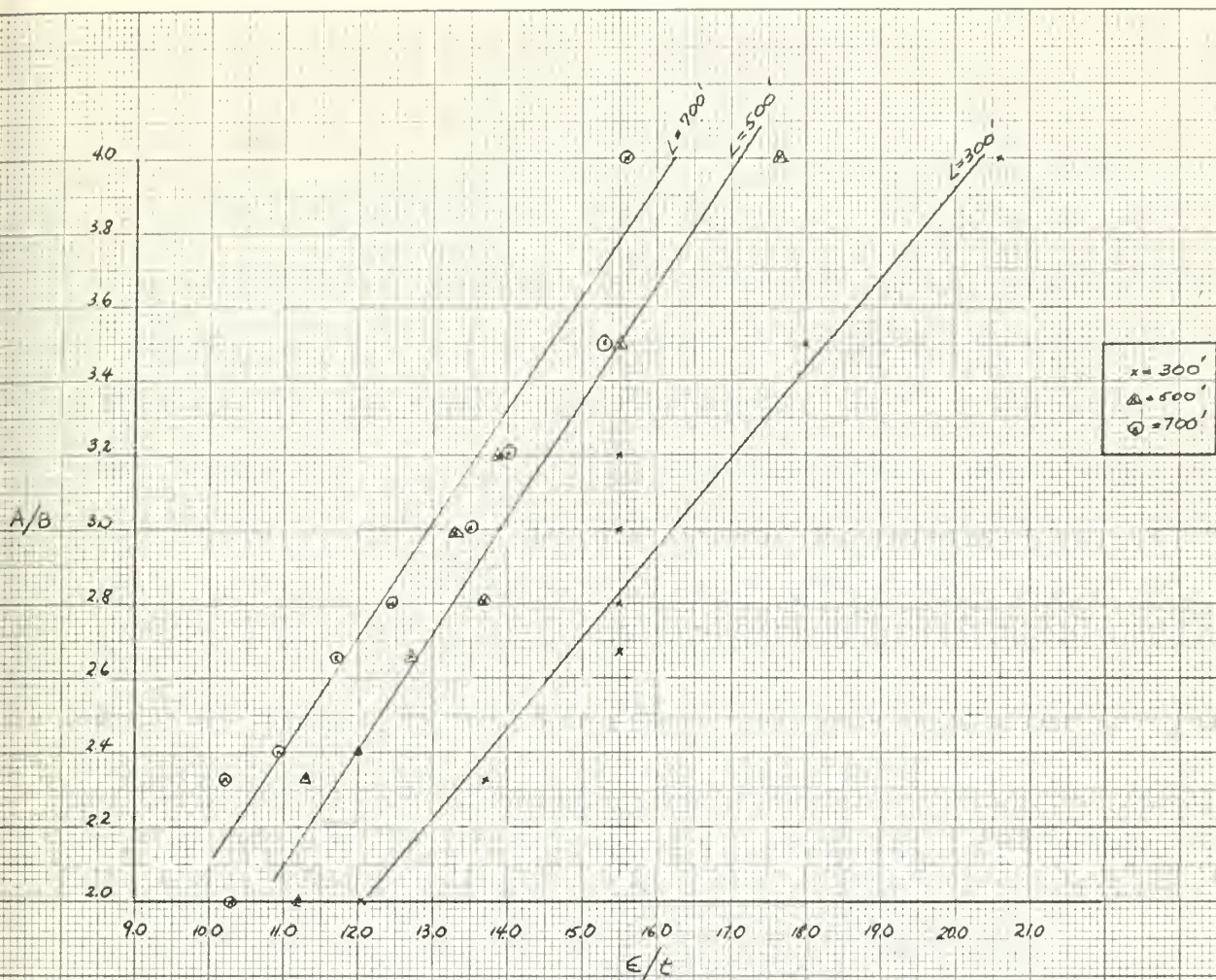
Table III. Non-dimensional Input Data

Figure V. Input data, depth ratio
(ϵ/t) vs. aspect ratio (a/b)

IV. RESULTS

The computer programs, Appendix D, were written to evaluate each of the infinite series presented as solutions for the plate stresses in Chapter III out to its tenth term. This extent was considered necessary to insure accuracy in the computation of the plate stresses, since the series representing the moments in the plate converge less rapidly than do those for deflection (i.e., as $1/m^3$ instead of as $1/m^5$).

Figures VI and VII are plots of the results obtained for the stresses, in the y direction only, using the simple support approximation. Figures VIII and IX show the same results obtained by use of the clamped approximation. These figures show only the results for case 1. As the general shape of the resultant curve was identical for all cases, differing only in magnitude, presentation of each case in this manner was considered superfluous.

Figures X through XV present a comparison of the actual tilt stresses obtained for each of the lateral load support approximations used. Again, only selected cases have been presented, but these are representative of the form obtained in each case examined.

Figures XVI through XXIII are plots of the results of all cases examined, both for the simple support and clamped approximations. These plots present the tilt stress

obtained, shown as a percentage of the lateral load stress,
versus the characteristic plate parameters in a non-
dimensional form, i.e., the depth ratio (c/t) and the aspect
ratio (a/b). These are shown for three different angles
of initial web tilt: three, five, and seven degrees.

In all cases shown in Figures XVI through XXIII,
data from the simple support approximation has been pre-
sented at the center of the plate panel ($x=a/2$, $y=0$) and
data from the clamped approximation has been shown at the
edge of the plate panel ($x=a/2$, $y=b/2$).

Tabulations of the data used to plot the figures
are presented concurrently in Tables IV through XIII.

Figure VI. Sample stress pattern,

σ_y stress along x=A/2 axis, Case 1.

Simple support approximation.

STRESS ALONG X = A/2 AXIS
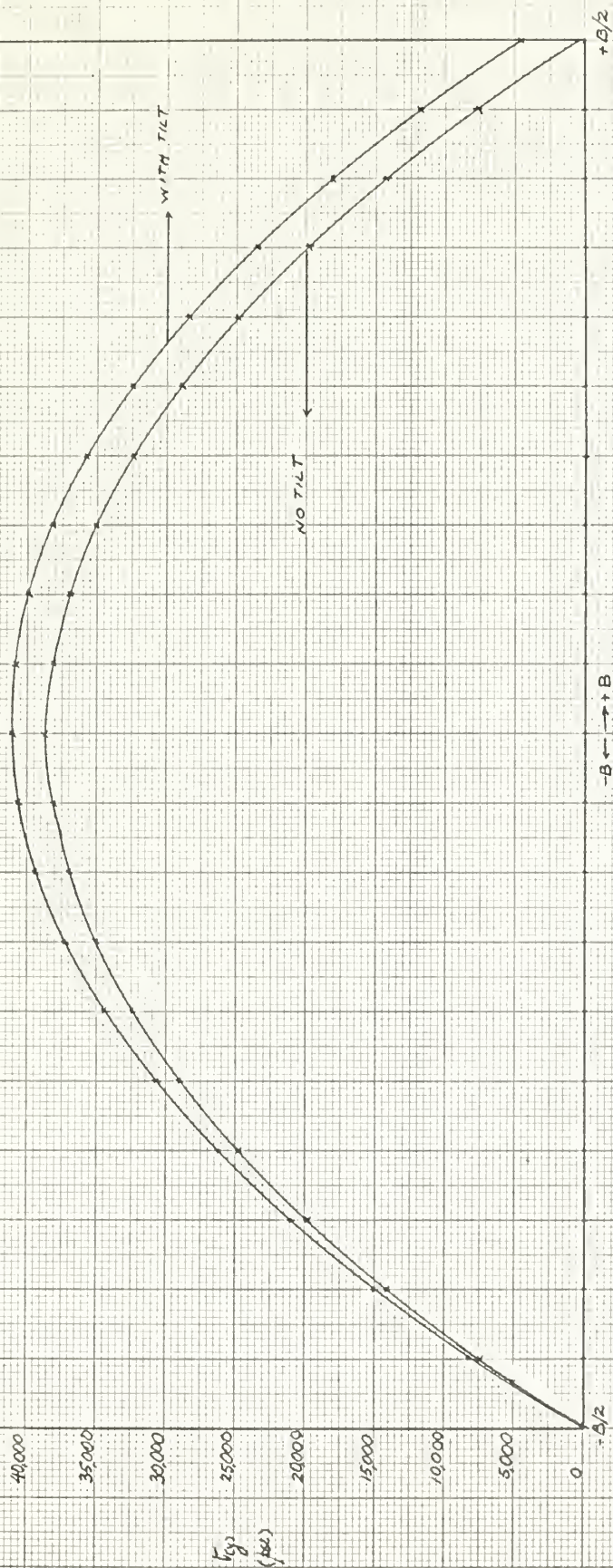
CASE / S.S. (φ=7°)

L = 300'
A = 72"
B = 24"
H = .375"
I = 11.4 in⁴
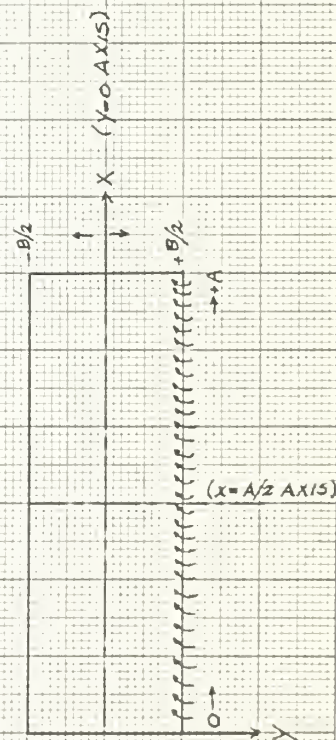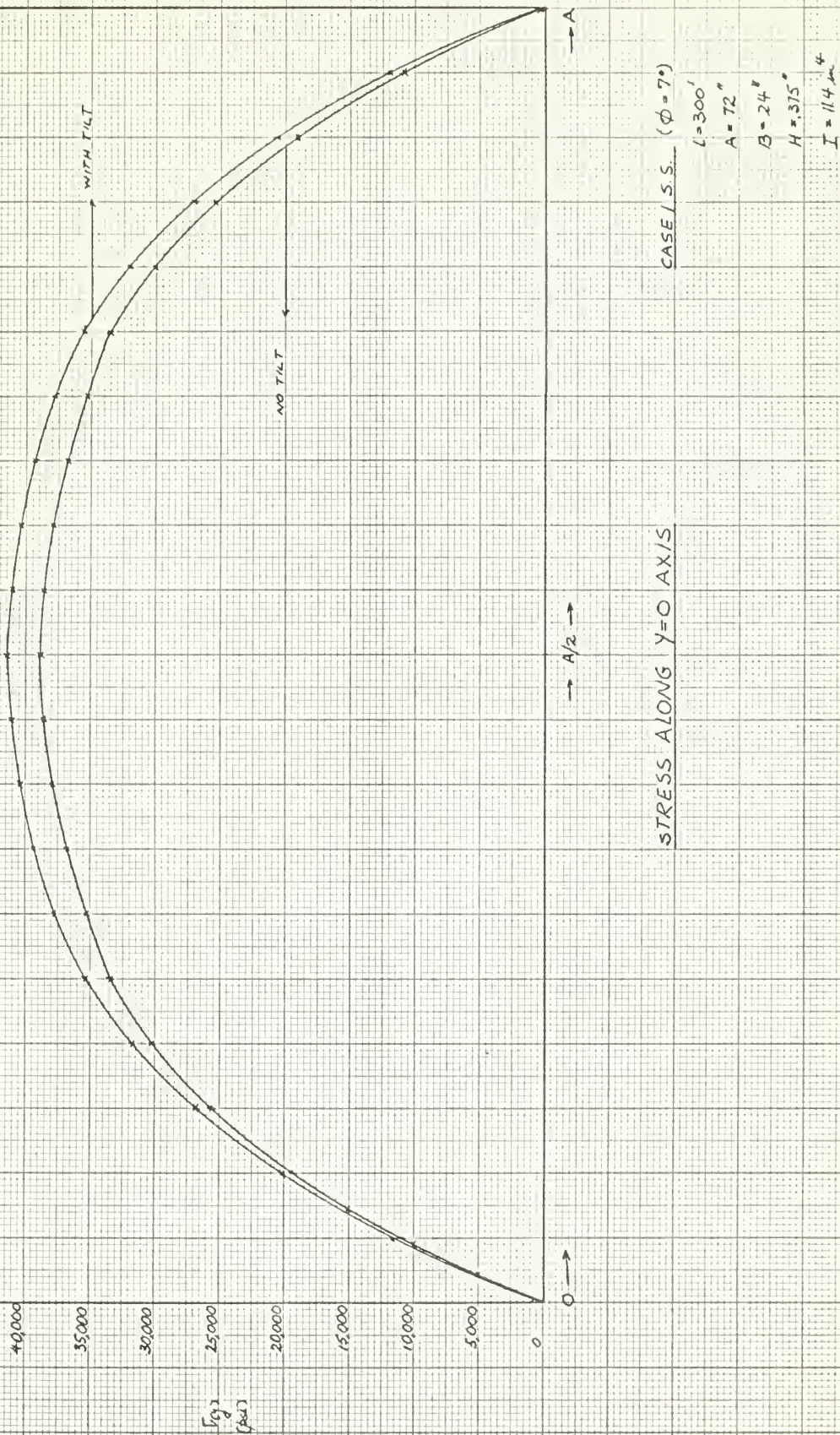
Figure VII. Sample stress pattern, σ_y stress along y=0 axis, case 1, simple support approximation
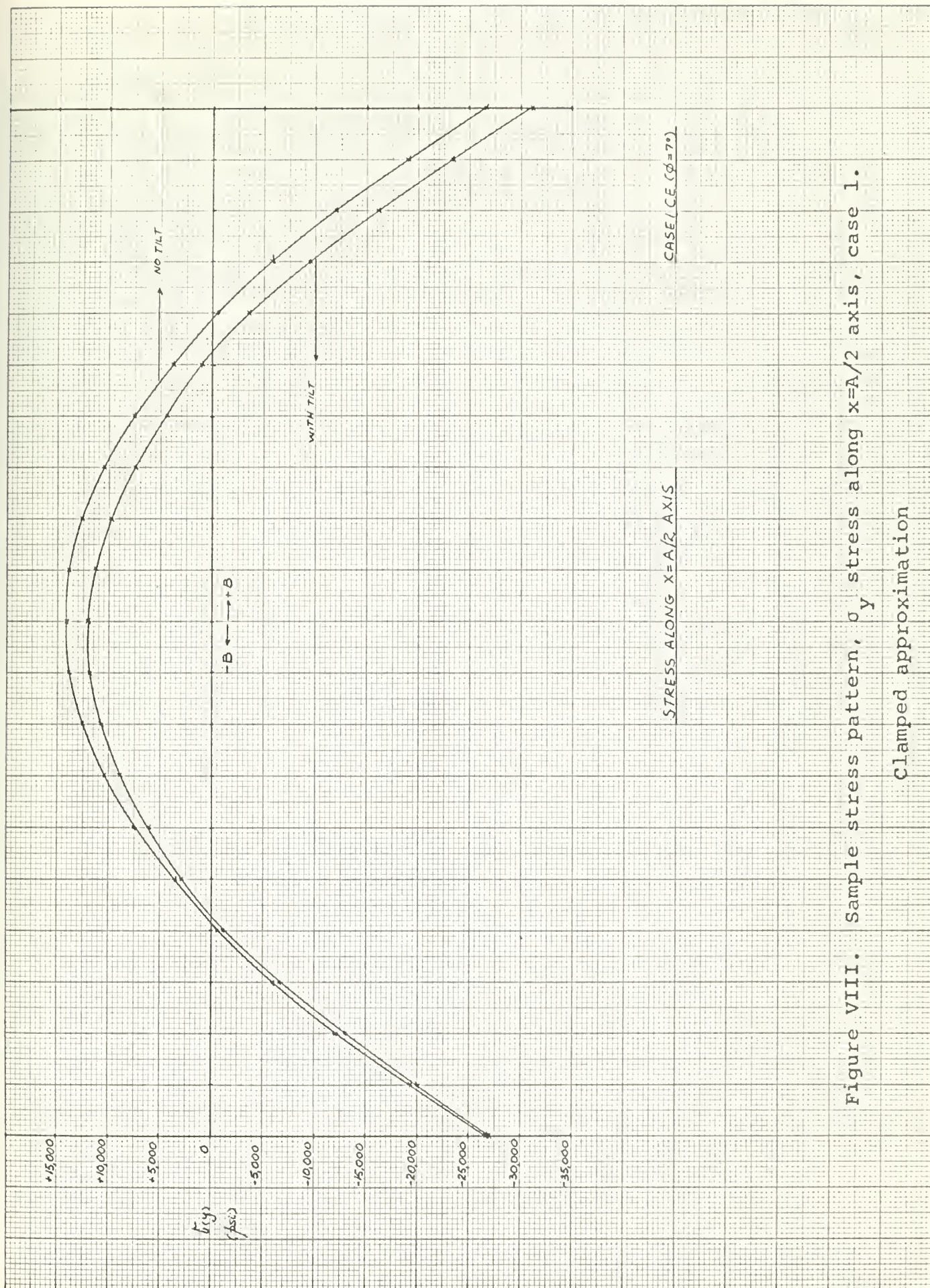
Figure VIII. Sample stress pattern, σ_y stress along x=A/2 axis, case 1.

Clamped approximation
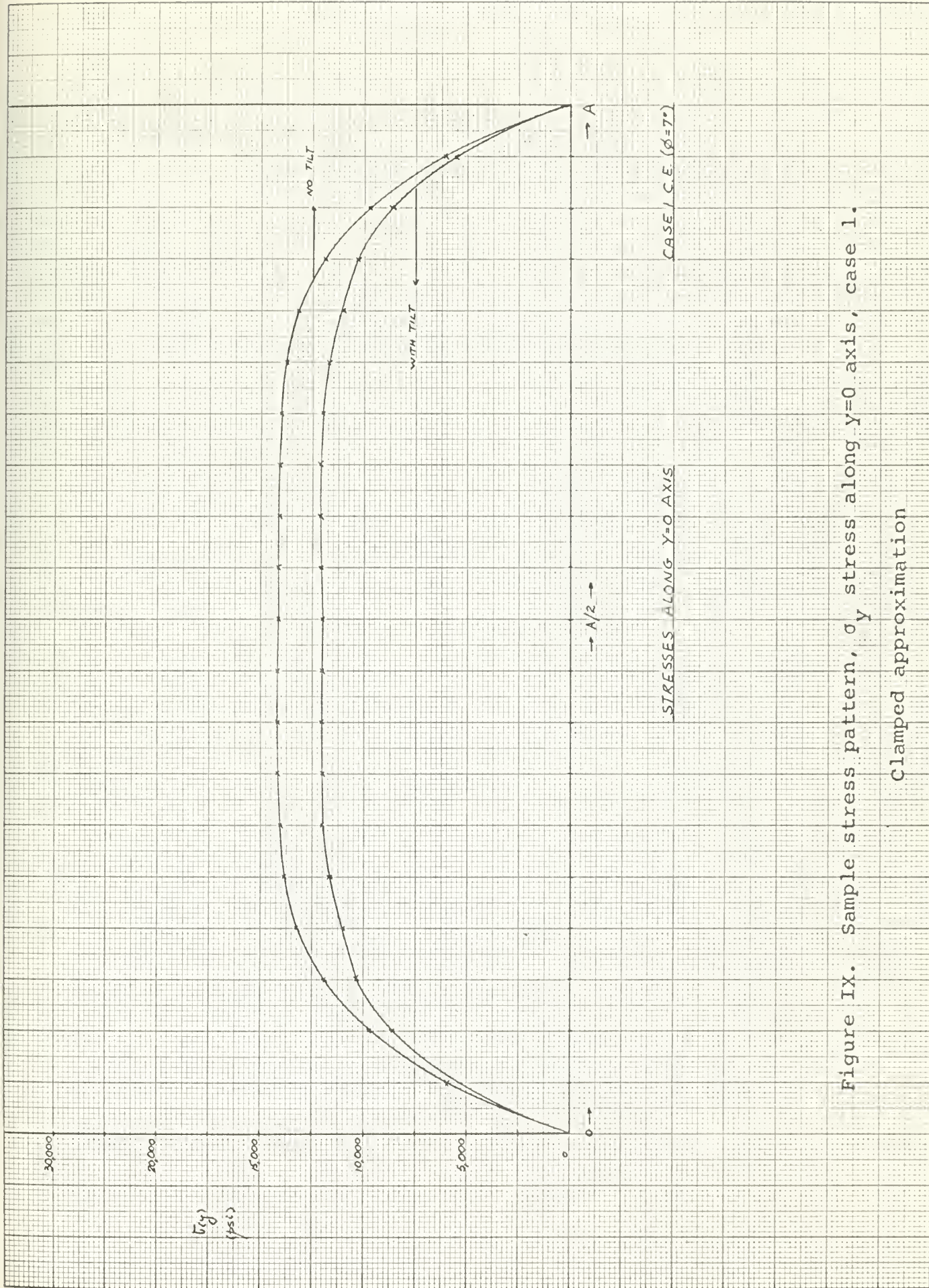
Figure IX. Sample stress pattern, σ_y stress along y=0 axis, case 1.

Clamped approximation

-39-

	3° tilt		5° tilt		7° tilt	
	S.S.	C.E.	S.S.	C.E.	S.S.	C.E.
-B/2	131.4psi.	128.0psi.	218.8psi.	213.1psi.	306.0psi.	298.0psi.
	211.6	209.6	352.4	350.4	492.6	490.5
	290.4	292.9	483.6	487.7	676.3	682.0
	369.4	374.2	615.2	623.1	860.2	871.3
	449.0	455.9	747.8	759.2	1045.6	1061.6
	529.7	538.5	882.1	895.4	1233.3	1253.9
	611.5	622.9	1018.3	1035.9	1424.0	1448.5
	694.8	706.8	1157.1	1177.0	1618.5	1645.9
	779.7	793.0	1298.5	1320.6	1815.6	1846.1
	866.4	880.5	1442.9	1466.4	2017.4	2050.4
0	955.0	969.4	1590.4	1614.7	2223.8	2257.8
	1045.6	1060.3	1741.3	1765.6	2434.8	2468.9
	1138.3	1152.5	1895.6	1919.2	2650.6	2683.6
	1232.9	1246.0	2053.3	2075.0	2871.1	2901.6
	1328.7	1341.1	2214.2	2233.3	3086.3	3122.2
	1422.8	1437.3	2378.3	2387.1	3380.8	3346.7
	1528.3	1534.4	2545.5	2555.1	3558.9	3572.9
	1630.1	1612.3	2714.5	2698.2	3795.6	3780.9
	1732.7	1730.2	3104.8	2881.3	4034.8	4028.9
	1835.4	1827.0	3056.3	3042.5	4273.9	4254.2
+B/2	1935.2	1918.3	3222.6	3194.6	4506.3	4467.0

Table IV. Comparison of tilt stresses for Case 1.
Clamped and simple support approximations.
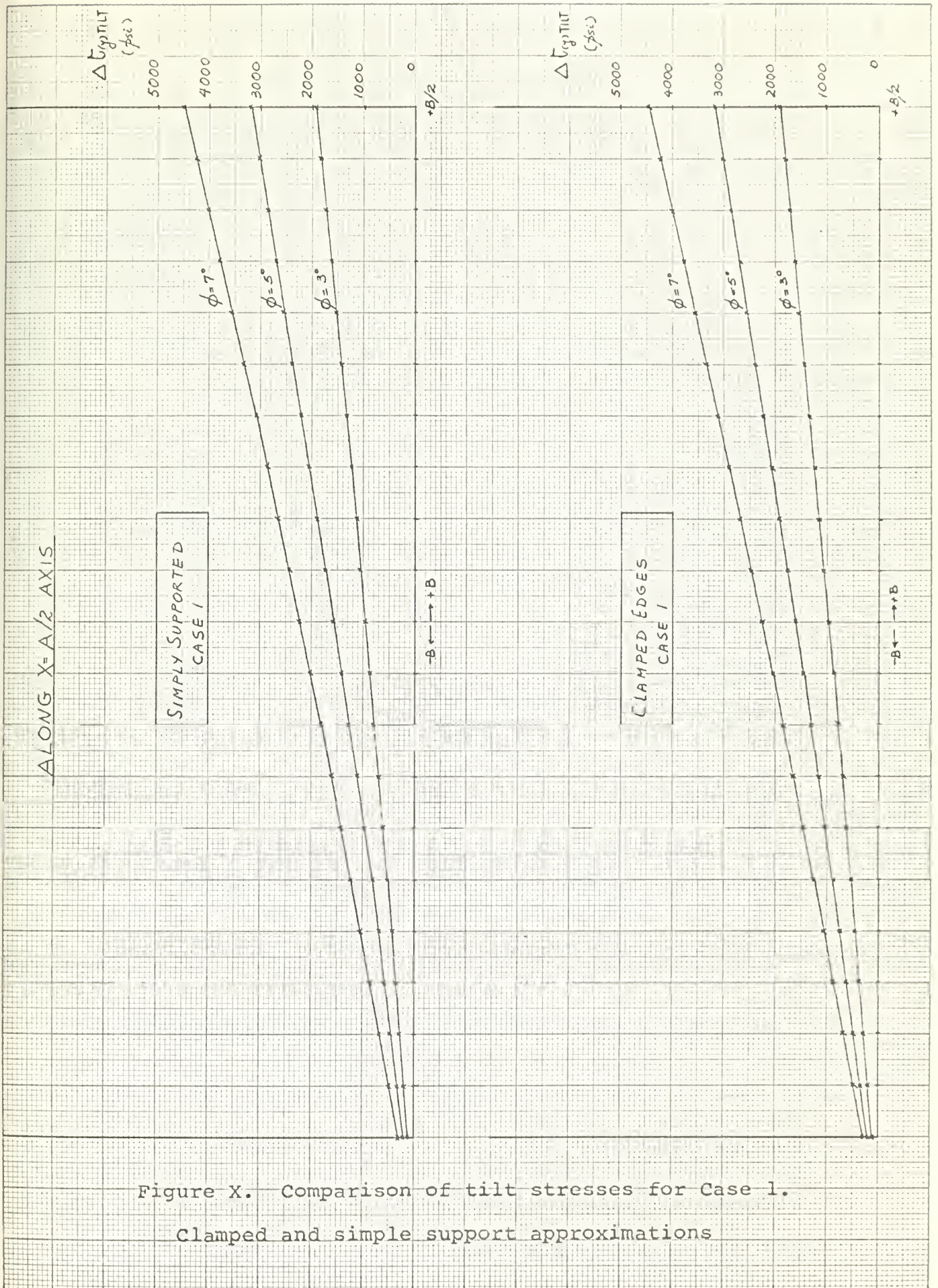
Figure X. Comparison of tilt stresses for Case 1. Clamped and simple support approximations

	Case 5		Case 10	
	S.S.	C.E.	S.S.	C.E.
3°				
-B/2	124.1psi.	120.6psi.	96.5psi.	93.9psi.
0	873.1	891.3	704.7	715.4
+B/2	1818.7	1804.5	1429.5	1416.9
5°				
-B/2	206.7	200.7	160.7	156.5
0	1453.8	1484.0	1173.6	1191.4
+B/2	3028.8	3004.0	2380.6	2359.4
7°				
-B/2	289.1	280.7	224.7	218.8
0	2032.9	2075.6	1641.0	1665.8
+B/2	4235.1	4201.8	3328.8	3299.3

Table V. Comparison of tilt stresses for random cases.

Clamped and simple support approximations

-42-

	Case 15		Case 22		Case 27	
	S.S.	C.E.	S.S.	C.E.	S.S.	C.E.
3°						
-B/2	79.9psi.	77.2psi.	97.6psi.	95.4psi.	74.5psi.	72.2psi.
0	502.8	523.1	746.2	750.7	1009.5	1091.8
+B/2	1157.0	1157.0	1449.7	1437.9	515.8	518.7
5°						
-B/2	133.1	128.5	162.5	159.0	124.2	120.1
0	837.4	871.2	1243.0	1250.2	859.0	880.6
+B/2	1926.7	1926.9	2414.2	2394.8	1831.1	1818.1
7°						
-B/2	186.0	179.6	227.3	222.5	173.6	168.0
0	1171.0	1218.1	1737.7	1748.2	1201.2	1231.3
+B/2	2694.2	2694.4	3375.7	3348.7	2560.4	2542.3

Table V. Comparison of tilt stresses for random cases.

Clamped and simple support approximations
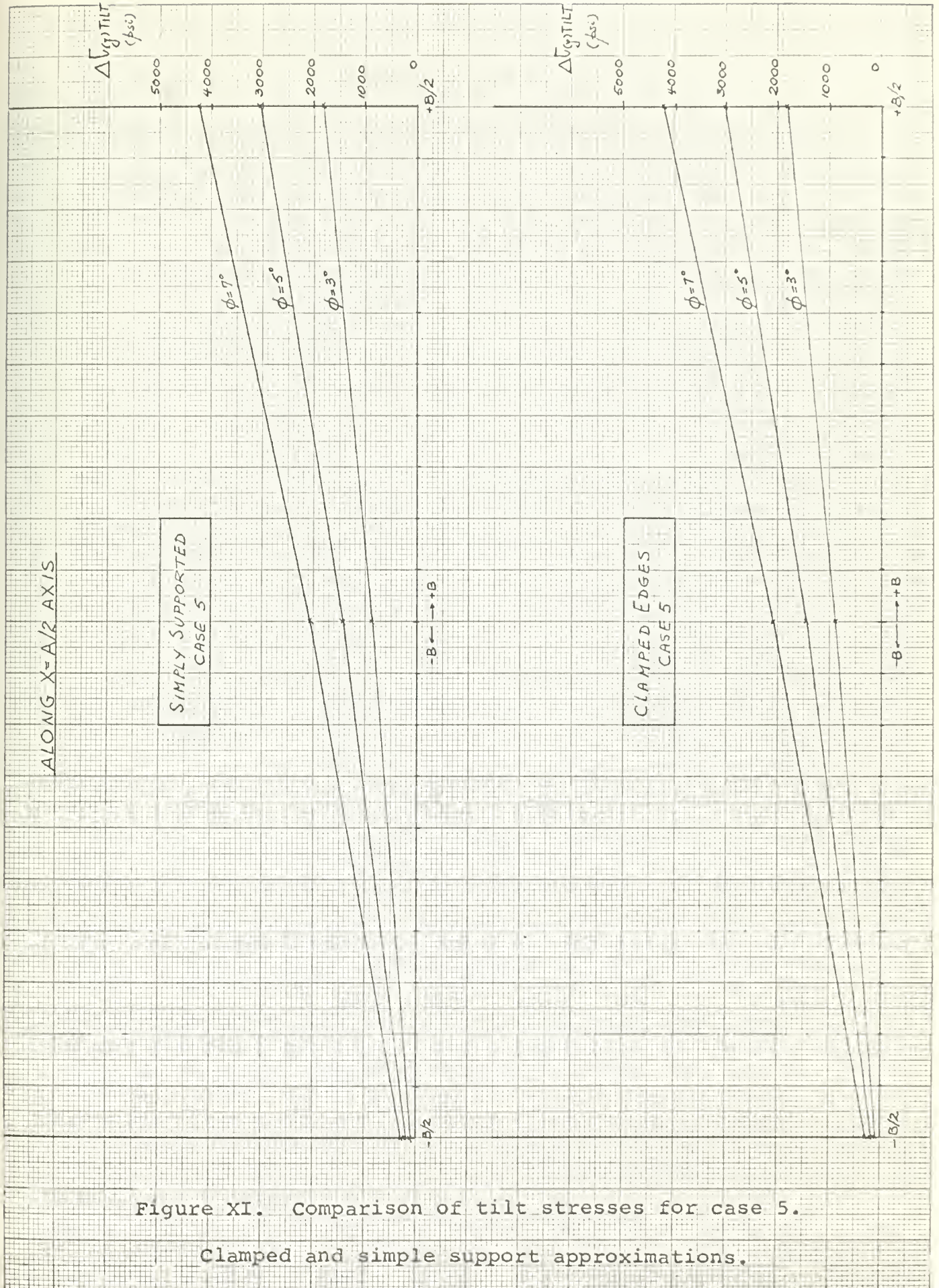
Figure XI. Comparison of tilt stresses for case 5.
Clamped and simple support approximations.
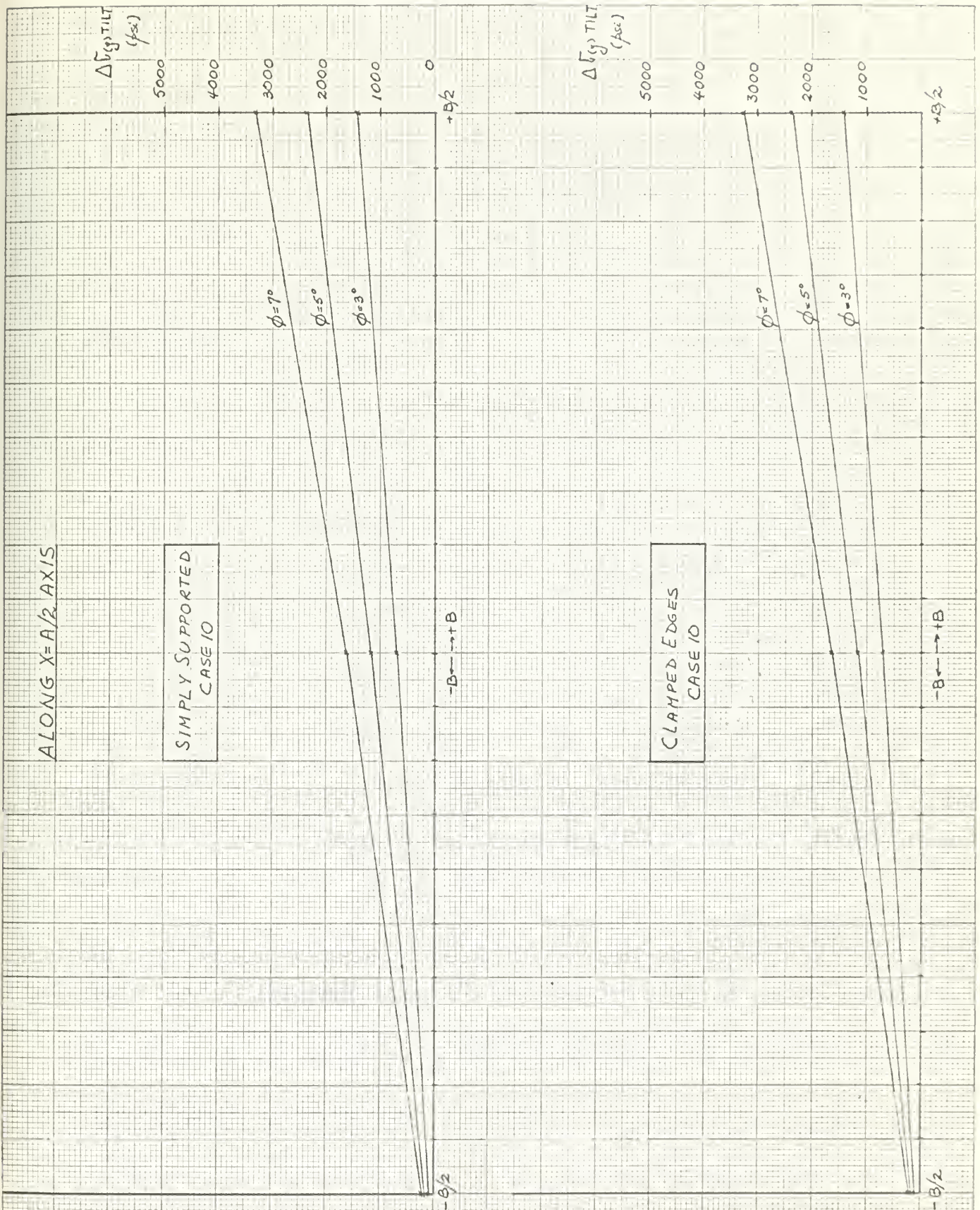
Figure XII. Comparison of tilt stresses for case 10.

Clamped and simple supported approximations
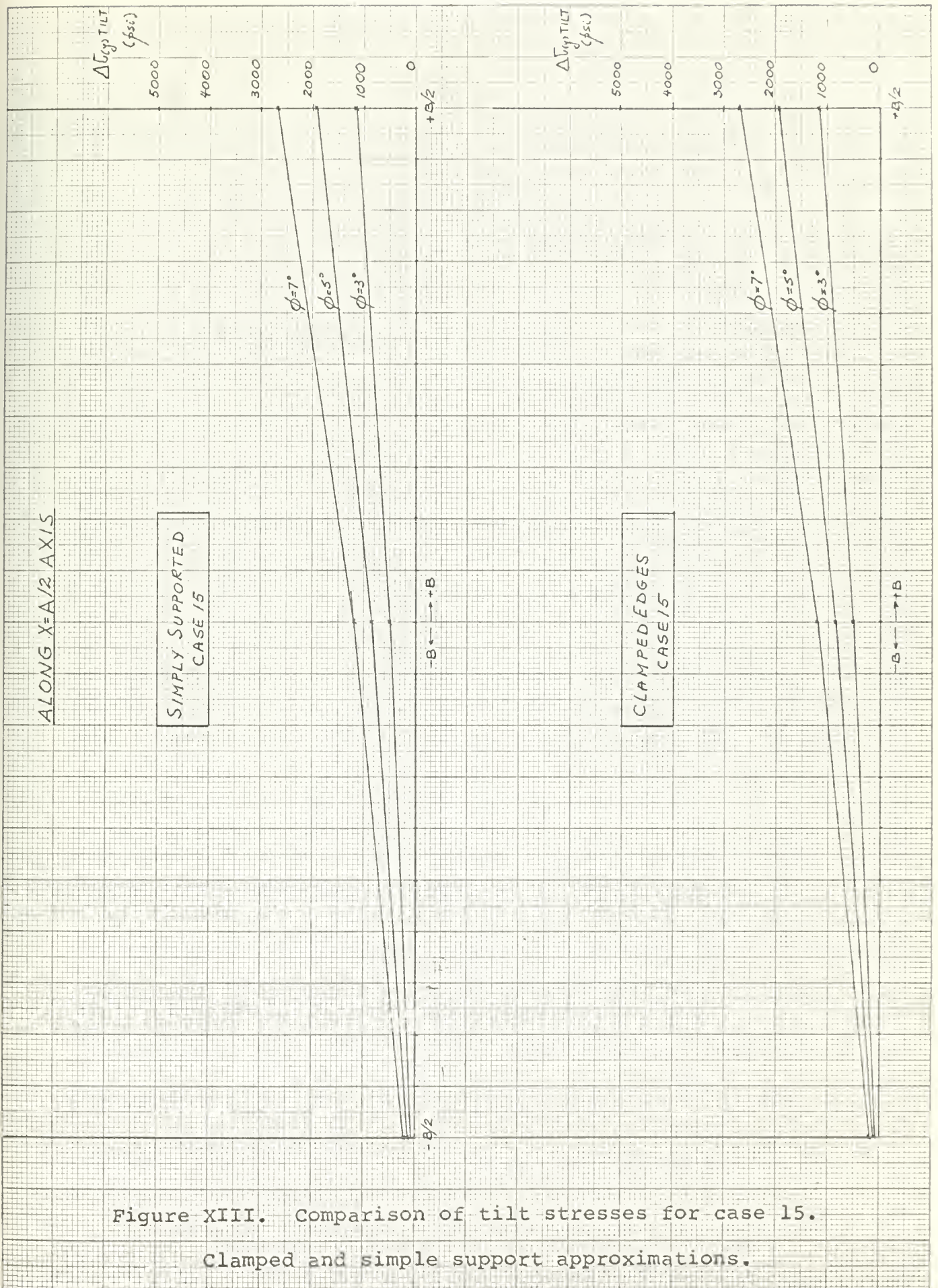
Figure XIII. Comparison of tilt stresses for case 15.
Clamped and simple support approximations.
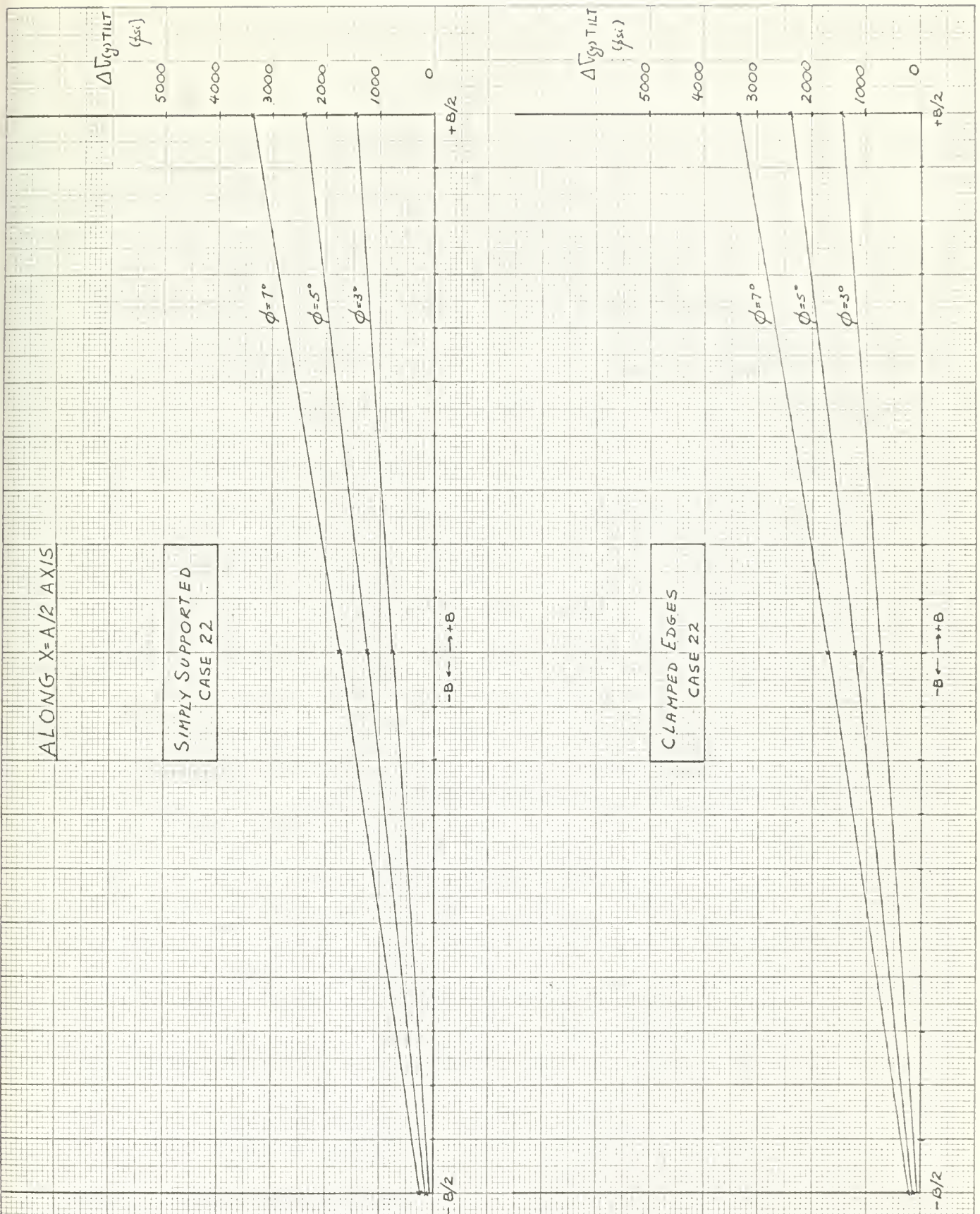
Figure XIV. Comparison of tilt stresses for case 22.
Clamped and simple support approximations.
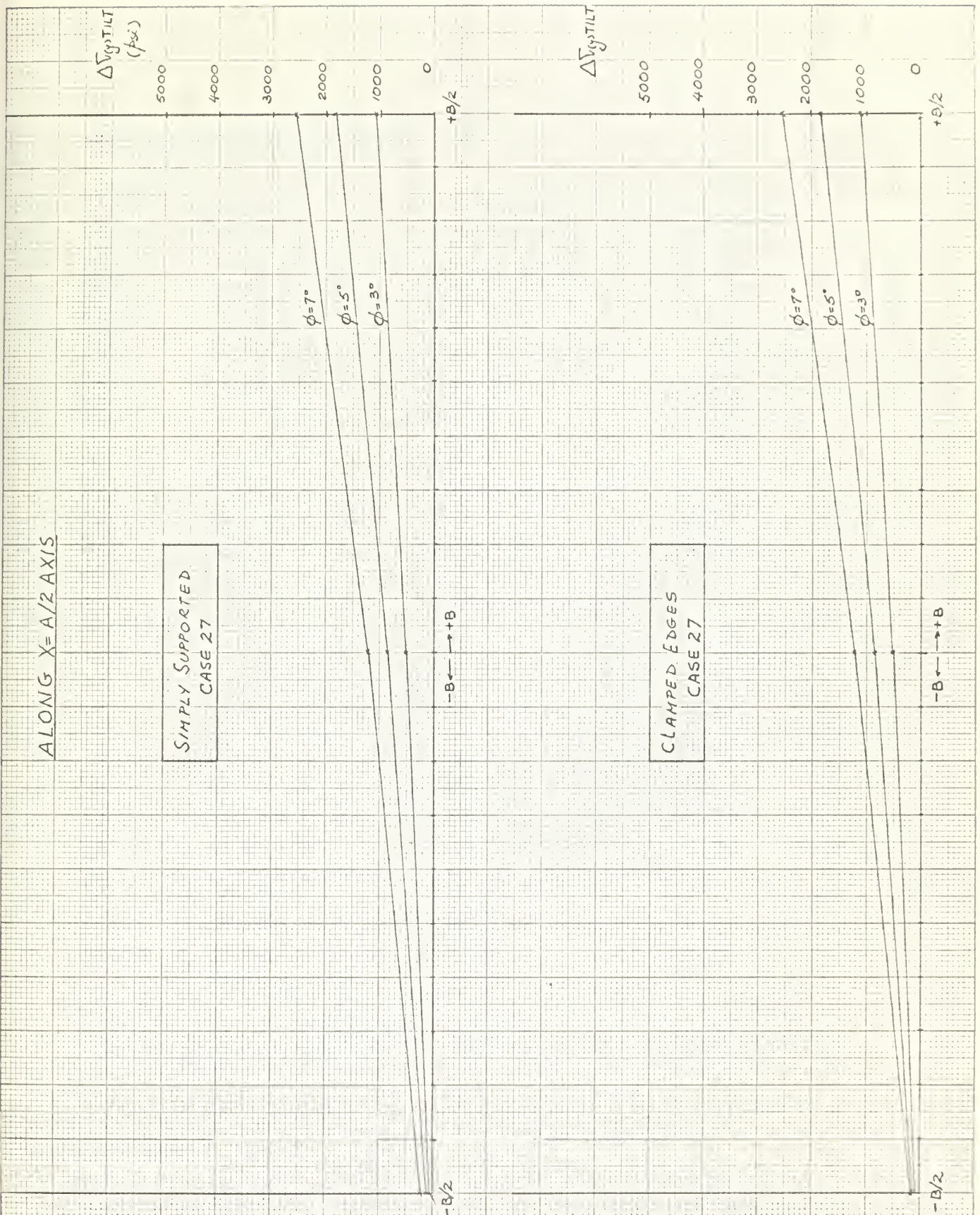
Figure XV. Comparison of tilt stresses for case 27.
Clamped and simple support approximations.

SIMPLY SUPPORTED CASE ($\emptyset = 7^{\circ}$)

L: 300'

ε/t	σ_y no tilt*	σ_y tilted	% increase
11.7	31,863.3psi.	33,278.2psi.	4.44
12.05	33,115.8	34,459.0	4.07
13.70	35,865.9	37,605.3	4.85
15.40	33,585.9	35,618.7	6.05
15.40	38,846.9	41,070.8	5.72
15.50	37,671.6	39,799.3	5.65
15.6	34,572.3	36,718.3	6.20
18.0	39,878.9	42,579.5	6.77
20.6	40,297.4	43,453.3	7.83

L: 500'

ε/t	σ_y no tilt	σ_y tilted	% increase
11.2	22,134.7psi.	25,145.5psi.	4.60
11.3	23,975.5	25,145.5	4.88
12.0	25,171.8	26,465.2	5.14
12.7	25,194.3	26,621.0	5.66
13.3	28,513.6	30,154.6	5.76
13.7	26,507.5	30,154.6	6.04
15.5	29,280.3	31,270.8	6.10
17.60	29,669.4	31,985.7	7.81

* These values remain constant for all angles of tilt and are not repeated in the subsequent tables

Table VI. Lateral and tilt stresses

vs. depth ratio (ε/t), 7° tilt angle.

All cases, simple support approximation.

L: 700'

ϵ/t	σ_y no tilt	σ_y tilted	% increase
10.30	18,571.5psi.	19,429.8psi.	4.62
10.30	20,116.3	21,076.5	4.77
10.90	20,364.4	21,414.4	5.15
11.70	21,153.1	22,354.3	5.68
12.45	21,462.0	22,769.0	6.09
13.50	21,829.2	23,283.9	6.67
14.00	22,090.3	23,624.4	6.94
15.40	22,416.5	24,154.2	7.75
15.60	22,708.6	24,492.0	7.86

Table VI.   Lateral and tilt stresses
vs. depth ratio (ϵ/t), 7° tilt angle.
All cases, simple support approximation.

Figure XVI. Stress magnification vs.
depth ratio (ϵ/t), 7° tilt angle.
Simple support approximation.

Figure XVI. Stress magnification vs. depth ratio (d/f), γ° tilt angle. Simple support approximation.

Top graph:

L = 700'
L = 500'
L = 300'

8.0
7.0
6.0
5.0
4.0
3.0

% INCREASE IN $\bar{\sigma}_{(y)}$ CENTER

SIMPLY SUPPORTED CASE
$\phi = 7°$

9.0   11.0   13.0   15.0   17.0   19.0   21.0

ϵ/t

Bottom graph:

L = 300'
L = 500'
L = 700'

40,000
35,000
30,000
25,000
20,000
15,000

$\bar{\sigma}_{(y)}$ CENTER "NO TILT" (psi)

9.0   11.0   13.0   15.0   17.0   19.0   21.0

ϵ/t
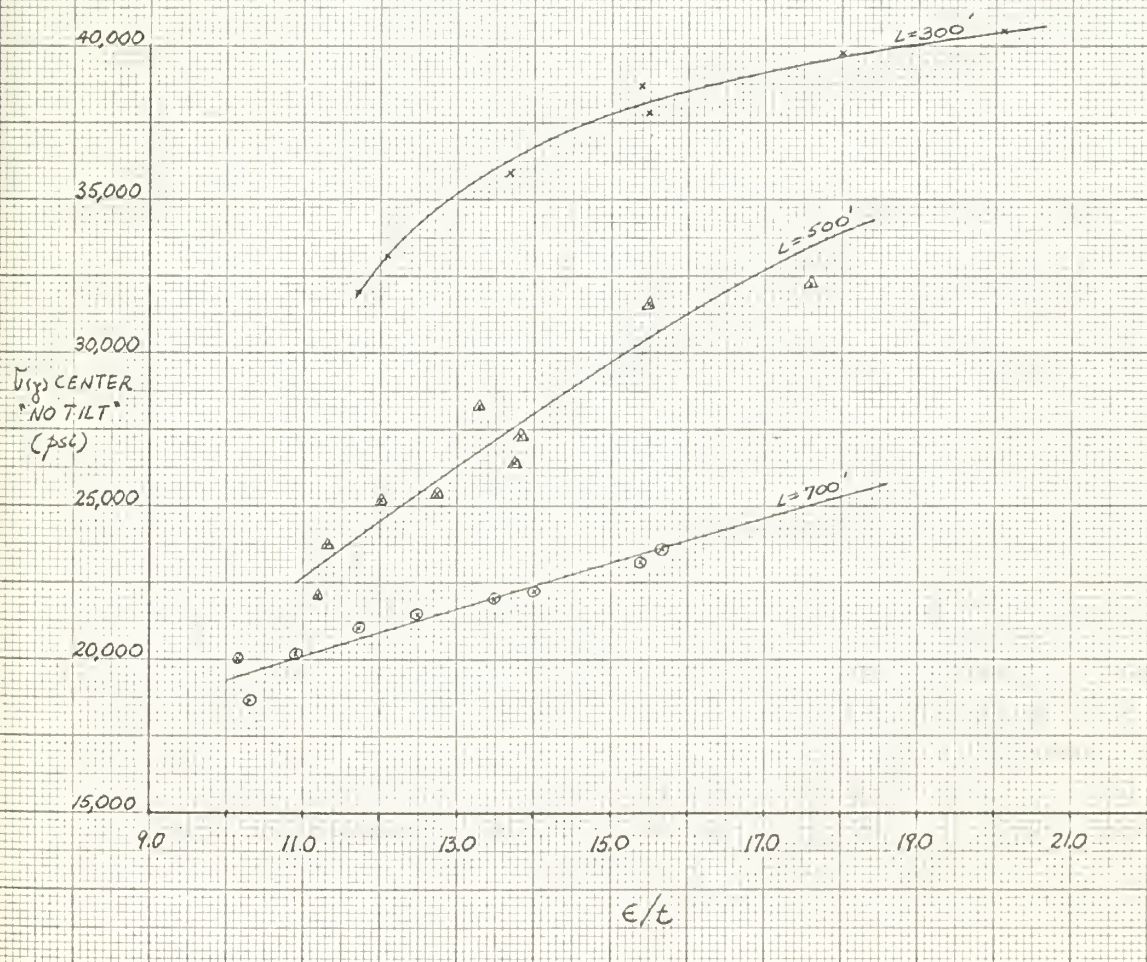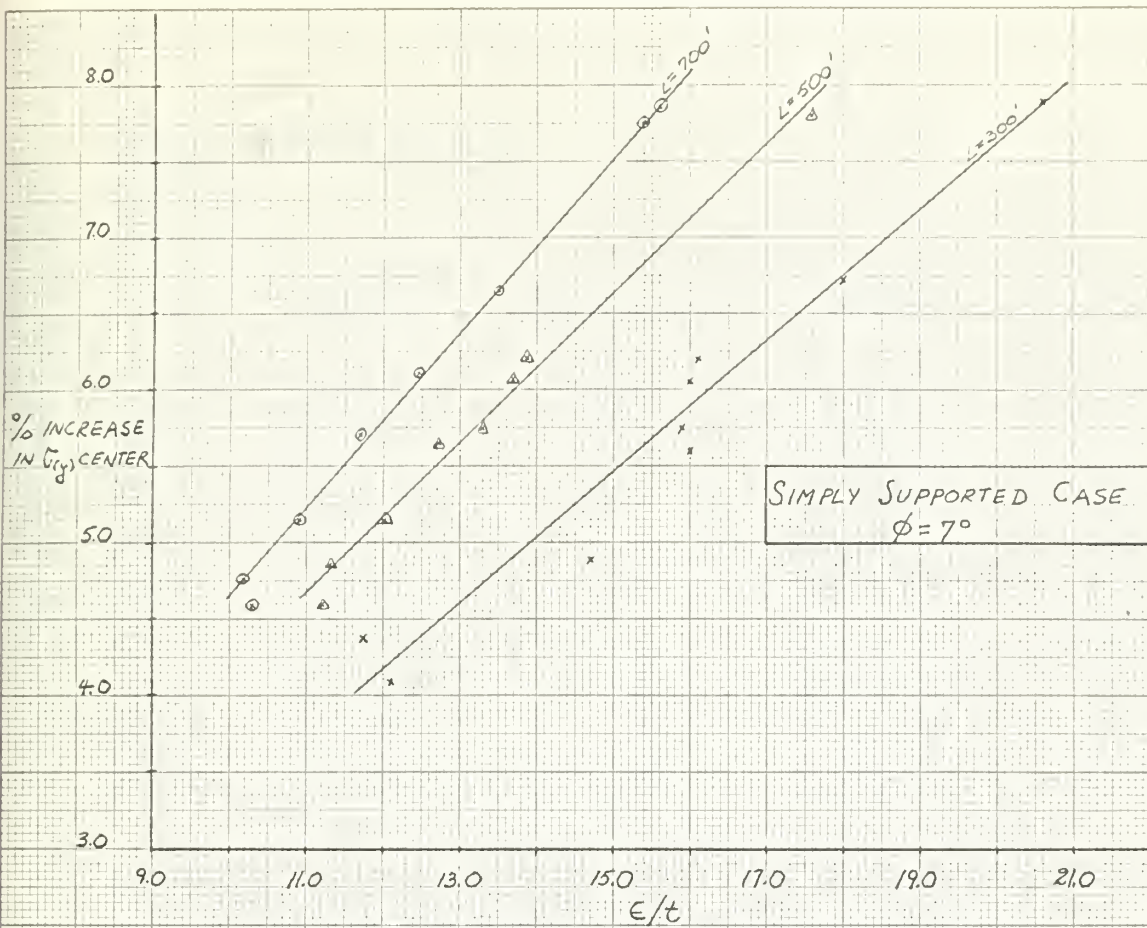
SIMPLY SUPPORTED CASE

L: 300'

ϵ/t	σ_y tilted, $(\emptyset=3^\circ)$	% increase	σ_y tilted, $(\emptyset=5^\circ)$	% increase
11.70	32,471.0	1.90	32,875.2	3.20
12.05	33,693.0	1.75	34,075.0	2.90
13.70	36,613.0	2.10	37,110.5	3.50
15.40	39,802.0	2.50	40,437.0	4.10
15.40	34,459.0	3.45	35,040.0	4.33
15.50	38,585.0	2.43	39,193.2	4.04
15.60	35,494.4	2.66	36,107.3	4.44
18.00	41,037.0	2.90	41,810.0	4.84
20.60	41,652.0	3.36	42,554.4	5.60

L: 500'

ϵ/t	σ_y tilted, $(\emptyset=3^\circ)$	% increase	σ_y tilted, $(\emptyset=5^\circ)$	% increase
11.20	22,572.0	1.98	22,864.0	3.30
11.30	24,478.4	2.10	24,813.0	3.50
12.00	25,727.2	2.21	26,096.8	3.70
12.70	25,807.2	2.43	26,214.7	4.05
13.30	29,218.0	2.47	29,687.0	4.12
13.70	27,195.8	2.60	27,653.8	4.32
13.85	28,027.0	2.70	28,509.7	4.43
15.50	31,135.1	2.92	30,703.8	4.86
17.60	30,664.0	3.35	31,325.8	5.58

Table VII. Lateral and tilt stresses vs. depth ratio (ϵ/t), 3° and 5° tilt angle. Simply supported approximation.

L: 700'

ε/t	σ_y tilted, ($\phi=3°$)	% increase	σ_y tilted, ($\phi=5°$)	% increase
10.30	18,490.0	1.98	19,185.3	3.30
10.30	20,528.8	2.05	20,803.1	3.41
10.90	20,815.3	2.21	21,115.3	3.35
11.70	21,668.9	2.44	22,012.1	4.06
12.45	22,023.2	2.61	22,396.9	4.35
13.50	22,453.9	2.86	22,869.0	4.77
14.00	22,749.1	2.98	23,187.5	4.97
15.40	23,162.7	3.33	23,659.2	5.54
15.60	23,475.6	3.38	23,986.0	5.63

Table VII.   Lateral and tilt stresses vs.
depth ratio (ε/t), $3°$ and $5°$ tilt angle.
Simply supported approximation.

Figure XVII. Stress magnification vs.
depth ratio (c/t), 3° and 5° tilt angle.
Simple support approximation.

Top figure: Plot of % increase in $\tau_{(y)}$ edge versus ϵ/t. Three lines labeled $L=700'$, $L=500'$, and $L=300'$. Box label: CLAMPED EDGES CASE $\phi = 5°$

Bottom figure: Plot of % increase in $\tau_{(y)}$ edge versus ϵ/t. Three lines labeled $L=700'$, $L=500'$, and $L=300'$. Box label: CLAMPED EDGES CASE $\phi = 3°$
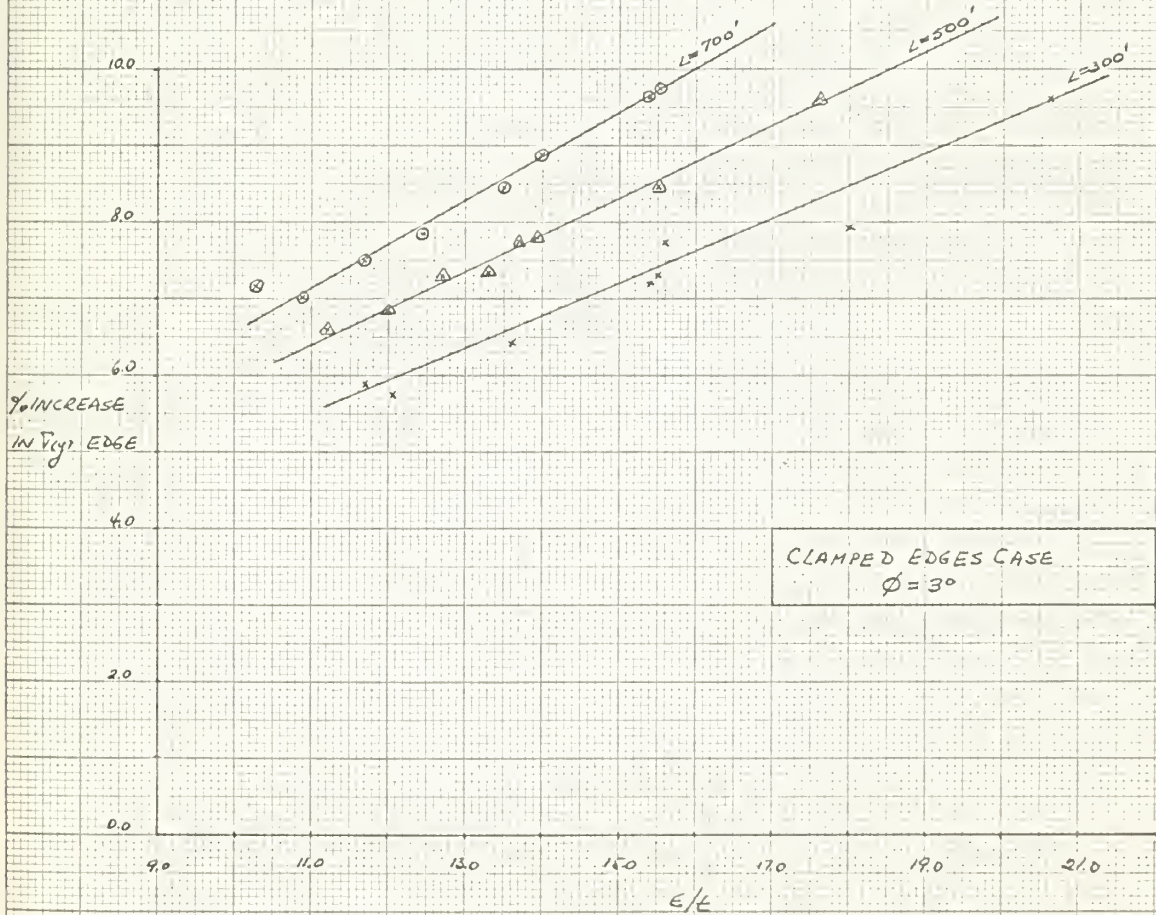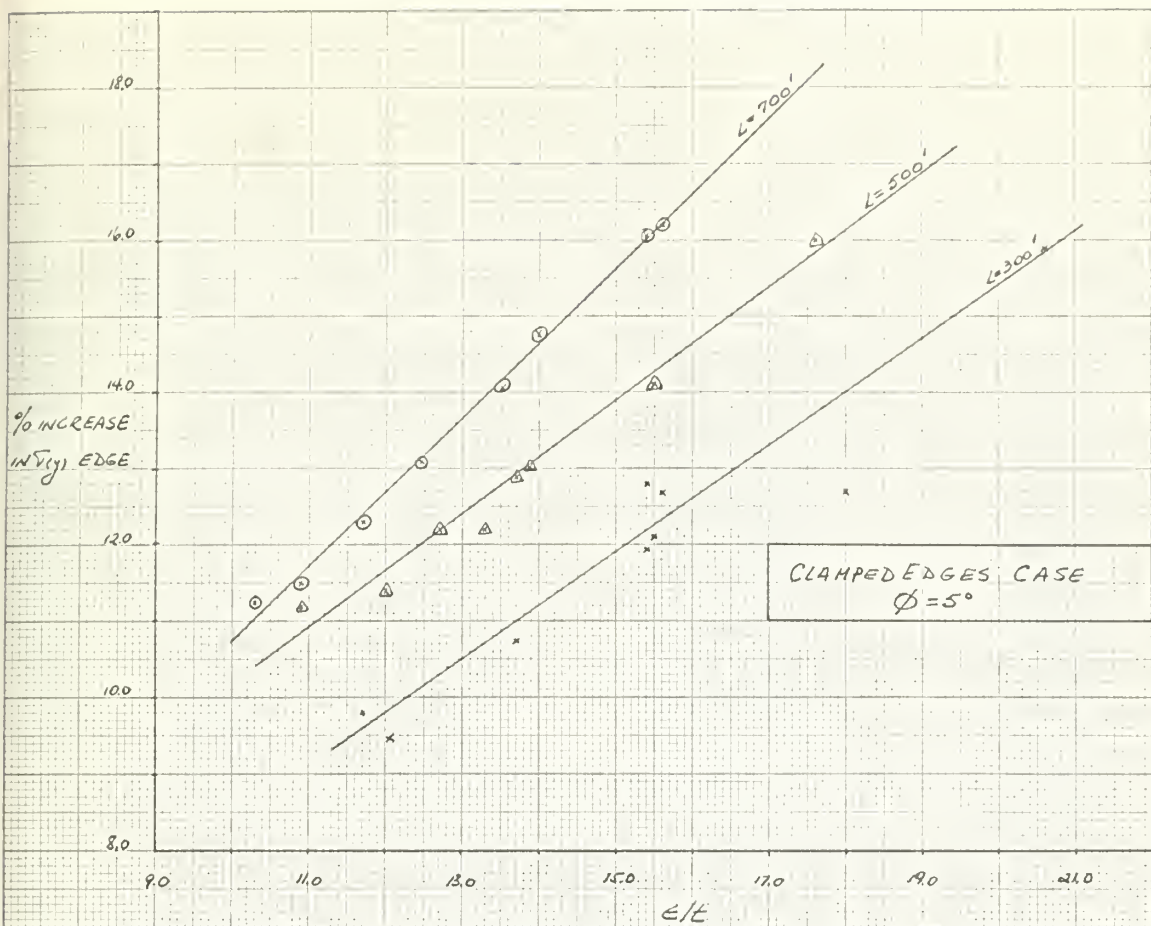
SIMPLY SUPPORTED CASE ($\emptyset$=7°)

L: 300'

A/B	σ_y no tilt	σ_y tilted	% increase
2.00	33,115.8psi.	34,459.0psi.	4.07
2.33	35,865.9	37,606.3	4.85
2.40	31,863.3	33,278.2	4.44
2.66	37,671.6	39,799.3	5.65
2.80	33,585.9	35,618.7	6.05
3.00	38,846.9	41,070.8	5.72
3.20	34,572.3	36,718.3	6.20
3.50	39,878.9	42,579.5	6.77
4.00	40,297.4	43,453.3	7.83

L: 500'

A/B	σ_y no tilt	σ_y tilted	% increase
2.00	22,134.7psi.	23,155.0psi.	4.60
2.33	23,975.5	25,145.5	4.88
2.40	25,171.8	26,465.2	5.14
2.66	25,194.3	26,621.0	5.66
2.80	26,507.5	28,110.4	6.04
3.00	28,513.6	30,154.6	5.76
3.20	27,300.0	28,993.0	6.20
3.50	29,280.3	31,270.8	6.10
4.00	29,669.4	31,985.7	7.81

Table VIII. Lateral and tilt stresses vs.
aspect ratio (a/b), 7° tilt angle.
Simple support approximation.

L: 700'

A/B	σ_y no tilt	σ_y tilted	% increase
2.00	18,571.5psi.	19,429.8psi.	4.62
2.33	20,116.6	21,076.5	4.77
2.40	20,364.4	21,414.4	5.15
2.66	21,153.1	22,354.3	5.68
2.80	21,462.0	22,769.0	6.09
3.00	21,829.2	23,283.9	6.67
3.20	22,090.3	23,624.4	6.94
3.50	22,416.5	24,154.2	7.75
4.00	22,708.6	24,492.0	7.86

Table VIII. Lateral and tilt stresses vs.
aspect ratio (a/b), 7° tilt angle.
Simple support approximation.

Figure XVIII.   Stress magnification vs.
aspect ratio (a/b), 7° tilt angle.
Simple Support Approximation

Figure XVIII. Stress magnification vs.
aspect ratio (a/b), 7° tilt angle.
Simple Support Approximation

SIMPLY SUPPORTED PLATE.
$\phi = 7°$

x 300'
△ 500'
⊘ 700'
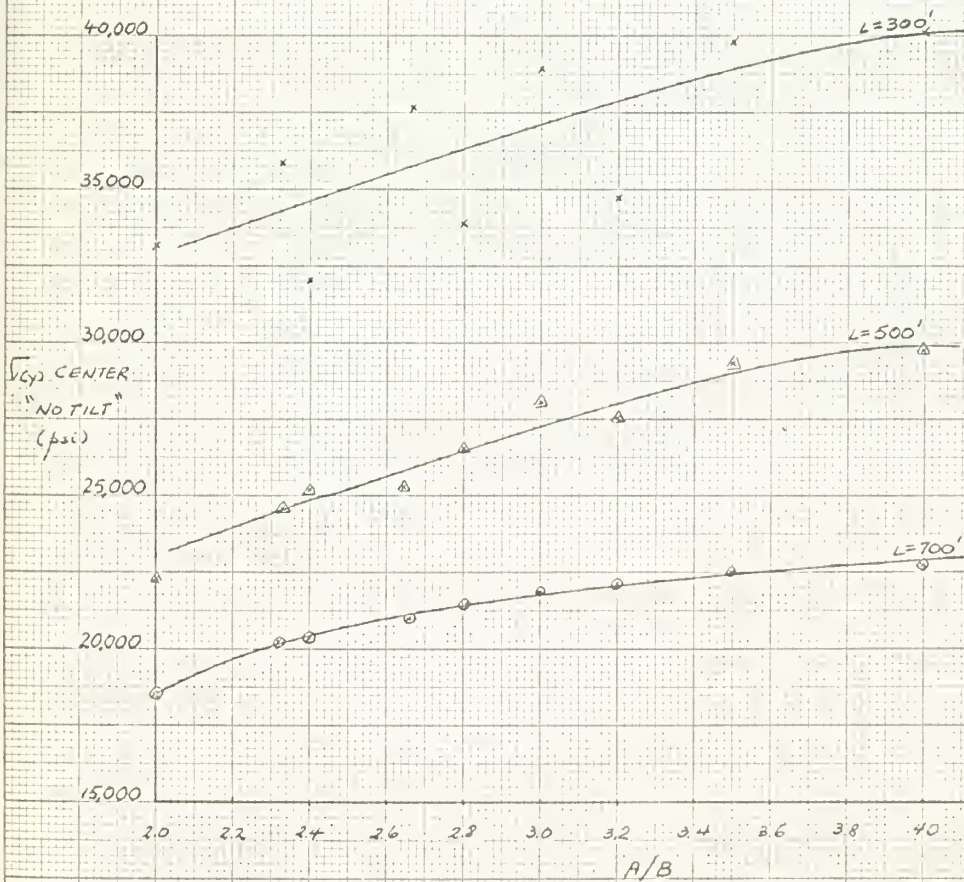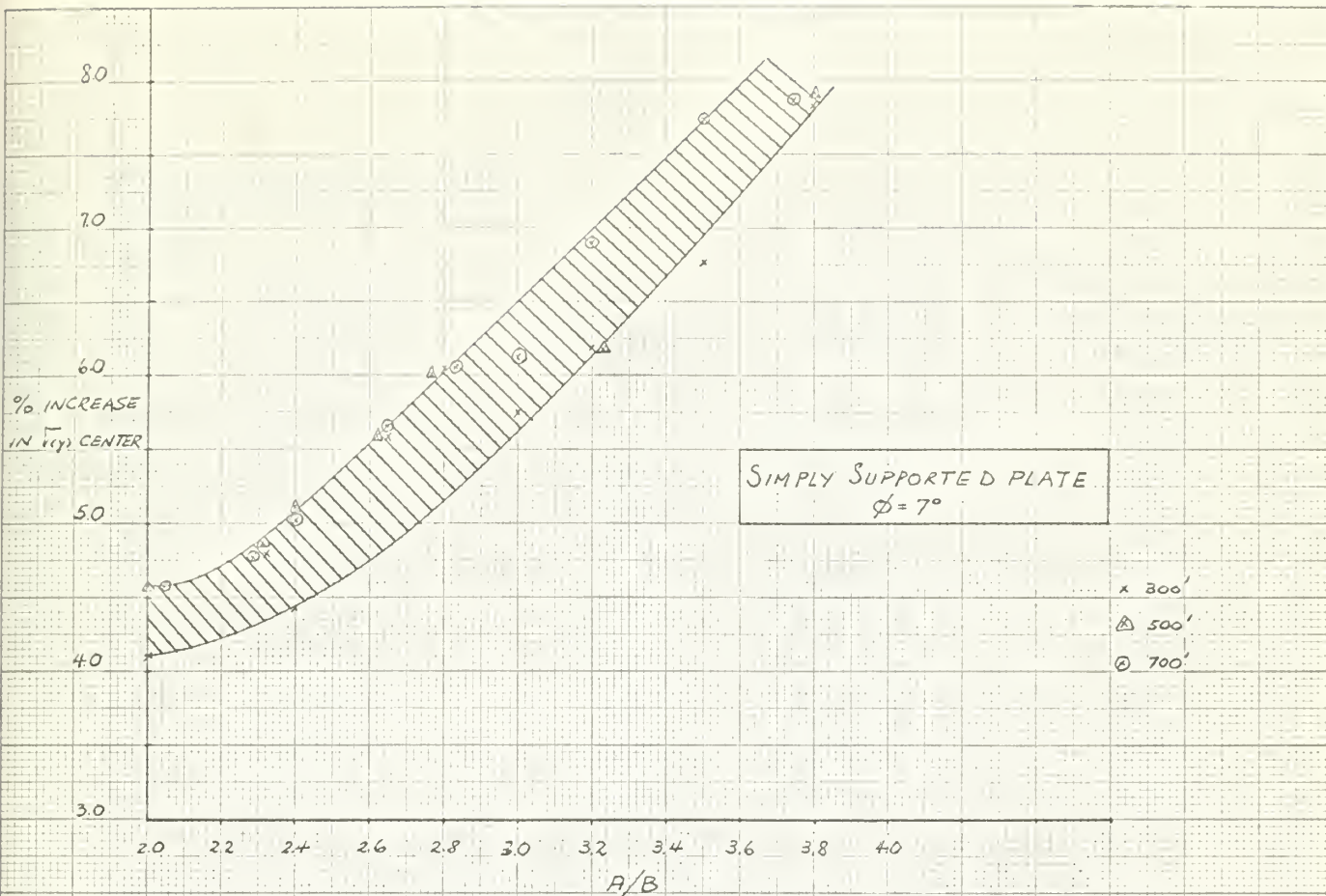
SIMPLY SUPPORTED CASE

L:300'

A/B	σ_y tilted ($\emptyset=3°$)	% increase	σ_y tilted ($\emptyset=5°$)	% increase
2.00	33,693.0psi.	1.75	34,075.0psi.	2.90
2.33	36,613.0	2.10	37,110.5	3.50
2.40	32,471.0	1.90	32,875.0	3.20
2.66	38,585.0	2.43	39,193.2	4.04
2.80	39,802.2	2.50	40,437.0	4.10
3.00	34,459.0	3.45	35,040.0	4.33
3.20	35,494.4	2.66	36,107.3	4.44
3.50	41,037.0	2.90	41,810.0	4.84
4.00	41,652.0	3.36	42,554.4	5.60

L:500'

A/B	σ_y tilted ($\emptyset=3°$)	% increase	σ_y tilted ($\emptyset=5°$)	% increase
2.00	22,574.0psi.	1.98	22,864.0psi.	3.30
2.33	24,478.4	2.10	24,813.0	3.50
2.40	25,727.2	2.21	26,096.8	3.70
2.66	25,807.2	2.43	26,214.7	4.05
2.80	27,195.8	2.60	27,653.8	4.32
3.00	29,218.0	2.47	29,687.0	4.12
3.20	28,027.0	2.70	28,509.7	4.43
3.50	30,135.1	2.92	30,703.8	4.86
4.00	30,664.0	3.35	31,325.8	5.58

Table IX. Lateral and tilt vs.
aspect ratio (a/b), 3° and 5° tilt angle.
Simple support approximation.

L:700'

A/B	σ_{y} tilted $(\emptyset=3^{o})$	% increase	σ_{y} tilted $(\emptyset=5^{o})$	% increase
2.00	18,490.0psi.	1.98	19,185.3psi.	3.30
2.33	20,528.8	2.05	20,803.1	3.41
2.40	20,815.3	2.21	21,153.0	3.35
2.66	21,668.9	2.44	22,012.1	4.06
2.80	22,023.2	2.61	22,396.9	4.35
3.00	22,453.9	2.86	22,869.0	4.77
3.20	22,769.1	2.98	23,187.5	4.97
3.50	23,162.7	3.33	23,659.2	5.54
4.00	23,475.7	3.38	23,986.0	5.63

Table IX. Lateral and tilt vs.
aspect ratio (a/b), 3° and 5° tilt angle.
Simple support approximation.

Figure XIX. Stress magnification vs. aspect ratio (a/b), 3° and 5° tilt angle. Simple support approximation

% INCREASE
IN √(y) CENTER

SIMPLY SUPPORTED PLATE
φ = 5°

x 300'
△ 500'
⊗ 700'

% INCREASE
IN √(y) CENTER

SIMPLY SUPPORTED PLATE
φ = 3°
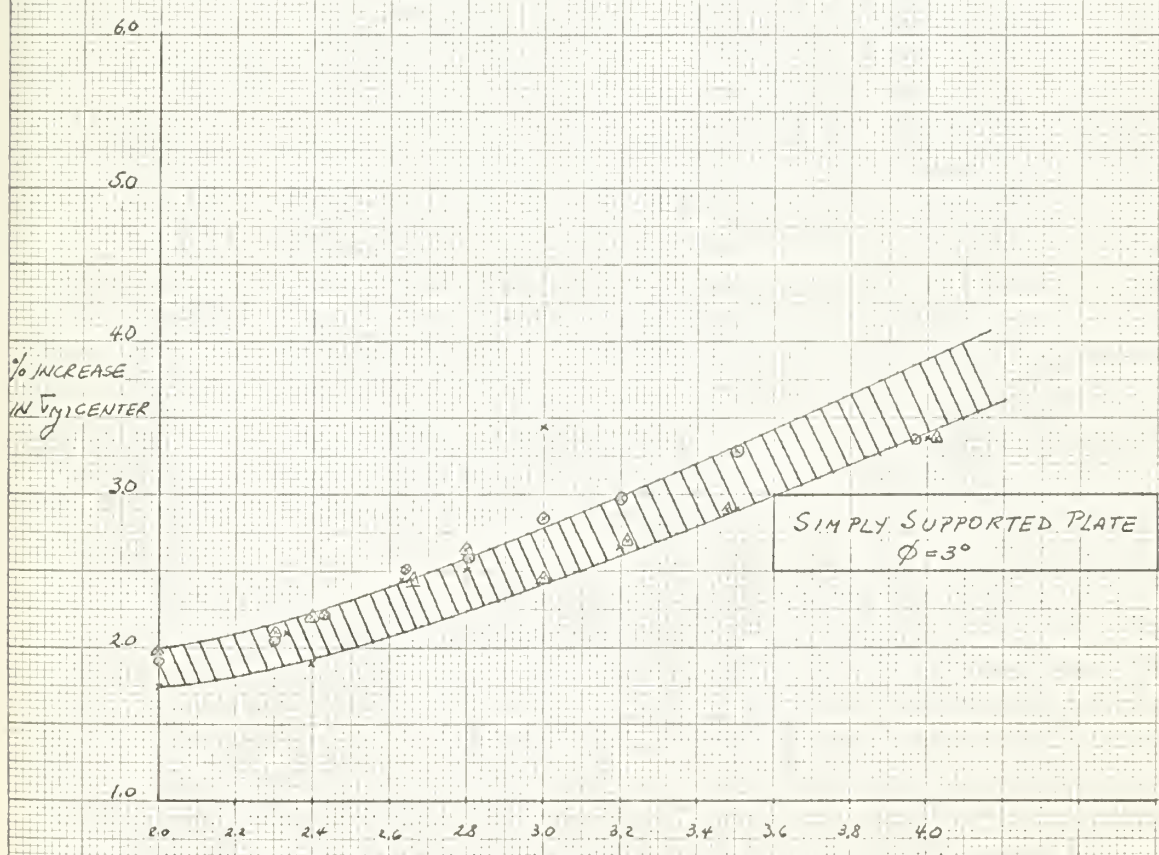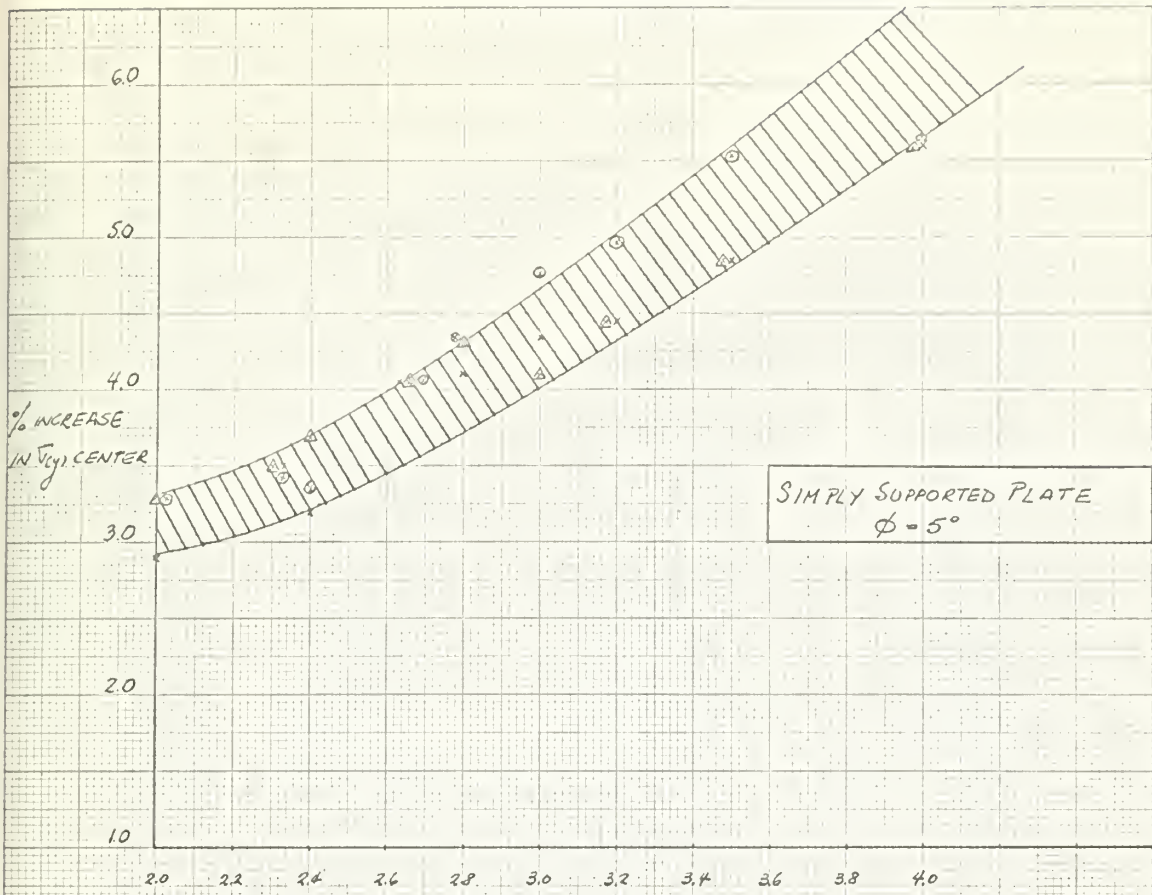
CLAMPED EDGES CASE ($\phi=7°$)

L:300'

c/t	σ_y no tilt	σ_y tilted	% increase (decrease)
11.70	23,247.0psi.	20,056.0psi.	13.30
12.05	26,542.0	23,006.0	13.30
13.70	26,666.0	22,662.0	15.00
15.40	26,680.0	22,213.0	16.75
15.40	23,499.0	19,298.0	17.90
15.50	26,669.0	22,167.0	16.90
15.60	23,421.0	19,198.0	18.00
18.00	26,629.0	21,559.0	19.00
20.60	26,775.0	20,817.0	22.20

L:500'

c/t	σ_y no tilt	σ_y tilted	% increase (decrease)
11.20	17,590.0psi.	14,900.0psi.	15.30
11.30	17,657.0	14,962.0	15.30
12.00	18,344.0	15,427.0	15.90
12.70	17,699.0	14,679.0	17.20
13.30	19,401.0	16,102.0	17.00
13.70	18,366.0	15,053.0	18.00
13.85	18,374.0	15,040.0	18.20
15.50	19,492.0	15,656.0	19.70
17.60	19,544.0	15,170.0	22.40

Table X. Lateral and tilt stresses vs.
depth ratio (c/t), 7° tilt angle.
Clamped approximation.

L:700'

ϵ/t	σy no tilt	σy tilted	% increase (decrease)
10.30	17,657.0psi.	14,962.0psi.	15.30
10.30	14,667.0	12,459.0	15.60
10.90	14,713.0	12,346.0	16.10
11.70	14,761.0	12,219.0	17.20
12.45	14,814.0	12,112.0	18.30
13.50	14,834.0	11,918.0	19.75
14.00	14,700.0	11,678.0	20.60
15.40	14,913.9	11,564.0	22.50
15.60	14,884.0	11,510.0	25.10

Table X. Lateral and tilt stresses vs.
depth ratio (ϵ/t), 7° tilt angle.
Clamped approximation.

Figure XX. Stress magnification vs. depth ratio (ϵ/t), 7° tilt angle. Clamped approximation.

CLAMPED EDGES CASE
$\phi = 7°$

Top graph:
Y-axis: % INCREASE IN $\bar{V}_{(y)}$ EDGE
X-axis: ϵ/t
Curves labeled: $L=700'$, $L=500'$, $L=200'$

Bottom graph:
Y-axis: $\bar{V}_{(y)}$ EDGE "NO TILT" (psi)
X-axis: ϵ/t
Curves labeled: $L=300'$, $L=500'$, $L=700'$

CLAMPED EDGES CASE

L:300'

ε/t	σ_y tilted ($\emptyset=3^{\circ}$)	% increase	σ_y tilted ($\emptyset=5^{\circ}$)	% increase
11.70	21,877.0psi.	5.90	20,965.5psi.	9.80
12.05	25,023.5	5.75	24,013.2	9.45
13.70	24,946.0	6.40	23,802.5	10.75
15.40	24,762.0	7.20	23,485.0	11.95
15.40	21,695.0	7.66	20,494.0	12.80
15.50	24,735.0	7.30	23,449.0	12.10
15.60	21,607.9	7.74	20,401.1	12.70
18.00	24,528.3	7.90	23,041.6	13.50
20.60	24,216.8	9.58	22,514.0	15.90

L:500'

ε/t	σ_y tilted ($\emptyset=3^{\circ}$)	% increase	σ_y tilted ($\emptyset=5^{\circ}$)	% increase
11.20	16,435.0psi.	6.60	15,666.0psi.	10.90
11.30	16,499.0	6.60	15,729.0	10.90
12.00	17,091.4	6.85	16,258.0	11.40
12.70	16,402.0	7.30	15,539.0	12.20
13.30	17,984.0	7.32	17,042.0	12.20
13.70	16,943.2	7.75	15,996.5	12.90
13.85	16,942.0	7.78	15,989.9	13.00
15.50	17,844.0	8.48	16,748.0	14.10
17.60	17,665.0	9.63	16,415.6	16.00

Table XI. Lateral and tilt stresses vs.
depth ratio (ε/t), 3° and 5° tilt angle.
Clamped approximation.

L:700'

ε/t	σ_y tilted ($\emptyset=3°$)	% increase	σ_y tilted ($\emptyset=5°$)	% increase
10.30	13,663.0psi.	7.10	13,016.0psi.	11.25
10.30	13,663.0	7.10	13,016.0	11.25
10.90	13,696.7	6.95	13,020.3	11.50
11.70	13,669.4	7.50	12,943.0	12.30
12.45	13,653.0	7.84	12,881.0	13.05
13.50	13,586.8	8.43	12,751.1	14.05
14.00	13,402.0	8.85	12,539.0	14.70
15.40	13,474.4	9.67	12,517.0	16.10
15.60	13,434.4	9.75	12,471.0	16.20

Table XI. Lateral and tilt stresses vs.
depth ratio (ε/t), 3° and 5° tilt angle.
Clamped approximation.

Figure XXI.   Stress magnification vs.
depth ratio (ϵ/t), 3° and 5° tilt angle.
Clamped approximation.

% INCREASE
IN $\sqrt{(y)}$ CENTER

SIMPLY SUPPORTED CASE
$\phi = 5°$

ϵ/t
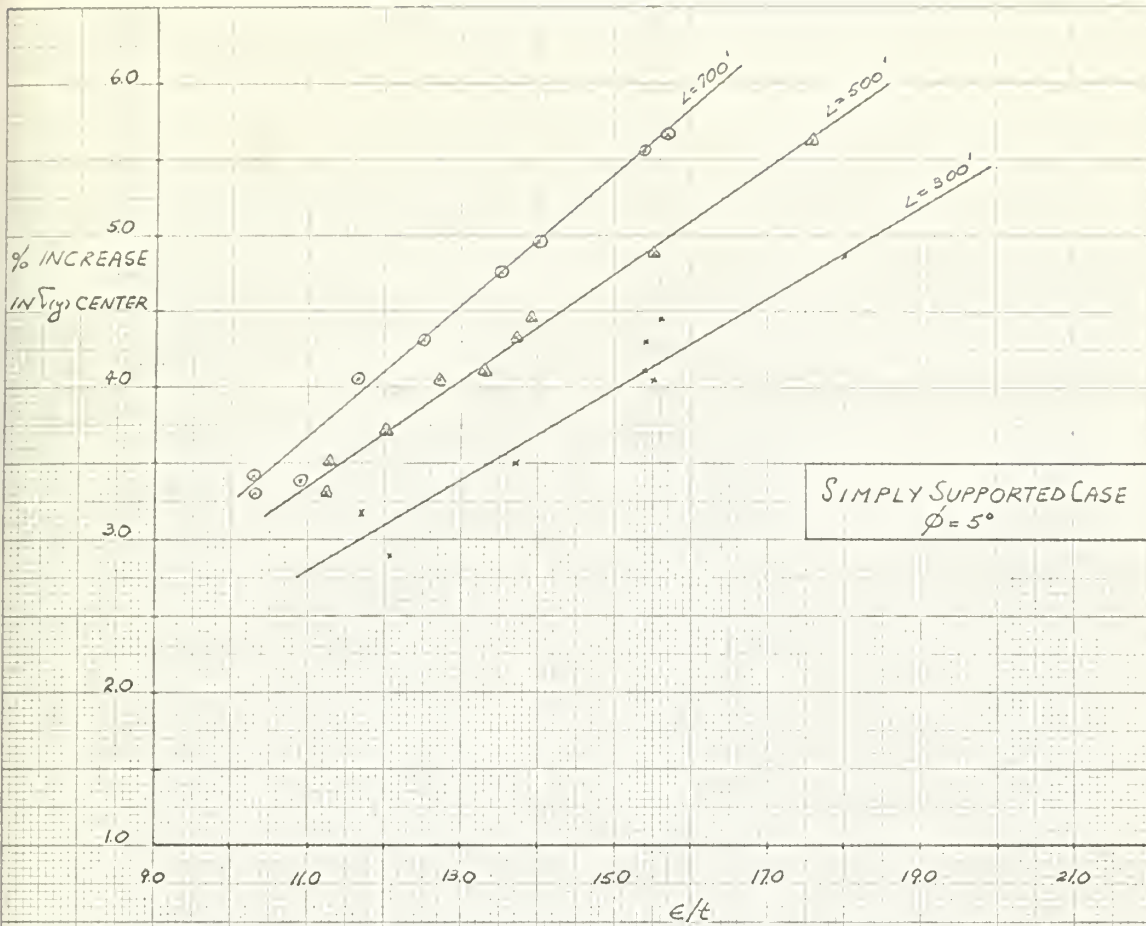
% INCREASE
IN $\sqrt{(y)}$ CENTER
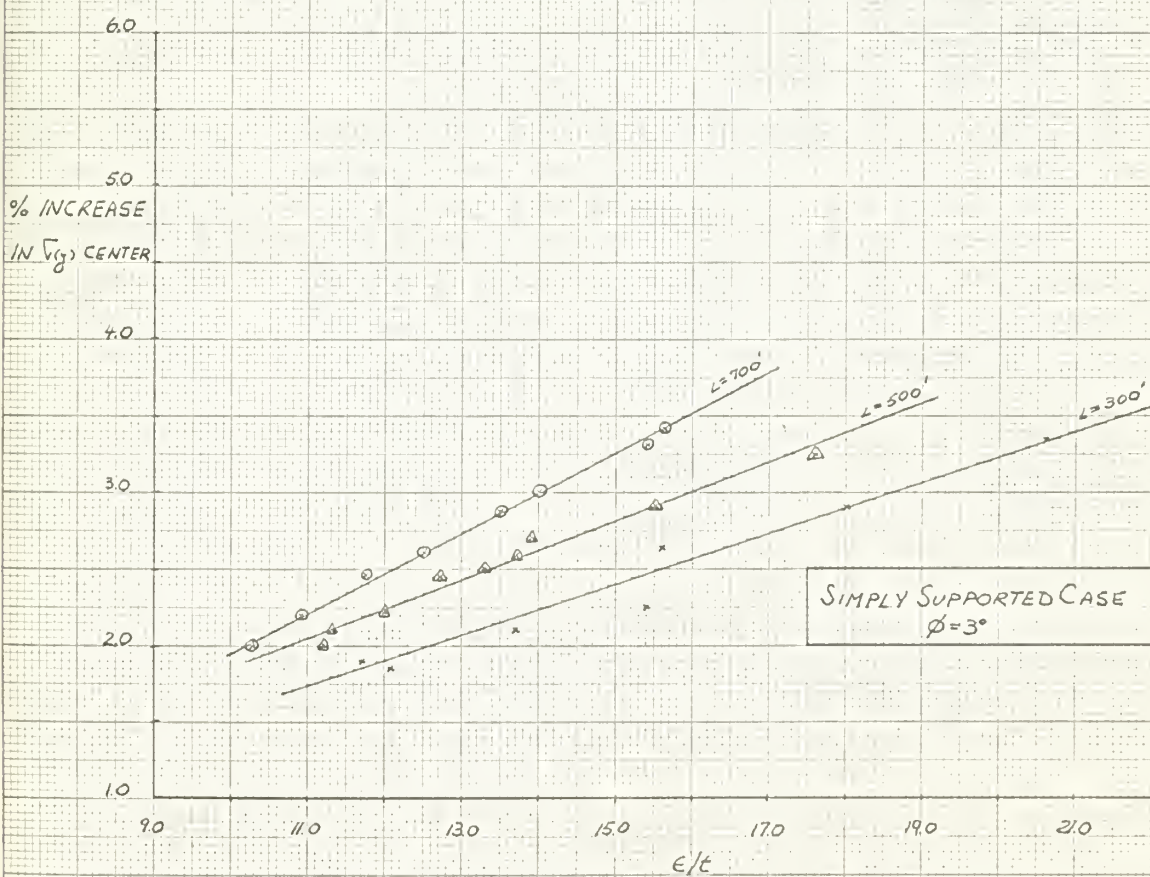
SIMPLY SUPPORTED CASE
$\phi = 3°$

ϵ/t

CLAMPED EDGES CASE ($\emptyset = 7^\circ$)

L:300'

A/B	σ_y no tilt	σ_y tilted	% increase (decrease)
2.00	26,542.0psi.	23,006.0psi.	13.30
2.33	26,666.0	22,662.0	15.00
2.40	23,247.0	20.056.0	13.30
2.66	26,669.0	22,167.0	16.90
2.80	23,499.0	19,298.0	17.90
3.00	26,680.0	22,213.0	16.75
3.20	23,421.0	19,198.0	18.00
3.50	26,629.0	21,559.0	19.00
4.00	26,775.0	20,817.0	22.20

L:500'

A/B	σ_y no tilt	σ_y tilted	% increase (decrease)
2.00	17,590.0psi.	14,990.0psi.	15.30
2.33	17,657.0	14,962.0	15.30
2.40	18,344.0	15,427.0	15.90
2.66	17,699.0	14,697.0	17.20
2.80	18,366.0	15,053.0	18.00
3.00	19,407.0	16,102.0	17.00
3.20	18,374.0	15,040.0	18.20
3.50	19,492.0	15,656.0	19.70
4.00	19,544.0	15,170.0	22.40

Table XII. Lateral and tilt stresses vs.
aspect ratio (a/b), 7° tilt angle.
Clamped approximation.

L:700'

A/B	σ_y no tilt	σ_y tilted	% increase (decrease)
2.00	14,634.0psi.	12,373.0psi.	15.60
2.33	14,667.0	12,459.0	15.60
2.40	14,713.0	12,346.0	16.10
2.66	17,699.0	14,679.0	17.20
2.80	14,814.0	12,112.0	18.30
3.00	14,843.0	11,918.0	19.75
3.20	14,700.0	11,678.0	20.60
3.50	14,913.0	11,664.0	22.50
4.00	14,884.0	11,510.0	25.10

Table XII. Lateral and tilt stresses vs.
aspect ratio (a/b), 7° tilt angle.
Clamped approximation.

Figure XXII. Stress magnification vs.
aspect ratio (a/b), 7° tilt angle.
Clamped approximation.

Figure XXII. Stress magnification vs.
aspect ratio (a/b), 7° tilt angle.
Clamped approximation.

% INCREASE IN
σ(y) EDGE

CLAMPED EDGES CASE
ϕ = 7°

x 300'
△ 500'
⊗ 700'

A/B

σ(y) EDGE
"NO TILT"
(psi)

L=300'

L=500'

L=700'

A/B
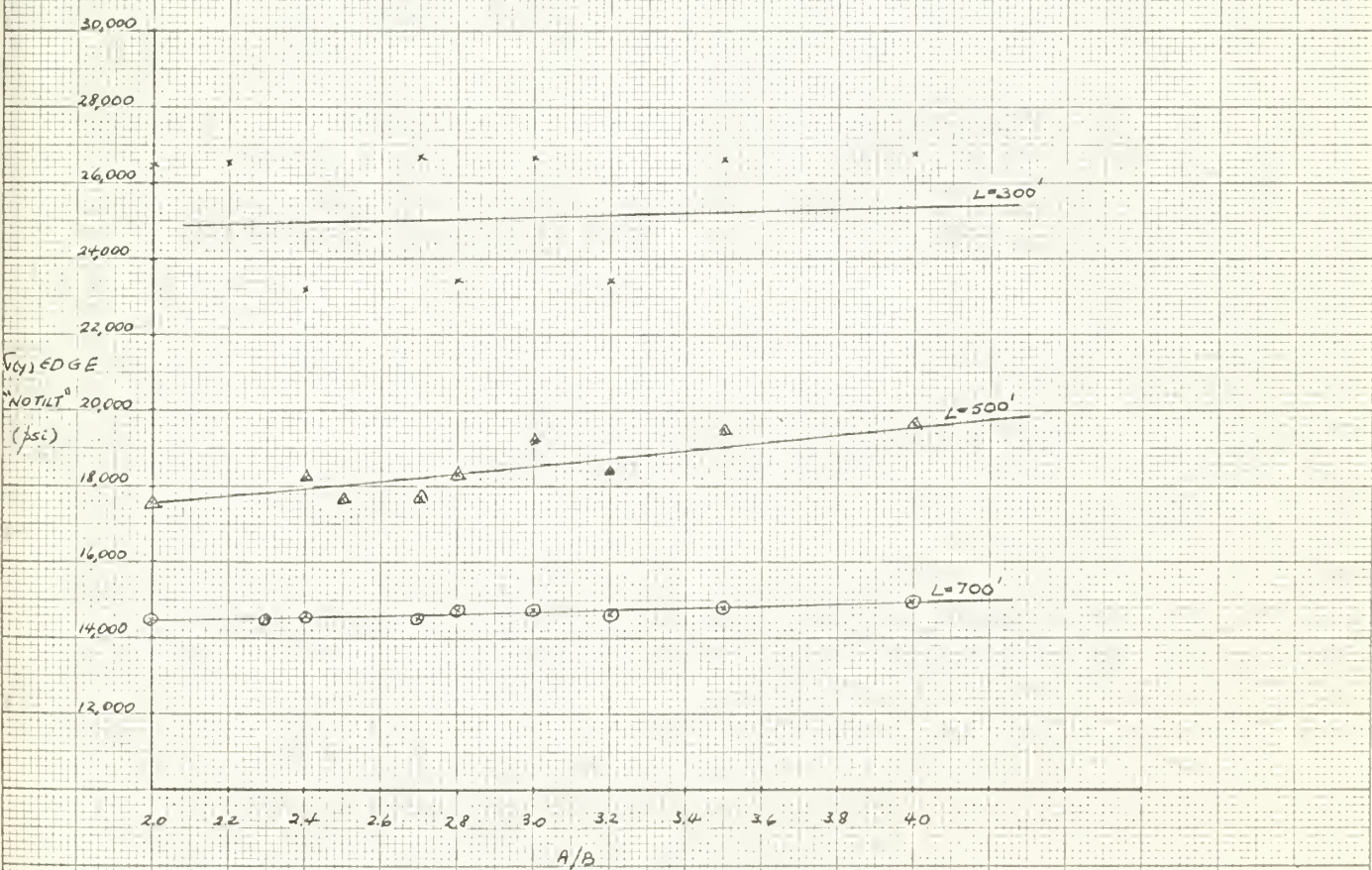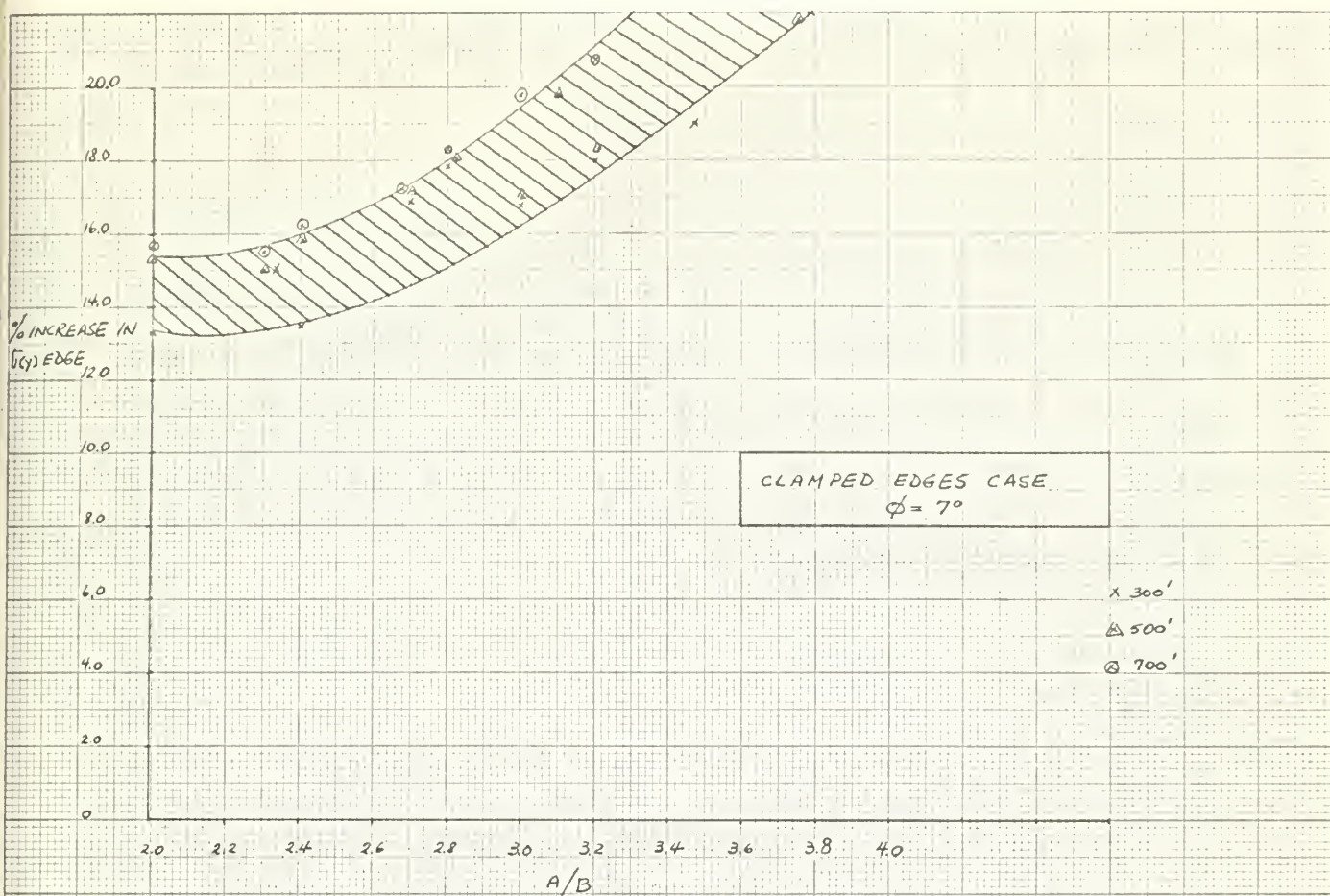
CLAMPED EDGES CASE

L:300'

A/B	σy tilted ($\emptyset=3^\circ$)	% increase	σy tilted ($\emptyset=5^\circ$)	% increase
2.00	25,023.5psi.	5.75	24,013.2psi.	9.45
2.33	24,946.0	6.40	23,802.5	10.75
2.40	21,877.0	5.90	20.965.5	9.80
2.66	24,735.0	7.30	23,449.0	12.10
2.80	24,762.0	7.20	23,485.0	11.95
3.00	21,695.0	7.66	20,494.0	12.80
3.20	21,607.9	7.74	20,401.1	12.70
3.50	24,528.3	7.90	23,041.6	13.50
4.00	24,216.8	9.58	22,514.0	15.90

L:500'

A/B	σy tilted ($\emptyset=3^\circ$)	% increase	σy tilted ($\emptyset=5^\circ$)	% increase
2.00	16,335.0psi.	6.60	15,666.0psi.	10.90
2.33	16,499.0	6.60	15,729.0	10.90
2.40	17,091.4	6.85	16,258.0	11.40
2.66	16,402.0	7.30	15,539.0	12.20
2.80	16,943.2	7.75	15,996.5	12.90
3.00	17,948.0	7.32	17,042.0	12.20
3.20	16,942.0	7.78	15,989.0	13.00
3.50	17,844.0	8.48	16,748.0	14.10
4.00	17,665.0	9.63	16,415.6	16.00

Table XIII. Lateral and tilt stresses vs. aspect ratio (a/b), 3° and 5° tilt angle. Clamped approximation.

L:700'

A/B	σ_y tilted ($\emptyset=3°$)	% increase	σ_y tilted ($\emptyset=5°$)	% increase
2.00	13,663.0psi.	7.10	13,016.0psi.	11.25
2.33	13,663.0	7.10	13,016.0	11.25
2.40	13,697.4	6.95	13,028.3	11.25
2.66	13,669.4	7.50	12,943.0	12.30
2.80	13,653.0	7.84	12,881.0	13.05
3.00	13,586.8	8.43	12,751.1	14.05
3.20	13,402.0	8.85	12,539.0	14.70
3.50	13,474.4	9.67	12,517.0	16.10
4.00	13,434.4	9.75	12,471.0	16.20

Table XIII. Lateral and tilt stresses vs.
aspect ratio (a/b), 3° and 5° tilt angle.
Clamped approximation.

Figure XXIII. Stress magnification vs.
aspect ratio (a/b), 3° and 5° tilt angle.
Clamped approximation.

% INCREASE
IN $\bar{V}_{(y)}$ EDGE

CLAMPED EDGES CASE
$\phi = 5°$

× 300'
△ 500'
⊕ 700'

A/B

% INCREASE
IN $\bar{V}_{(y)}$ EDGE

CLAMPED EDGES CASE
$\phi = 3°$

A/B
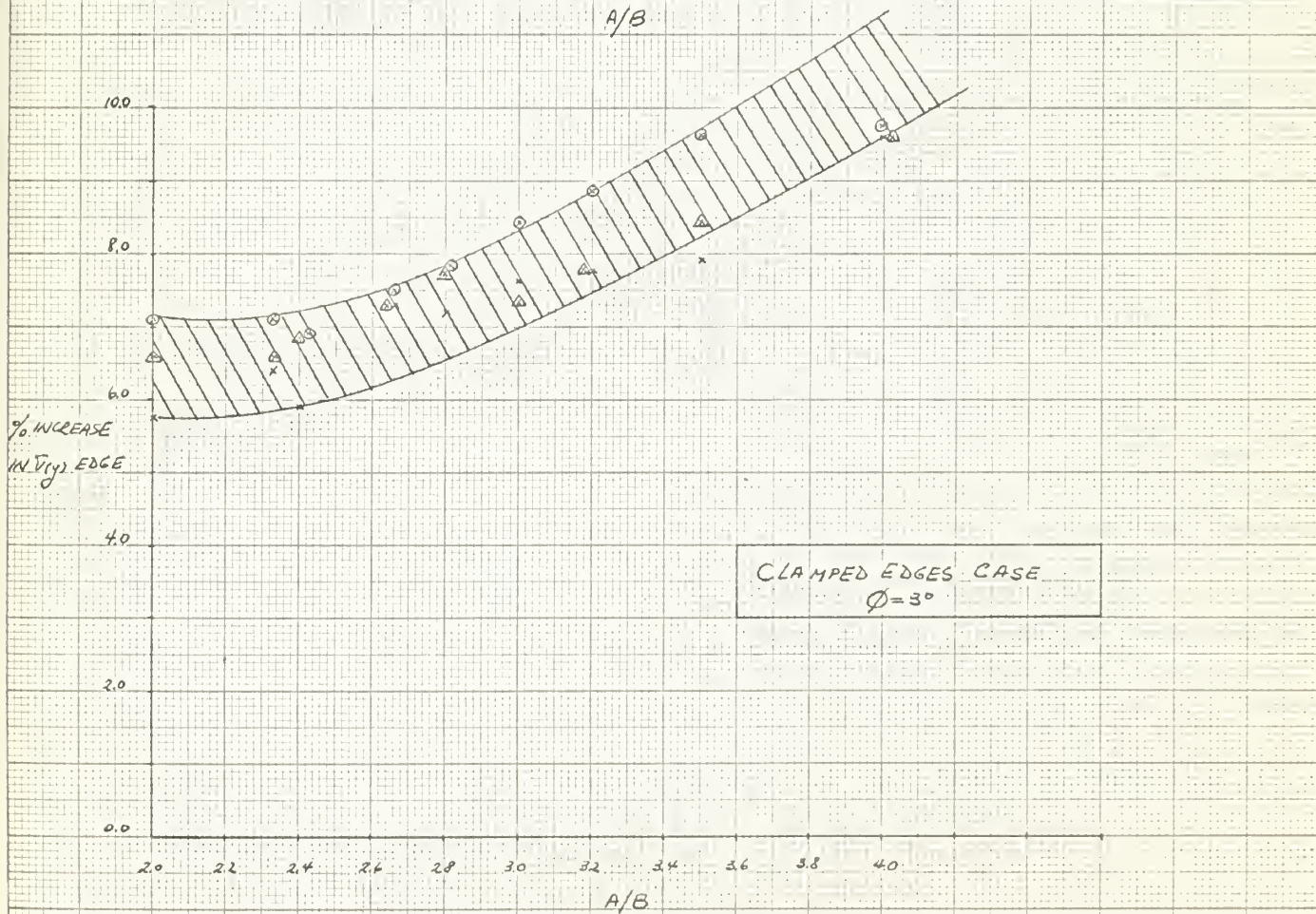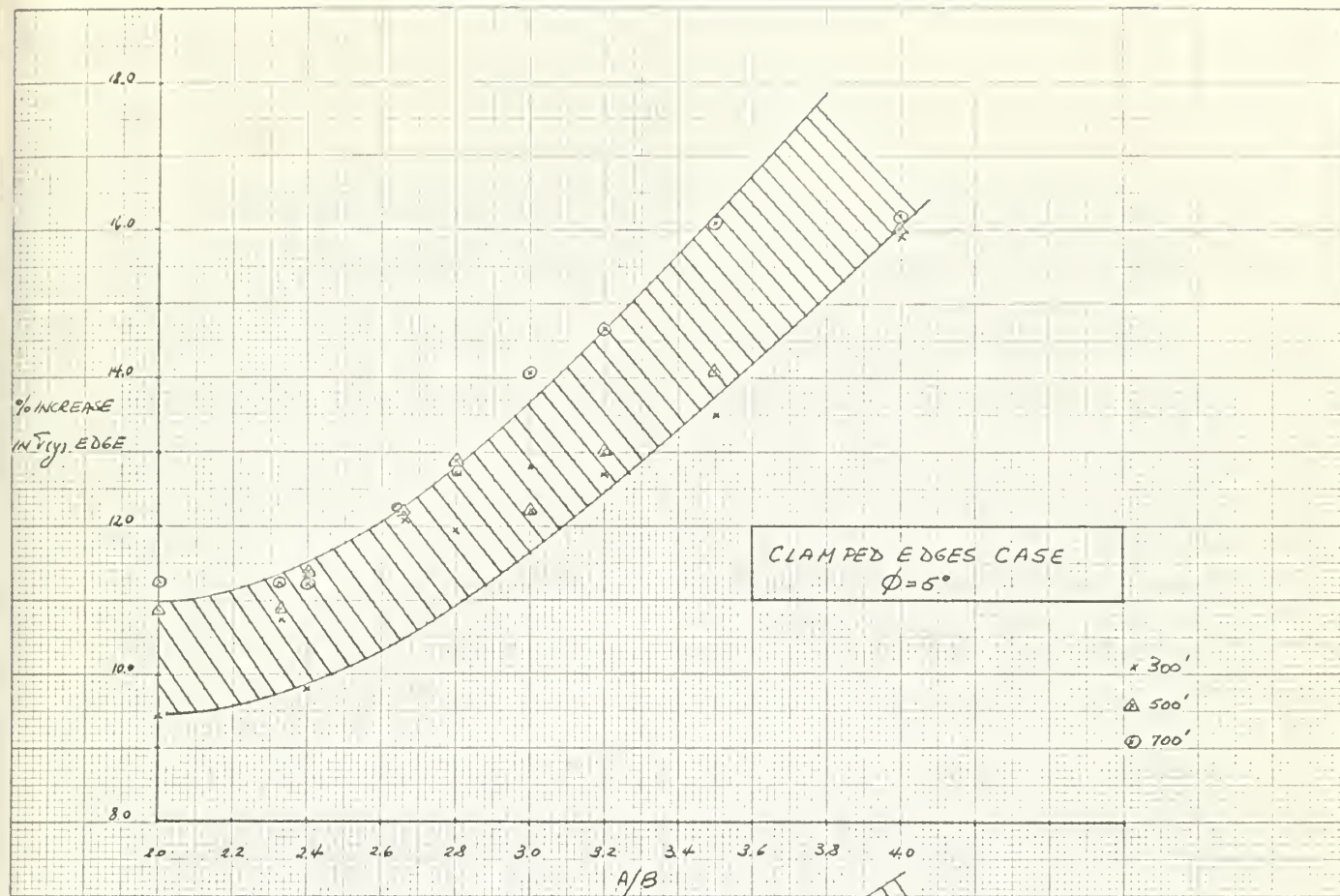
V. DISCUSSION OF RESULTS

Upon examination of the results of the computer study for all fifty-four cases, it was apparent that the effect of web tilt, while present to some degree at any point in the plate, had real significance only for the stress in the "y" direction (σ_y). That this should be so seemed intuitive at the outset, since the vector of the applied tilt moment parallelled the "x" direction of the plate panel. The results confirmed this, and hence the values of lateral and tilt stresses in the "x" direction (σ_x) have not been presented in the results.

Another intuitive conclusion, that the major effect, or tilt stress variation, would occur along the central plate axis x=a/2, normal to the vector of the applied moment, was also borne out by the results. Figures VII and IX show the total stress (σ_y) variation along the y=0 axis for both support approximations. The maximum stress magnification occurs at the plate center in each case. This is also the point of maximum stress due to lateral load in each case, arising from the assumption that the plate was simply supported along its transverse edges. Consideration of Figures VI and VIII, total stress (σ_y) patterns along the x=a/2 axis, shows that the magnitude of the tilt stress is a maximum at its point of application, and diminishes across the plate axis. Since the additional stress is largest along

-72-

the x=a/2 axis as well, the discussion will be limited to
this effect.

Figure X and XV are presentations of the stress
arising from web tilt alone, shown along the axis x=a/2 for
several cases and angles of tilt. Each pair of plots com-
pares the effect produced under similar geometry for the
two support approximations. Consideration of these figures,
as well as of the accompanying tables, IV and V, reveals that
the actual magnitude of the tilt stress is very nearly in-
dependent of the support conditions assumed for the plate
panel. This says, in effect, that the shear pressure at
the plate edge does not vary measurably with the edge sup-
port conditions. This fact is not obvious from an examina-
tion of equations (34), (13), (14), (21), and (22), the
analytical expressions for the shear pressure coefficient.

The chief conclusion to be drawn from the state-
ments above lies in the fact that the major factor in stress
amplification due to web tilt, the shear pressure, can be
considered a constant under the most widely varying support
conditions normally made for plate analysis.

It is worth noting at this point, that the actual
values of tilt stress obtained in this analysis must be con-
sidered low when extrapolated to an actual ship plating
problem. To demonstrate the reasoning behind this statement,
consider again the analogy to a simple beam under a

distributed load (q). For a single span, analogous to the single panel examined in this thesis, the shear force at either edge is of the order of "qa/2," whereas for a double span, analogous to a continuous panel system, the shear force at the central support is of the order of "qa." Thus, in a real case, the tilt stresses might be expected to exceed those found in this analysis.

Before any discussion of the results presented in Figures XVI through XXIII, it is pertinent to discuss the non-dimensional parameters against which these results are presented. In most work which has been done on plate panels and systems, the fundamental identifying characteristic of the panel is the aspect ratio (a/b). In this work, it was apparent from the initial assumption of the magnitude of the tilt moment arm, (ϵ SIN $\emptyset$), that the value of "ϵ" would have an important bearing on the results. Additionally, since the plate stresses are inversely proportional to the square of the plate thickness, (t), the non-dimensional depth ratio (ϵ/t) seemed pertinent. Analysis of the input data, all selected by standard design techniques, revealed that a rough but generally consistent relationship exists between these two ratios (Figure V), that is, as the plate aspect ratio increases, an increase in the depth ratio is to be expected as well. Since both of these ratios are readily obtainable in an engineering situation, (ϵ can be

taken to be equal to the full depth of the stiffener with
very little sacrifice of accuracy), the results shown in
Figures XVI through XXIII have been presented against both
of these parameters. Any other non-dimensional relationship
for further analysis may be obtained by reference to Table
III. The results shown are plotted for each assumed ship
length, showing, in the lower figure of each group, the
corresponding design stress levels. The difference in
allowable stress magnitude arises from the design technique
employed [10] which permits a higher level of plate bending
stress in a shorter ship, where the girder stress would
presumably be smaller.

Figures XVI through XIX show results at the panel
center for the simple support approximation, while figures
XX through XXIII show results at the center of the longi-
tudinal edge (x=a/2, y=b/2) for the clamped approximation.
In both situations the magnification has been presented at
the point of maximum plate stress due to the lateral load
alone. The fact that the stress magnification shown for
the clamped approximation is in all cases the greater arises
from two facts:

1. The stress at the panel center under a simple
support approximation is greater than the stress which ob-
tains at the plate edge under the clamped approximation, and,

2. the magnitude of the tilt stress remains es-
sentially constant for varying support conditions, as has
been pointed out, and decreases nearly linearly as the
distance from the plate edge increases (Figure X through
XV).

Of particular interest in the results is the fact
that a fairly regular relationship is implied between the
value of stress magnification and the plate aspect ratio
(Figures XVIII, XIX, XXII, and XXIII). Thus, while still
not defining the absolute value of the tilt effect, it may
be concluded that the effect of web tilt increases in im-
portance for a particular plate panel as the aspect ratio
of the panel itself increases.

The question which this thesis seeks to answer asks
not only the magnitude of the tilt effect, but, more funda-
mentally, whether the effect is large enough to be of con-
cern in surface ship construction. In order to properly
define an answer to this question, it is necessary to con-
sider first the nature of the design method used for scantling
selection on surface ships. To a very simplified first
approximation, the plating thickness of a particular panel
is selected to withstand the lateral load or to resist in-
stability failure in compressive loading, whichever is the
more limiting. The stiffener scantlings are selected

principally to withstand the girder bending of the ship, that
is, the chief considerations are usually the area of material
in the stiffener and its section modulus. The choice between
a number of stiffeners which all satisfy the required values
of section modulus is generally based upon considerations of
weight or such characteristics as instability of the web
itself. In any event, the ratio of the depth of the stif-
fener to the plating thickness (c/t) has been merely a de-
rived value, never a design consideration.

From Figures X through XV, it can be seen that the
maximum value of tilt stress, for the conditions examined,
is measured in thousands of pounds per square inch, and even
this, as has already been discussed, is to be considered a
low value. Stresses of this magnitude are certainly not to
be ignored in any design consideration.

As a general conclusion then, it may be stated that
initial web tilt can indeed have an important effect upon
plate bending stresses. This is especially true upon con-
sideration of the improvements presently being made in
structural design. As design techniques improve, effects
which have been heretofore hidden within the "factor of
safety" will become increasingly important. Construction
methods which allow the depth of a stiffening member to
be increased and its orientation to the plate changed for
such reasons as support for an item within the hull or for

a more favorable connection to another member are to be con-
sidered suspect. In such cases, an estimate of the effect
of the change might be obtained by reference to a plot such
as is shown in Figure XXII or XX.

VI. CONCLUSIONS

Recounting the conclusions developed in the pre-
vious section, they are

1. The value of tilt-induced bending stress is es-
sentially independent of the support conditions of the
plate.

2. The effect of an initial web tilt increases in
a regular manner as both the panel aspect ratio (a/b) and
depth ratio (ϵ/t) increase.

3. The ratio of stiffener depth to plate thick-
ness (ϵ'/t), where ϵ' can be taken as very nearly equal to
ϵ, should be considered a design parameter, and its effect
accounted for in any case of an intentionally skew stif-
fening member.

4. The magnitude of tilt-induced stress, while not
catastrophic, is large enough to merit further considera-
tion in any design technique which seeks to optimize the
structure, i.e., reduce the factor of safety in the design.

VII.   RECOMMENDATIONS

Having concluded that the effect of initial web tilt can be of importance in structural design under the assumptions made in this thesis, the logical recommendations follow that

1.   the investigation be extended, and,

2.   the assumptions in the present investigation be themselves investigated, and experimentally verified.

In line with these general statements, specific recommendations are put forth as follows:

1.   An analysis of ship design procedures should be made to determine what general relationship between the aspect ratio (a/b) and the depth ratio (ε/t) exists. If no good relationship can be found, the use of the depth ratio (ε/t) as a basic design parameter for cases of skew stiffeners should be further developed.

2.   The present investigation should be extended to stronger materials and higher lateral loads to verify the consistancy of the data presented herein.

3.   An analysis of the actual deflection behavior of an initially tilted stiffening member under lateral load should be undertaken to determine the effect of such a deflection upon the actual angle of tilt along the member.

Appendix A

Detailed Solution of Lateral Load Case,
Clamped Approximation

In this case, the boundary conditions are, as men-
tioned before

$$w = 0, \quad \frac{\partial^2 w}{\partial x^2} = 0 \qquad\qquad \text{at } x = 0, a \qquad\qquad (5)$$

$$EI \frac{\partial^4 w}{\partial x^4} = D \left[\frac{\partial^3 w}{\partial y^3} + (2-\nu) \frac{\partial^3 w}{\partial x^2 \partial y} \right] \quad \text{at } y = \pm b/2 \qquad (6)$$

$$\frac{\partial w}{\partial y} = 0 \qquad\qquad\qquad \text{at } y = \pm b/2 \qquad\qquad (9)$$

The fundamental equation of the deflection surface which
must be solved is

$$\frac{\partial^4 w}{\partial x^4} + 2 \frac{\partial^4 w}{\partial x^2 \partial y^2} + \frac{\partial^4 w}{\partial y^4} = q/D \qquad\qquad (26)$$

or

$$\nabla^4 w = q/D \qquad\qquad (2a)$$

Assuming a general solution form of

$$w = w_1 + w_2 \qquad\qquad (48)$$

where w_1 is the displacement of a simply supported strip
parallel to the x-axis, then,

-81-

$$\nabla^4 \omega_1 = \frac{q}{D} \qquad (49) \qquad \text{and} \qquad \nabla^4 \omega_2 = 0 \qquad (50)$$

For the case of a uniform load, as can be shown in [5],

$$\omega_1 = \frac{q}{24D} (x^4 - 2a\,x^3 + a^3 x) \qquad (51)$$

and, in order to solve for ω_2, let

$$\omega_2 = \sum_{m=1,3,\ldots}^{\infty} Y_m \, \text{SIN} \, \frac{m\pi x}{a} \qquad (3)$$

where,

$$Y_m = \frac{qa^4}{D} \left[A_m \, \text{COSH} \, \frac{m\pi y}{a} + B_m \, \frac{m\pi y}{a} \, \text{SINH} \, \frac{m\pi y}{a} + C_m \, \text{SINH} \, \frac{m\pi y}{a} \right.$$

$$\left. + D_m \, \frac{m\pi y}{a} \, \text{COSH} \, \frac{m\pi y}{a} \right] \qquad (4)$$

This form of solution was developed by Nádai [7] and Lévy [8], and has been presented by Timoshenko [5].

To evaluate the constant terms in Y_m, it can be seen that the deflection surface under a purely lateral load will by symmetric, that is

$$\omega(x,b) = \omega(x,-b) \qquad (52)$$

hence the equation for the deflection surface must be an even function of the variable "y" by considerations of symmetry. The terms "y COSH(y)" and "SINH(y)" are in themselves

odd functions and hence the coefficients of these terms
must vanish, i.e.,

$$C_m = D_m = 0 \tag{53}$$

Thus, the solution can now be expressed as

$$w = w_1 + w_2$$

$$= \frac{q}{24D} \left[x^4 - 2a \, x^3 + a^3 x \right] + \frac{qa^4}{D} \sum_{m=1,3,\ldots}^{\infty} (A_m \text{COSH} \frac{m\pi y}{a}$$

$$+ \, B_m \frac{m\pi y}{a} \text{SINH} \frac{m\pi y}{a}) \, \text{SIN} \frac{m\pi x}{a} \tag{54}$$

this can also be expressed as a single series, viz.,

$$w = \frac{qa^4}{D} \sum_{m=1,3,\ldots}^{\infty} (\frac{4}{m^5 \pi^5} + A_m \text{ COSH} \frac{m\pi y}{a} + B_m \frac{m\pi y}{a} \text{ SINH} \frac{m\pi y}{a}) \text{SIN} \frac{m\pi x}{a}$$

$$\tag{55}$$

By inspection, it can be seen that this equation
satisfies boundary condition (5), since both the sine term
and its second derivative vanish at $x = 0$, a. Further, since
symmetry has been considered, the remaining boundary condi-
tions need only be satisfied at $y = + b/2$ to complete the
solution.

Differentiating the deflection equation above, and
substituting into boundary condition (6), gives

$$\frac{4\alpha_m}{m^5\pi^5} = A_m \left[(\nu-1)SINH\ \lambda_m - \alpha_m COSH\ \lambda_m \right]$$

$$+ B_m \left[(1+\nu-\alpha_m\lambda_m)SINH\ \lambda_m + \lambda_m(1-\nu)COSH\ \lambda_m \right] \tag{56}$$

where

$$\lambda_m = \frac{m\pi b}{2a} \tag{15}$$

and

$$\alpha_m = \frac{EI}{D} \cdot \frac{m\pi}{a} \tag{16}$$

as before.

Differentiating again, and substituting into boundary condition (9) gives

$$0 = A_m\ SINH\ \lambda_m + B_m(SINH\ \lambda_m + \lambda_m\ COSH\ \lambda_m) \tag{57}$$

Solving these two expressions simultaneously for the coefficients A_m and B_m, gives

$$A_m = \frac{4}{m^5\pi^5} \left[\frac{-\alpha_m(SINH\ \lambda_m + \lambda_m COSH\ \lambda_m)}{\alpha_m\lambda_m + \alpha_m SINH\ \lambda_m COSH\ \lambda_m + 2SINH^2\ \lambda_m} \right] \tag{58}$$

$$B_m = \frac{4}{m^5\pi^5} \left[\frac{\alpha_m SINH\ \lambda_m}{\alpha_m\lambda_m + \alpha_m SINH\ \lambda_m COSH\ \lambda_m + 2SINH^2\ \lambda_m} \right] \tag{59}$$

If the constant term $\frac{4}{m^5\pi^5}$ is factored out of these two

expressions, the final solution for this case can then be
written in the following form.

$$\omega = \frac{4qa^4}{\pi^5 D} \sum_{m=1,3,...}^{\infty} \frac{1}{m^5} \left[1+A_m COSH \frac{m\pi y}{a} + B_m \frac{m\pi y}{a} SINH \frac{m\pi y}{a} \right] SIN \frac{m\pi x}{a}$$

(12)

where,

$$A_m = - \frac{\alpha_m SINH \lambda_m + \lambda_m COSH \lambda_m}{\alpha_m \lambda_m + \alpha_m SINH \lambda_m COSH \lambda_m + 2 SINH^2 \lambda_m}$$

(21)

and,

$$B_m = \frac{\alpha_m SINH \lambda_m}{\alpha_m \lambda_m + \alpha_m SINH \lambda_m COSH \lambda_m + 2 SINH^2 \lambda_m}$$

(22)

Appendix B

Detailed Solution of Tilt Load Case

As stated in the discussion in the body of the paper, the boundary conditions applicable to this case are

$$\omega = 0, \quad \frac{\partial^2 \omega}{\partial x^2} = 0 \qquad \text{at } x = 0, \text{ a} \qquad (5)$$

$$EI \frac{\partial^4 \omega}{\partial x^4} = D \left[\frac{\partial^3 \omega}{\partial y^3} + (2-\nu) \frac{\partial^3 \omega}{\partial x^2 \partial y} \right] \quad \text{at } y = \pm b/2 \qquad (6)$$

$$-D \left[\frac{\partial^2 \omega}{\partial y^2} + \nu \frac{\partial^2 \omega}{\partial x^2} \right] = f_1(x) \quad \text{at } y = + b/2 \qquad (10)$$

$$-D \left[\frac{\partial^2 \omega}{\partial y^2} + \nu \frac{\partial^2 \omega}{\partial x^2} \right] = f_2(x) \quad \text{at } y = -b/2 \qquad (11)$$

Assuming a general deflection form, as in the previous cases, of

$$\omega = \sum_{m=1}^{\infty} Y_m \, \text{SIN} \, \frac{m\pi x}{a} \qquad (3)$$

which satisfies boundary condition (5) and where

$$Y_m = A_m \text{SINH} \frac{m\pi y}{a} + B_m \text{COSH} \frac{m\pi y}{a} + C_m \frac{m\pi y}{a} \text{SINH} \frac{m\pi y}{a}$$

$$+ D_m \frac{m\pi y}{a} \text{COSH} \frac{m\pi y}{a} \qquad (4)$$

This is the same form of solution technique as was used in the solution of phase one, the difference in the expressions

for Y_m arises from the fact that there is no lateral loading to be considered in this case.

Considering first a symmetrical loading form, in which

$$M_y\bigg|_{y=+b/2} = M_y\bigg|_{y=-b/2} \tag{60}$$

and assuming that

$$f_1(x) = f_2(x) = \sum_{m=1}^{\infty} E_m \; SIN \; \frac{m\pi x}{a} \tag{61}$$

now, from consideration of symmetry, the odd functions present in Y_m must be eliminated, and hence

$$A_m = D_m = 0 \tag{62}$$

Then

$$\omega = \sum_{m=1}^{\infty} (B_m COSH \; \frac{m\pi y}{a} + C_m \; \frac{m\pi y}{a} \; SINH \; \frac{m\pi y}{a}) \; SIN \; \frac{m\pi x}{a} \tag{63}$$

Having made use of symmetry to eliminate the odd functions, this deflection surface need satisfy the remaining boundary conditions at $y = +b/2$ only.

Differentiating this deflection equation, and substituting into (6) gives

$$B_m = C_m(\rho) \tag{64}$$

where

$$\rho = \frac{(1+\nu-\alpha_m\lambda_m)\text{SINH } \lambda_m-(1-\nu)\lambda_m\text{COSH } \lambda_m}{(1-\nu)\text{SINH } \lambda_m+\alpha_m\text{COSH } \lambda_m} \qquad (25)$$

and, as before

$$\lambda_m = \frac{m\pi b}{2a} \qquad (15) \quad \text{and} \quad \alpha_m = \frac{EI}{D} \cdot \frac{m\pi}{a} \qquad (16)$$

The deflection surface now can be reduced to

$$w = \sum_{m=1}^{\infty} C_m \left[\rho \text{ COSH } \frac{m\pi y}{a} + \frac{m\pi y}{a} \text{ SINH } \frac{m\pi y}{a} \right] \text{ SIN } \frac{m\pi x}{a} \qquad (64)$$

Differentiating again, and substituting into (10) gives

$$C_m = -\frac{E_m}{D} \left(\frac{a}{m\pi}\right)^2 \frac{1}{R_1} \qquad (65)$$

where

$$R_1 = \left[\rho(1-\nu)+2\right] \text{COSH } \lambda_m+\lambda_m(1-\nu)\text{SINH } \lambda_m \qquad (27)$$

and hence, for a symmetrical moment loading,

$$w = -\frac{a^2}{\pi^2 D} \sum_{m=1}^{\infty} \frac{E_m}{m^2} \left[\frac{\rho}{R_1} \text{ COSH } \frac{m\pi y}{a} + \frac{m\pi y}{aR_1} \text{ SINH} \frac{m\pi y}{a} \right] \text{ SIN } \frac{m\pi x}{a} \qquad (66)$$

Considering now a parallel case in which the loading is completely unsymmetric, i.e.,

$$M_y \bigg|_{y=b/2} = - M_y \bigg|_{y=-b/2} \tag{67}$$

and

$$f_1(x) = -f_2(x) = \sum_{m=1}^{\infty} E_m \, SIN \, \frac{m\pi x}{a} \tag{68}$$

from symmetry, it can be seen that, in this case, the coefficients of the even functions of "y" must vanish, i.e.,

$$B_m = C_m = 0 \tag{69}$$

and hence

$$\omega = \sum_{1}^{\infty} (A_m \, SINH \, \frac{m\pi y}{a} + D_m \, \frac{m\pi y}{a} \, COSH \, \frac{m\pi y}{a}) \, SIN \, \frac{m\pi x}{a} \tag{70}$$

Proceedings as before, differentiating and substituting into (5)

$$A_m = D_m(\gamma) \tag{71}$$

where

$$\gamma = \frac{(\nu+1-\alpha_m \lambda_m) COSH \, \lambda_m - (1-\nu)\lambda_m SINH \, \lambda_m}{\alpha_m SINH \, \lambda_m + (1-\nu) COSH \, \lambda_m} \tag{26}$$

and then

$$\omega = \sum_{1}^{\infty} D_m \left[\gamma \, SINH \, \frac{m\pi y}{a} + \frac{m\pi y}{a} \, COSH \, \frac{m\pi y}{a} \right] SIN \, \frac{m\pi x}{a} \tag{72}$$

Differentiating again, and substituting into (10) gives

$$D_m = - \frac{E_m}{D} \left(\frac{a}{m\pi}\right)^2 \frac{1}{R_2} \tag{73}$$

where

$$R_2 = \left[\gamma(1-\nu)+2\right] \text{SINH } \lambda_m + \lambda_m(1-\nu)\text{COSH } \lambda_m \tag{28}$$

Thus, for an unsymmetrical loading,

$$\omega = - \frac{a^2}{\pi^2 D} \sum_{m=1}^{\infty} \frac{E_m}{m^2} \left[\frac{\gamma}{R_2} \text{SINH } \frac{m\pi y}{a} + \frac{m\pi y}{aR_2} \text{COSH } \frac{m\pi y}{a} \right] \text{SIN } \frac{m\pi x}{a} \tag{74}$$

In the completely general case both of these solutions may be combined, as

$$\omega = - \frac{a^2}{\pi^2 D} \sum_{m=1}^{\infty} \frac{E_m}{m^2} \left[\frac{\rho}{R_1} \text{COSH } \frac{m\pi y}{a} + \frac{m\pi y}{aR_1} \text{SINH } \frac{m\pi y}{a} \right.$$

$$\left. + \frac{\gamma}{R_2} \text{SINH } \frac{m\pi y}{a} + \frac{m\pi y}{aR_2} \text{COSH } \frac{m\pi y}{a} \right] \text{SIN } \frac{m\pi x}{a} \tag{75}$$

since, under an arbitrary moment, all of the deflection functions, both odd and even, must be considered acting on the plate.

To specialize this general solution for the case in which the moment is applied only along one edge of the plate, the given moment functions may be divided into both symmetrical and unsymmetrical components, as

$$M_y'\bigg|_{y=b/2} = M_y'\bigg|_{y=-b/2} = \frac{1}{2}\left[\, f_1(x)+f_2(x)\,\right] \tag{76}$$

$$M_y''\bigg|_{y=b/2} = M_y''\bigg|_{y=-b/2} = \frac{1}{2}\left[\, f_1(x)-f_2(x)\,\right] \tag{77}$$

and, representing these separate functions as series,

$$M_y' = \sum_{m=1}^{\infty} E_m' \; SIN \; \frac{m\pi x}{a} \tag{78}$$

$$M_y'' = \sum_{m=1}^{\infty} E_m'' \; SIN \; \frac{m\pi x}{a} \tag{79}$$

Now, if the applied moment is to be distributed only along the edge $y = + b/2$, then,

$$f_2(x) = 0 \tag{80}$$

and

$$E_m' = E_m'' = \frac{1}{2} E_m \tag{81}$$

thus the solution becomes

$$\omega = - \frac{a^2}{2\pi^2 D} \sum_{m=1}^{\infty} \frac{E_m}{m^2} \left[\frac{\rho}{R_1} \; COSH \; \frac{m\pi y}{a} + \frac{m\pi y}{aR_1} \; SINH \; \frac{m\pi y}{a} \right.$$

$$\left. + \frac{\gamma}{R_2} \; SINH \; \frac{m\pi y}{a} + \frac{m\pi y}{aR_2} \; COSH \; \frac{m\pi y}{a} \right] \; SIN \; \frac{m\pi x}{a} \tag{24}$$

Appendix C

Evaluation of the Second Order Shear Term

In this analysis, the magnitude of the tilt moment acting on the plate is a direct function of the shear pressure or reaction which the plate exerts on the stiffener under a lateral load. There is, however, another shear pressure present, that arising from the tilt moment itself, which could add or detract from the initial value, depending upon the direction of application of the tilt moment, and so change the overall effect on the plate.

In order to gain some insight into the magnitude of this increment of shear, it is helpful to consider a simple beam under lateral load, and compare the form of the result to those obtained in the body of the paper.

$$V = \frac{WL}{2} \qquad\qquad V_1 = \frac{W}{2} \in \sin \phi$$

$$T_2 = V \in \sin \phi$$
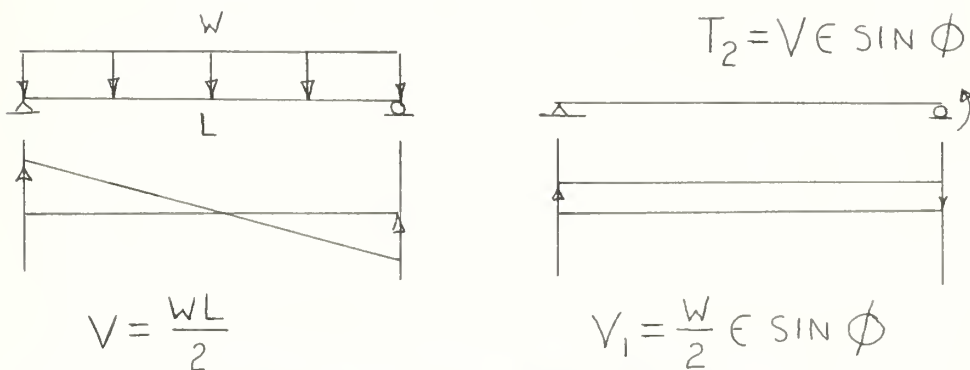
Figure XXIV Simple Beam Analogy

Since, in the example pictured, the value of the shear force used in computing the tilt moment would have to be corrected by the amount of shear it itself created in the plate, it

-92-

can be seen that a corrected moment would be, when carried
out through several steps,

$$T_2 = \frac{WL\epsilon}{2} \, SIN \, \emptyset + \frac{W}{2} \, (\epsilon \, SIN \, \emptyset)^2 + \frac{W}{2L} \, (\epsilon \, SIN \, \emptyset)^3 + \, \ldots$$

(82)

By inspection, it can be seen that the relationship between
terms is

$$\frac{\epsilon \, SIN \, \emptyset}{L}$$

(83)

Considering a numerical example with values consistent with
those used in this investigation, assume:

$$L = 72 \text{ inches}$$
$$\epsilon = 7 \text{ inches}$$
$$\emptyset = 7 \text{ degrees}$$

the ratio of the first two terms is then,

$$\frac{7(0.12)}{72} = 0.015$$

or, the error in neglecting this term is of the order of
1.5%. The following terms decrease rapidly and can be
neglected as well.

Considering the case in point, it has already been
shown that the shear pressure (reaction) at the plate edge
is

$$\frac{4\alpha a}{\pi^2} \sum_{m=1}^{\infty} \frac{1}{m^2} \, F_m \, SIN \, \frac{m\pi x}{a}$$

(84)

where F_m is a series constant developed from equation (32) and arises from the lateral load alone. From this has been derived the tilt loading factor, E_m,

$$E_m = \frac{4qa}{\pi^2 m^2} \; F_m \; \epsilon \; SIN \; \emptyset \tag{85}$$

The shear loading on the plate from this, i.e., the moment load, alone can be obtained by differentiating (24) and substituting into the expression,

$$- V_y = D \left[\frac{\partial^3 \omega}{\partial y^3} + (2-\nu) \frac{\partial^3 \omega}{\partial x^2 \partial y} \right] \quad \text{at } y = +b/2 \tag{30}$$

This results in

$$- V_y = \frac{\pi}{2a} \sum_{m=1}^{\infty} m \; E_m \left[\left\{ \frac{(\nu-1)\rho + (\nu+1)}{R_1} \right\} \; SINH \; \lambda_m + \frac{(\nu-1)}{R_1} \lambda_m COSH \; \lambda_m \right.$$

$$+ \left\{ \frac{(\nu-1)\gamma + (\nu+1)}{R_2} \right\} \; COSH \; \lambda_m + \frac{(\nu-1)\lambda_m}{R_2} \; SINH \; \lambda_m \right] SIN \; \frac{m\pi x}{a} \tag{86}$$

or, simplified by grouping the series constant into a term R_m,

$$- V_y' = \frac{\pi}{a} \sum_1^{\infty} m \; E_m \; R_m \; SIN \; \frac{m\pi x}{a} \tag{87}$$

hence, the order of magnitude of the increment of tilt moment is

$$E_m' = \frac{4q}{2\pi m} \, F_m \, R_m \, (\epsilon \, SIN \, \emptyset)^2 \qquad (88)$$

Again, this is related to E_m by the ratio

$$\frac{\pi \, \epsilon \, SIN \, \emptyset}{2a} \qquad (89)$$

as was true for the beam analogy. This correction is then of second order in $(\epsilon \, SIN \, \emptyset)^2$ as well, and may be neglected with little error.

Appendix D

Computer Programs

1. Program for the stresses in a plate subject to lateral load. This program is presented for both of the support approximations. In addition this program calculates the value of the coefficients of the shear pressure term (E_m).

```
*       FORTRAN
C       STRESSES IN A LATERALLY LOADED FLAT PLATE
C
C       INTERNAL FUNCTIONS
        SINHF(X) = (EXPF(X)-EXPF(-X))/2.0
        COSHF(X) = (EXPF(X)+EXPF(-X))/2.0
```

```
C       FOR THE SIMPLE SUPPORT APPROXIMATION
        AAMF(X,Y)=(EN*(1.0+EN)*SINHF(X)-EN*(1.0-EN)*COSHF(X)
     1    -Y*(2.0*COSHF(X)+X*SINHF(X)))/((3.0+EN)*(1.0-EN)
     2    *SINHF(X)*COSHF(X)-(1.0-EN)**2*X+2.0*Y*(COSHF(X)**2))
        BBMF(X,Y)=(EN*(1.0-EN)*SINHF(X) Y*COSHF(X))/((3.0+EN)
     1    *(1.0-EN)*SINHF(X)*COSHF(X)-(1.0-EN)**2*X+2.0*Y*
     2    (COSHF(X)**2))
```

```
C       FOR THE CLAMPED APPROXIMATION
        AAMF(X,Y)=Y*(-SINHF(X)-X*COSHF(X))/(X*Y+Y*SINHF(X)
     1    *COSHF(X) 2.0*(SINHF(X)**2))
```

-96-

```
      BBMF(X,Y) Y*SINHF(X)/(X*Y+Y*SINHF(X)*COSHF(X)+2.0
    1    *(SINHF(X)**2))
C        READ COUNTER FOR NUMBER OF DATA RUNS
         LITEM=0
         READ 920, INDEX
    5    LITEM=LITEM+1
C        READ INPUT DATA
         READ 900,SHIP,YIELD,A,B,H,S,Q,EN
         PRINT 921,SHIP,YIELD,A,B,H,S
         PI=3.141592654
         FRONT=(24.0*Q*A**2)/(H**2*PI**3)
         ONE=(12.0*S*(1.0-EN**2)IPI)/(H**3*A)
C        SECTION TO CALCULATE STRESSES ALONG THE X=A/2 AXIS
         II=0
         DO 250 L=1,11
         I=L-1
         Y=FLOATF(I)*B/20.0
C        SET UP TO COMPUTE TEN SERIES VALUES
         AMDA=PI*Y/A
         SIGMAX=0.0
         SIGMAY=0.0
         DO 200 M=1,19,2
         FM=FLOATF(M)
         FIRST=(SINF(FM*PI/2.0))/(FM**3)
         AX=FM*ONE
```

```
        C1=FM*PI*B/(2.0*A)

        P1=AAMF(C1,AX)

        P2=BBMF(C1,AX)

        XTERM=1.0+P1*(1.0-EN)*COSHF(FM*AMDA)-2.0*EN*P2

      1    *COSHF(FM*AMDA)+P2*(1.0-EN)*FM*AMDA*SINHF(FM*AMDA)

     10 UP1=XTERM*FIRST*FRONT

        SIGMAX=SIGMAX+UP1

C       VALUES OF STRESS IN THE Y DIRECTION

        YTERM=EN+((EN-1.0)*P1-2.0*P2)*COSHF(FM*AMDA)

      1    +(EN-1.0)*P2*FM*AMDA*SINHF(FM*AMDA)

        UP2=YTERM*FIRST*FRONT

        SIGMAY=SIGMAY+UP2

    200 CONTINUE

        SIGYX(II)=SIGMAX

        SIGYY(II)=SIGMAY

    250 CONTINUE

C

C       SECTION TO CALCULATE STRESSES ALONG THE Y 0 AXIS

        II=0

        DO 350 L=1,11

        I=L-1

        II=II+1

        X=((FLOATF(I)*A)/20.0)+A/2.0

C       VALUES COMPUTED AT TEN EQUAL STATIONS ON Y AXIS

        SIGMAX=0.0
```

```
            SIGMAY=0.0

            DO 300 M=1,19,2

            ZM=FLOATF(M)

            ZLEAD=(SINF(ZM*PI*X/A))/(ZM**3)

            AZ=ZM*ONE

            Z1=ZM*PI*B/(2.0*A)

            Z11=AAMF(Z1,AZ)

            Z12=BBMF(Z1,AZ)

            ZTERM=1.0+Z11*(1.0-EN)-2.0*EN*Z12

            UP3=ZTERM*ZLEAD*FRONT

            SIGMAX=SIGMAX+UP3

C           STRESS IN THE Y DIRECTION

            YITEM=EN+Z11*(EN-1.0)-2.0*Z12

            UP4=YITEM*ZLEAD*FRONT

            SIGMAY=SIGMAY+UP4

  300       CONTINUE

            SIGXX(II)=SIGMAX

            SIGXY(II)=SIGMAY

  350       CONTINUE

C

C           PRINT HEADINGS

C

            PRINT 923

            PRINT 901

            L=-1
```

```
      DO 400 N=1,11
      L=L+1
      PRINT 912,L,SIGYX(N),SIGYY(N)
400   CONTINUE
      PRINT 907
      J=9
      DO 450 N=1,11
      J=J+1
      PRINT 913,J,SIGXX(N),SIGXY(N)
450   CONTINUE
C
C     CALCULATION OF COEFFICIENTS FOR TILT MOMENT
C
      PRINT 915
      DO 500 N=1,19,2
      FN=FLOATF(N)
      C3=FN*PI*B/(2.0*A)
      AN=FN*ONE
      P3=AAMF(C3,AN)
      P4=BBMF(C3,AN)
      EM=4.0*Q*A(((EN-1.0)*P3+(EN+1.0)*P4)*SINHF(C3)
     1    +(EN-1.0)*P4*C3*COSHF(C3))/(PI**2*FN**2)
500   PRINT 909,N,EM
C
C     CHECK FOR OTHER CASES
```

```
        IF(INDEX-LITEM) 15,15,5
 15     CALL EXIT
C       FORMAT STATEMENTS
C
 900    FORMAT(F5.1,F10.1,3F8.5,F8.2,2F8.5)
 901    FORMAT(35X,29HSTRESSES ALONG THE X=A/2 AXIS//)
 907    FORMAT(1H1,35X,27HSTRESSES ALONG THE Y=0 AXIS//)
 909    FORMAT(10X,2HM=,I2,5X,5HE(M)=,E20.9//)
 912    FORMAT(10X,2HY=,I3,4HB/20,5X,9HSIGMA(X)=,E20.9,5X,
    1      9HSIGMA(Y)=,E20.9//)
 913    FORMAT(10X,2HX=,I3,4HB/20,5X,9HSIGMA(X)=,E20.9,5X,
    1      9HSIGMA(Y)=,E20.9//)
 915    FORMAT(1H1,20X,21HTABLE OF COEFFICIENTS///)
 920    FORMAT(I2)
 921    FORMAT(1H1,7HLENGTH=,F5.1,5X,6HYIELD=,Flo.1/30X,
    1      2HA=,F8.5,5X,2HB=,F8.5,5X,2HH=,F8.5,5X,2HI=,
    2      F8.2////)
 923    FORMAT(30X,41HSTRESSES IN A LATERALLY LOADED FLAT
        PLATE//)
        END
```

2. This section of coding is designed to receive
the output from the first section already presented, examine
the tilt induced stresses for all angles up to seven degrees,
and compare the results.

```
*        FORTRAN

C

C        TILTED STIFFENER

C

         DIMENSION EM(25),SIGYX(50),SIGYY(50),SIGXX(50),
      1     SIGXY(50),SIGTYX(50),SIGTYY(50),SIGTXX(50),
      2     SIGTXY(50),TSIGYX(50),TSIGYY(50),TSIGXX(50),
      3     TSIGXY(50),SLFYX(50),SLFYY(50),SLFXX(50),SLFXY(50)

C

C        INTERNAL FUNCTIONS

C

         SINHF(X)=(EXPF(X)-EXPF(-X))/2.0
         COSHF(X)=(EXPF(X)+EXPF(-X))/2.0
         RHOF(X,Y)=((1.0+EN-(Y*X))*SINHF(X)-(1.0-EN)*X*
      1     *COSHF(X))/((1.0-EN)*SINHF(X)+Y*COSHF(X))
         GAMF(X,Y)=((1.0+EN-(Y*X))*COSHF(X)-(1.0-EN)*X
      1     *SINHF(X))/(Y*SINHF(X)+(1.0-EN)*COSHF(X))
         ADENF(X,Y)=(RHOF(X,Y)*(1.0-EN)+2.0)*COSHF(X)+X
      1     *(1.0-EN)*SINHF(X)
         BDENF(X,Y)=(GAMF(X,Y)*(1.0-EN)+2.0)*SINHF(X)+X
      1     *(1.0-EN)*COSHF(X)
         READ 910,INDEX
         LCOUNT=0
   30    LCOUNT=LCOUNT+1
```

```
      READ 900,A,B,EN,EPS,S,(EM(I),I=1,20),(SIGYX(I),
1     I=1,24),(SIGYY(I),I=1,24),(SIGXX(I),I=1,24),
2      (SIGXY(I),I=1,24)
    OUT=3.0/(H**2)
    PI=3.141592654
    AMDA=(PI*B)/(2.0*A)
    ALPH=(12.0*S*(1.0-EN**2)*PI)/(A*H**3)
C
C     CYCLE TILT ANGLE FROM ONE TO SEVEN DEGREES
    DO 800 K=1,7
    THETA=(FLOATF(K)*PI)/180.0
C
C     STRESSES ALONG THE A/2 AXIS, 21 POINTS
    Y=-B/2.0
    DELTAY=0.0
    DO 250 I=1,21
    SIGTX=0.0
    SIGTY=0.0
    Y=Y+DELTAY
    DO 200 M=1,19,2
    FM=FLOATF(M)
    X1=FM*AMDA
    AX=FM*ALPH
    P1=RHOF(X1,AX)
    P2=GAMF(X1,AX)
```

```
      R1=ADENF(X1,AX)

      R2=BDENF(X1,AX)

      XTERM=((P1*(EN-1.0)+2.0*EN/R1+FM*PI*Y*(EN-1.0)/
     1      (A*R2))*COSHF(FM*PI*Y/A)+(FM*PI*Y*(EN-1.0)/
     2      (A*R1)+(P2*(EN-1.0)+2.0*EN)/R2)*SINHF(FM*PI*Y/A)
      FRONT=EM(M)*SINF(FM*PI/2.0)*EPS*SINF(THETA)
      YTERM=((P1*(1.0-EN)+2.0)/R1+FM*PI*Y*(1.0-EN)/
     1      (A*R2))*COSHF(FM*PI*Y/A)+(FM*PI*Y(1.0-EN)/
     2      (A*R1)+(P2*(1.0-EN)+2.0)/R2)*SINHF(FM*PI*Y/A)
      UPX=OUT*FRONT*XTERM

      UPY=OUT*FRONT*YTERM

      SIGTX=SIGTX+UPX

      SIGTY=SIGTY+UPY

  200 CONTINUE

      SIGTYX(I)=SIGTX

      SIGTYY(I)=SIGTY

      DELTAY=B/20.0

  250 CONTINUE

C

C     STRESSES ALONG THE Y AXIS, 21 POINTS

      X=0.0

      DELTAX=0.0

      DO 350 I=1,21

      SIGTX=0.0

      SIGTY=0.0
```

```
        X=X+DELTAX

        DO 300 J=1,19,2

        FM=FLOATF(J)

        X1=FM*AMDA

        AX=FM*ALPH

        P1=RHOF(X1,AX)

        P2=GAMF(X1,AX)

        R1=ADENF(X1,AX)

        FRONT=EM(J)*SINF(FM*PI*X/A)*EPS*SINF(THETA)

        XTERM=(P1*(EN-1.0)+2.0*EN)/R1

        YTERM=(P1*(1.0-EN)+2.0)/R1

        UPX=OUT*FRONT*XTERM

        UPY=OUT*FRONT*YTERM

        SIGTX=SIGTX+UPX

        SIGTY=SIGTY+UPY

 300    CONTINUE

        SIGTXX(I)=SIGTX

        SIGTXY(I)=SIGTY

        DELTAX=A/20.0

 350    CONTINUE

C

C       SUM STRESSES AND GET RATIOS

C       ALONG A/2.0 AXIS

        DO 450 N=1,21

        TSIGYX(N)=SIGTYX(N)+SIGYX(N)
```

```
        SLFYX(N)=TSIGYX(N)/SIGYX(N)

        TSIGYY(N)=SIGTYY(N)+SIGYY(N)

        SLFYY(N)=TSIGYY(N)/SIGYY(N)

C       ALONG Y AXIS

        TSIGXX(N)=SIGTXX(N)+SIGXX(N)

        SLFXX(N)=TXIGXX(N)/SIGXX(N)

        TSIGXY(N)=SIGTXY(N)+SIGXY(N)

        SLFXY(N)=TSIGXY(N)/SIGXY(N)

450     CONTINUE

C       PRINT OUT VALUES FOR THIS ANGLE OF TILT

        PRINT 901,K,A,B,H,EPS,EN,S

        PRINT 902

        DO 600 N=1,21

        L=-11 N

        PRINT 903,L,TSIGYX(N), SLFYX(N), TSIGYY(N), SLFYY(N)

600     CONTINUE

        PRINT 904

        DO 700 N=1,21

        L=N-1

        PRINT 903,L,TSIGXX(N), SLFXX(N), TSIGXY(N), SLFXY(N)

700     CONTINUE

800     CONTINUE

        IF(INDEX-LCOUNT) 20,20,30

20      CALL EXIT

C
```

```
C        FORMAT STATEMENTS
  900    FORMAT(6F10.5/(4E20.9))
  901    FORMAT(1H1,50X,15HANGLE OF TILT=,I3,7HDEGREES//5X,
       1    2HA=,F10.5,5X,2HH=,F10.5,5X,4HEPS=,F10.5,3HNU=,
       2    F6.4,2HI=,F10.5//)
  902    FORMAT(45X,29HSTRESSES ALONG THE X=A/2 AXIS,/7X,
       1    5H20Y/B,15X,8HSIGMA(X),18X,6HFACTOR,18X,
       2    8HSIGMA(Y),18X,6HFACTOR)
  903    FORMAT(7X,I4,7X,E20.9,5X,E20.9,5X,E20.9,5X,E20.9)
  904    FORMAT(//,45X,27HSTRESSES ALONG THE Y=0 AXIS,/7X,
       1    5H20X/A,15X,8HSIGMA(X),18X,6HFACTOR,18X,
       2    8HSIGMA(Y),18X,6HFACTOR)
  910    FORMAT(I2)
         END
```

APPENDIX E.   SAMPLE COMPUTER OUTPUT

STRESSES IN A LATERALLY LOADED FLAT PLATE

NO ROTATION AT EDGE

STRESSES ALONG THE X=A/2 AXIS

Y=   0B/20   SIGMA(X)=   .521761447E 04   SIGMA(Y)=   .124697912E 05

Y=   1B/20   SIGMA(X)=   .511002660E 04   SIGMA(Y)=   .121101363E 05

Y=   2B/20   SIGMA(X)=   .478728227E 04   SIGMA(Y)=   .110312090E 05

Y=   3B/20   SIGMA(X)=   .424943384E 04   SIGMA(Y)=   .923312195E 04

Y=   4B/20   SIGMA(X)=   .349658694E 04   SIGMA(Y)=   .671608068E 04

Y=   5B/20   SIGMA(X)=   .252891973E 04   SIGMA(Y)=   .348038904E 04

Y=   6B/20   SIGMA(X)=   .134676848E 04   SIGMA(Y)=   -.473492999E 03

Y=   7B/20   SIGMA(X)=   -.492672767E 02   SIGMA(Y)=   -.514478810E 04

Y=   8B/20   SIGMA(X)=   -.165810406E 04   SIGMA(Y)=   -.105317420E 05

Y=   9B/20   SIGMA(X)=   -.347826432E 04   SIGMA(Y)=   -.166293642E 05

Y= 10B/20   SIGMA(X)=   -.550958335E 04   SIGMA(Y)=   -.234217828E 05

STRESSES ALONG THE Y=0 AXIS

X= 10A/20	SIGMA(X)=	.521761447E 04	SIGMA(Y)=	.124697912E 05
X= 11A/20	SIGMA(X)=	.525706410E 04	SIGMA(Y)=	.124843946E 05
X= 12A/20	SIGMA(X)=	.519326940E 04	SIGMA(Y)=	.124690130E 05
X= 13A/20	SIGMA(X)=	.524406433E 04	SIGMA(Y)=	.124721640E 05
X= 14A/20	SIGMA(X)=	.524751537E 04	SIGMA(Y)=	.124035531E 05
X= 15A/20	SIGMA(X)=	.548132330E 04	SIGMA(Y)=	.122588511E 05
X= 16A/20	SIGMA(X)=	.574323140E 04	SIGMA(Y)=	.118138900E 05
X= 17A/20	SIGMA(X)=	.626007430E 04	SIGMA(Y)=	.108760871E 05
X= 18A/20	SIGMA(X)=	.629734270E 04	SIGMA(Y)=	.890050985E 04
X= 19A/20	SIGMA(X)=	.517292477E 04	SIGMA(Y)=	.547697902E 04
X= 20A/20	SIGMA(X)=	.260068882E-02	SIGMA(Y)=	.212254321E-02

TABLE OF COEFFICIENTS

```
M = 1        E(M) =        .253185555E 03

M = 3        E(M) =        .788349740E 02

M = 5        E(M) =        .380002800E C2

M = 7        E(M) =        .207794638E C2

M = 9        E(M) =        .127463059E 02

M =11        E(M) =        .855609901E 01

M =13        E(M) =        .613001220E C1

M =15        E(M) =        .460549772E 01

M =17        E(M) =        .358615320E 01

M =19        E(M) =        .287124272E 01
```

ANGLE OF TILT = 3 DEGREES

A = 96.00000   B = 30.00000   H = .50000   EPS = 7.78000 NU = .3000 I = 37.80000

STRESSES ALONG THE X=A/2 AXIS

20Y/B	SIGMA(X)	FACTOR	SIGMA(Y)	FACTOR
-10	-.545691565E 04	.990440734E 00	-.233007757E 05	.994833574E 00
-9	-.339790225E 04	.976895936E 00	-.164272875E 05	.987848215E 00
-8	-.154994916E 04	.934771955E 00	-.102505284E 05	.973298475E 00
-7	.863957494E 02	-.175361328E 01	-.478471432E 04	.930011950E 00
-6	.150957689E 04	.112088820E 01	-.342388302E 02	.723111652E-01
-5	.271847565E 04	.107495530E 01	.399941228E 04	.114912793E 01
-4	.371245004E 04	.106173538E 01	.731562503E 04	.108926998E 01
-3	.449111424E 04	.105687354E 01	.991406195E 04	.107374972E 01
-2	.505424075E 04	.105576411E 01	.117945162E 05	.106919523E 01
-1	.540168218E 04	.105707515E 01	.129568528E 05	.106991800E 01
0	.553335555E 04	.106051446E 01	.134010036E 05	.107467746E 01
1	.544922531E 04	.106637905E 01	.131269442E 05	.108396337E 01
2	.514930934E 04	.107562267E 01	.121346938E 05	.110003298E 01
3	.463367376E 04	.109042143E 01	.104243129E 05	.112901282E 01
4	.390245002E 04	.111607408E 01	.799592294E 04	.119056387E 01
5	.295584816E 04	.116881850E 01	.484970871E 04	.139343867E 01
6	.179423012E 04	.133224837E 01	.985969618E 03	-.208233200E 01
7	.418199353E 03	-.848837979E 01	-.359476022E 04	.698718823E 00
8	-.117117641E 04	.706334688E 00	-.889120676E 04	.844229452E 00
9	-.297233570E 04	.854545668E 00	-.148996277E 05	.895983018E 00
10	-.498431228E 04	.904662304E 00	-.216078898E 05	.922555298E 00

STRESSES ALONG THE Y=0 AXIS

20X/A	SIGMA(X)	FACTOR	SIGMA(Y)	FACTOR
0	.260068879E-02	.100000000E 01	.212254319E-02	.100000000E 01
1	.533412829E 04	.103116294E 01	.567775071E 04	.103665739E 01
2	.657353401E 04	.104385841E 01	.929106720E 04	.104388034E 01
3	.659577943E 04	.105362639E 01	.114307920E 05	.105100225E 01
4	.609859720E 04	.106187560E 01	.124979515E 05	.105790315E 01
5	.583501898E 04	.106452742E 01	.130374659E 05	.106351451E 01
6	.559114501E 04	.106548425E 01	.132473923E 05	.106803205E 01
7	.557645574E 04	.106338432E 01	.133587228E 05	.107108301E 01
8	.551657617E 04	.106225496E 01	.133817885E 05	.107320352E 01
9	.557471350E 04	.106042336E 01	.134112028E 05	.107423734E 01
10	.553335555E 04	.106051446E 01	.134010036E 05	.107467746E 01
11	.557471350E 04	.106042336E 01	.134112028E 05	.107423734E 01
12	.551657617E 04	.106225496E 01	.133817885E 05	.107320352E 01
13	.557645574E 04	.106338432E 01	.133587228E 05	.107108301E 01
14	.559114501E 04	.106548425E 01	.132473923E 05	.106803207E 01
15	.583501898E 04	.106452742E 01	.130374661E 05	.106351451E 01
16	.609859720E 04	.106187560E 01	.124979517E 05	.105790318E 01
17	.659577951E 04	.105362640E 01	.114307922E 05	.105100226E 01
18	.657353416E 04	.104385842E 01	.929106750E 04	.104388037E 01
19	.533412859E 04	.103116299E 01	.567775108E 04	.103665745E 01
20	.293595087E-02	.112891279E 01	.250889767E-02	.118202431E 01

ANGLE OF TILT = 5DEGREES

A = 96.00000   8= 30.00000   H=   .50000   EPS=   7.78000NU= .30001= 37.80000

STRESSES ALONG THE X=A/2 AXIS

20Y/B	SIGMA(X)	FACTOR	SIGMA(Y)	FACTOR
-10	-.542187534E 04	.984080844E 00	-.232202685E 05	.991396286E 00
-9	-.334443640E 04	.961524509E 00	-.162928436E 05	.979763485E 00
-8	-.147799235E 04	.891374908E 00	-.100634336E 05	.955533624E 00
-7	.176654115E 03	-.358562779E 01	-.454515275E 04	.883448012E 00
-6	.161789544E 04	.120131668E 01	.258002613E 03	-.544892140E 00
-5	.284458969E 04	.112482402E 01	.434472512E 04	.124834467E 01
-4	.385606661E 04	.110280874E 01	.771450967E 04	.114866245E 01
-3	.465190735E 04	.109471225E 01	.103671003E 05	.112281636E 01
-2	.523185171E 04	.109286468E 01	.123023544E 05	.111523174E 01
-1	.559572443E 04	.109504802E 01	.135201845E 05	.111643538E 01
0	.574342236E 04	.110077553E 01	.140205514E 05	.112436134E 01
1	.567489862E 04	.111054190E 01	.138034398E 05	.113982529E 01
2	.539017066E 04	.112593543E 01	.128688565E 05	.116658623E 01
3	.488931358E 04	.115057998E 01	.112168279E 05	.121484673E 01
4	.417247601E 04	.119329967E 01	.884741858E 04	.131734846E 01
5	.323988922E 04	.128113564E 01	.576073483E 04	.165519852E 01
6	.209193211E 04	.155329749E 01	.195696885E 04	-.413304709E 01
7	.729210921E 03	-.148011209E 02	-.256350677E 04	.498272572E 00
8	-.847217187E 03	.510955378E 00	-.779973760E 04	.740593307E 00
9	-.263573494E 04	.757773049E 00	-.137488119E 05	.826779179E 00
10	-.463484276E 04	.841232911E 00	-.204010837E 05	.871030353E 00

STRESSES ALONG THE Y=0 AXIS

20X/A	SIGMA(X)	FACTOR	SIGMA(Y)	FACTOR
0	.260068879E-02	.100000000E 01	.212254319E-02	.100000000E 01
1	.544137917E 04	.105189607E 01	.581132680E 04	.106104603E 01
2	.675728783E 04	.107303798E 01	.955091022E 04	.107307452E 01
3	.681912847E 04	.108930472E 01	.117998444E 05	.108493471E 01
4	.633502677E 04	.110304224E 01	.129530666E 05	.109642688E 01
5	.607033737E 04	.110745838E 01	.135554885E 05	.110577152E 01
6	.581976630E 04	.110905181E 01	.138088094E 05	.111329467E 01
7	.579760015E 04	.110555474E 01	.139485620E 05	.111837544E 01
8	.573167637E 04	.110367399E 01	.139890701E 05	.112190677E 01
9	.578604981E 04	.110062379E 01	.140278203E 05	.112362840E 01
10	.574342236E 04	.110077553E 01	.140205514E 05	.112436134E 01
11	.578604981E 04	.110062379E 01	.140278203E 05	.112362840E 01
12	.573167644E 04	.110367401E 01	.139890701E 05	.112190677E 01
13	.579760015E 04	.110555474E 01	.139485620E 05	.111837544E 01
14	.581976630E 04	.110905181E 01	.138088096E 05	.111329469E 01
15	.607033737E 04	.110745838E 01	.135554887E 05	.110577155E 01
16	.633502677E 04	.110304224E 01	.129530668E 05	.109642690E 01
17	.681912862E 04	.108930476E 01	.117998446E 05	.108493473E 01
18	.675728805E 04	.107303802E 01	.955091074E 04	.107307456E 01
19	.544137970E 04	.105189615E 01	.581132740E 04	.106104615E 01
20	.315900505E-02	.121468015E 01	.276594434E-02	.130312745E 01

A = 96.00000   8 = 30.00000   H = .50000   EPS = 7.78000 NU = .3000 I = 37.80000

STRESSES ALONG THE X=A/2 AXIS

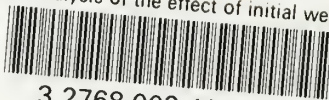| 20Y/B	SIGMA(X)	FACTOR	SIGMA(Y)	FACTOR
-10	-.538694188E 04	.977740355E 00	-.231400065E 05	.987969480E 00
-9	-.329113357E 04	.946199961E 00	-.161588097E 05	.971703410E 00
-8	-.140625495E 04	.848110199E 00	-.987690911E 04	.937822938E 00
-7	.266637225E 03	-.541205525E 01	-.430632170E 04	.837026067E 00
-6	.172588367E 04	.128149990E 01	.549352862E 03	-.116021329E 01
-5	.297031909E 04	.117454070E 01	.468898498E 04	.134725884E 01
-4	.399924520E 04	.114375683E 01	.811217785E 04	.120787380E 01
-3	.481221005E 04	.113243558E 01	.108187571E 05	.117173339E 01
-2	.540892102E 04	.112985212E 01	.128086438E 05	.116112784E 01
-1	.578917503E 04	.113290507E 01	.140817981E 05	.116281088E 01
0	.595284842E 04	.114091382E 01	.146382097E 05	.117389373E 01
1	.589988381E 04	.115457009E 01	.144778723E 05	.119551688E 01
2	.563029751E 04	.117609475E 01	.136007803E 05	.123293651E 01
3	.514417373E 04	.121055507E 01	.120069259E 05	.130041886E 01
4	.444167856E 04	.127028976E 01	.969631746E 04	.144374643E 01
5	.352306403E 04	.139311027E 01	.666898265E 04	.191616012E 01
6	.238872629E 04	.177367255E 01	.292500708E 04	-.617750868E 01
7	.103927401E 04	-.210946105E 02	-.153539818E 04	.298437599E 00
8	-.524245940E 03	.316171918E 00	-.671159692E 04	.637273200E 00
9	-.230016064E 04	.661295526E 00	-.126015056E 05	.757786378E 00
10	-.428643901E 04	.777996957E 00	-.191979576E 05	.819662526E 00

STRESSES ALONG THE Y=0 AXIS

20X/A	SIGMA(X)	FACTOR	SIGMA(Y)	FACTOR
0	.260068879E-02	.100000000E 01	.212254319E-02	.100000000E 01
1	.554830298E 04	.107256595E 01	.594449557E 04	.108536030E 01
2	.694048114E 04	.110212856E 01	.980996080E 04	.110217964E 01
3	.704179645E 04	.112487428E 01	.121677713E 05	.111876369E 01
4	.657073528E 04	.114408333E 01	.134067938E 05	.113483313E 01
5	.630493812E 04	.115025841E 01	.140719315E 05	.114789970E 01
6	.604769044E 04	.115248647E 01	.143685147E 05	.115841926E 01
7	.601807006E 04	.114759655E 01	.145366022E 05	.116552366E 01
8	.594612069E 04	.114496673E 01	.145944994E 05	.117046149E 01
9	.599674165E 04	.114070166E 01	.146425573E 05	.117286884E 01
10	.595284842E 04	.114091382E 01	.146382097E 05	.117389373E 01
11	.599674165E 04	.114070166E 01	.146425573E 05	.117286884E 01
12	.594612069E 04	.114496673E 01	.145944994E 05	.117046149E 01
13	.601807006E 04	.114759655E 01	.145366022E 05	.116552366E 01
14	.604769036E 04	.115248647E 01	.143685147E 05	.115841926E 01
15	.630493812E 04	.115025841E 01	.140719319E 05	.114789973E 01
16	.657073535E 04	.114408335E 01	.134067941E 05	.113483317E 01
17	.704179659E 04	.112487429E 01	.121677718E 05	.111876372E 01
18	.694048144E 04	.110212861E 01	.980996154E 04	.110217974E 01
19	.554830365E 04	.107256607E 01	.594449639E 04	.108536045E 01
20	.338137906E-02	.130018594E 01	.302220710E-02	.142386129E 01

BIBLIOGRAPHY

1. NAVSHIPS 250-637-3, Fabrication, Welding, and Inspection
   of HY-80 Submarine Hulls, Navy Department.

2. E. Wenk Jr. and E. H. Kennard, "The Weakening Effect of
   Initial Tilt and Lateral Buckling of Ring Stif-
   feners on Cylindrical Pressure Vessels," David W.
   Taylor Model Basin Research and Development Report
   No. 1073, Navy Department, December, 1960.

3. E. H. Kennard, "Tripping of T-Shaped Stiffening Rings on
   Cylinders Under External Pressure," David W. Taylor
   Model Basin Research and Development Report No.
   1079. Navy Department, November, 1959.

4. J. J. Roark, Formulas for Stress and Strain, New York:
   The McGraw-Hill Book Company, Inc., 1954.

5. S. Timoshenko and S. Woinowsky-Krieger, Theory of Plates
   and Shells, New York: The McGraw-Hill Book Company,
   1959.

6. Manual of Steel Construction, American Institute of Steel
   Construction, Inc., Sixth Edition, New York, 1964.

7. A. Nádai, Elastiche Platten, Berlin, 1925.

8. M. Lévy, Comptes Rendu Hebdomadaires des Seances de
   l'Academic des Sciences, Vol. 129, Paris, 1899.

9. F. Bleich, Buckling Strength of Metal Structures, New
   York: The McGraw-Hill Book Company, Inc., 1952.

10. M. St. Denis, "On the Structural Design of the Midship
    Section," David W. Taylor Model Basin Report No.
    NC 555 Navy Department, October, 1954.

11. Manual of Properties of Combined Beam and Plate, Part 1,
    Tees and Angles, Office of Technical Services, U.S.
    Department of Commerce, Washington, D. C.